MONASH University

Dynamics of iron bound phosphorus within sediments of the Gippsland Lakes

RASHID IFTIKHAR
Master of Science

A thesis submitted in fulfilment of the requirements for the degree of
Doctor of Philosophy
at
Monash University in June 2022
Faculty of Science
School of Chemistry

Copyright notice

Abstract

Estuaries are highly productive ecosystems that are impacted by the algal blooms due to excessive nitrogen (N) and phosphorus (P) loading. The dynamics of P in lake sediment is mainly controlled by factors including, but not limited to, the presence of iron oxyhydroxides (FeOOH), oxygen condition, inflow events and bioirrigation by fauna. The present thesis deals with the impact of these factors on sediment P cycling using in-situ field data, lab experiments and modelling approaches.

First, a decade long study of water quality parameters and sediment P speciation was linked with river flow to investigate the variables related to Fe bound P dynamics. No legacy P build-up was observed in the lake sediments even after longer periods of oxygenation. Principal component analysis (PCA) showed a strong positive association of the iron bound P fraction (ascorbate extractable) with bottom water total phosphorus (TP) and (counter-intuitively) low bottom water dissolved oxygen (DO) associated with river inflow. The PCA analysis suggests that the delivery of new Fe and P is a major factor in Gippsland Lakes, controlling the sediment phosphorus fractions.

Second, a laboratory experiment approach was used to quantify the influence of faunal irrigation on P release rates from sediments to the overlying water column under cyclic anoxic-hypoxic conditions. A sequential extraction method using ascorbate as an extractant for Fe and P was used to disentangle the presence of various P pools in the sediment. The study shows that *Capitella capitata* activity led to an enhanced accumulation of P in the sediment under oxic condition. Cyclic hypoxic-anoxic conditions led to an enhanced P release from the sediment in sediment colonised by *C. capitata*. Benthic P fluxes equal to 1166 μmol m^{-2} d^{-1} correspond to some of the highest P fluxes out of the sediment reported in literature. The study also reiterates the ability of *C. capitata* to adapt well to low oxygen conditions and show increased physical activity when stressed.

Finally, a modelling investigation was used to further investigate the lab outcome based hypothesis that cyclic anoxic-hypoxic conditions will lead to an enhanced P release from the sediments and oxic conditions will result in an enhanced P accumulation. The study reveals limitations of a 1D model as a tool to explain some of the bioirrigation based lab experimental observations. The 1D model assumes a well-mixed sediment that means it cannot have deep pockets of FeOOH neighbouring reduced sediment; consequently, the model may not be applicable in situations involving faunal activity into the sediments. A 2D model with lateral heterogeneity can most likely better demonstrate the mechanistic effects of benthic fauna activity on sediment P dynamics.

Declaration

This thesis is an original work of my research and contains no material which has been accepted for the award of any other degree or diploma at any university or equivalent institution and that, to the best of my knowledge and belief, this thesis contains no material previously published or written by another person, except where due reference is made in the text of the thesis.

Acknowledgements

I would like to express my gratitude to a number of people without their support my doctoral research would not have been possible. Firstly, I would like to thank my supervisor Prof. Perran Cook for his support and motivation throughout my project. He was always available to guide me and helped me learn and explore the new world of marine biogeochemistry. Because of him, I have been able to explore ways of developing ideas and converting them into stories through scientific writing. I can simply wish that one day I will be able to build ideas and do writing like him. Secondly, I would like to thank my co-supervisor, Dr. Adam Kessler, for his countless support and guidance. You were always encouraging me and giving me confidence through motivational words. Whenever I felt down, I used to go back to your emails as a source of motivation. Of course, you have also played an important role in helping me achieve my Ph.D. goals particularly modelling. Your different way of viewing my project helped me alot in building new skills and improving research quality.

My heartiest thank to all the members of the WSC laboratory for their support throughout my research. I am very grateful to Vera Eate for her support in the fieldwork especially in the early stages of my project. I have learned the skills of performing fieldwork and sample analysis from her. Her work energy and positive work attitude were a boost for me whenever I felt down and tired. I am also very thankful to Maha Alharbi and Tess Hutchinson. They were always available to support me whenever I needed them. Sample extraction would not have been possible without the invaluable assistance of Maha Alharbi particularly during the last year. I am also very grateful to Wei Wen Wong and Tina Hines for providing me valuable guidance, equipment access and lab supplies whenever I needed them. To the rest of the members within the Water Studies Centre, I thank you all for your support particularly Associate Prof. Michael Grace.

I am also thankful to my friends and family, who were always motivating me during my three years of stay in Australia. I would like to thank my parents for having faith in my abilities and allowing me to pursue whatever endeavour I choose, as long as it made me happy. Lastly, to my wife, Munaza Liaqat, I thank her for the efforts she put in making me achieve my goal and I appreciate the tough times she had to face because of COVID. This Ph.D. would not have been possible without your continual support.

TABLE OF CONTENTS

Contents

Table of Figures

List of Tables

1. Introduction

The occurrence of harmful algal blooms (HABs) is on rise in coastal areas and in freshwater bodies around the world, and arguably linked to climate change and nutrient pollution (Hallegraeff et al, 2021). These blooms have serious implications for the ecological functions and economic activity (fishing, boating etc.) associated with them. This makes algae an important part of the aquatic ecosystem as their concentration may control the ecological balance of any ecosystem. A number of environmental factors such as light intensity, pH, nutrients, temperature, salinity, UV radiation, wind, trace metals and environmental pollutants can influence the growth of the cyanobacterial species and their cyanotoxin production (Pilskaln et al., 2014). Among the above-mentioned factors, nutrient loading (N, P and micro-nutrients) as a result of anthropogenic activities is major driving factor for increased rate of HABs over the past few decades. Both nitrogen and phosphorus are essential macronutrients and depending upon their availability can limit primary production in aquatic systems. Phosphorus is critical to the aquatic system in the sense that the only way to manage phosphorus is either through its burial within the system leading to the formation of phosphate rich sedimentary rocks or export from the system (Hartzell et al., 2010). This makes phosphorus an important component of the aquatic system.

An estuary is a partly enclosed aquatic system, characterized by fresh river water mixing with salty ocean water. Estuaries are critical reactive water bodies furnishing ecological services and economical value to human beings (Wei et al., 2022). Anthropogenic activities may lead to accelerated input of nutrients into estuaries and uncontrolled supply of nutrient may stress the system by stimulating excessive algal growth that leads to eutrophication (Withers & Jarvie, 2008). The fate and cycling of the nutrient entering the marine coastal environment may include, but is not limited to, sedimentation and burial through chemical and physical processes, release through resuspension and hypoxic/anoxic events, assimilation and regeneration through organisms, and decomposition of organic matter (Xu et al., 2021). Nutrients (especially N and P) are also important managers of carbon cycling in estuarine environments imparting primary production and widespread eutrophication (Colborne et al., 2019; Wang et al., 2021). Algal blooms and hypoxia are two main indicators of eutrophication that can pose serious threat to aquatic life. Environmental pressures such as hypoxia tend to threaten ecosystem stability and they are closely linked with the nutrient source-sink patterns (Tao et al., 2021). An aquatic system can switch between P and N limitation either seasonally or depending upon the inflow events or interannual variability (Howarth et al., 2021). Phosphorus as a limiting nutrient is critical to the ecosystem as it can act as a key control on primary productivity and harmful algal bloom (Robson, 2014). Studies into P dynamics show that the balance between sources and sinks regulate P concentrations in the water column until equilibrium is reached which reduces variability (Li et al., 2021). Sediments function as a phosphorus warehouse as they act as a store of external P and source of internal P resulting in continuous exchange of phosphorus with the overlying water column (Cai et al., 2020). A range of environmental factors including temperature, pH, redox potential, mixing and bioturbation are regarded as to influence the release mechanism within sediments. (Carstensen et al., 2014; Chen et al., 2015).

The internal and external P loads need to be considered while establishing a management strategy for an aquatic system. The occurrence of cyanobacterial blooms are also found to have a positive feedback loop where release of P from the sediment fuels algal bloom, which in turn produce dense organic matter layer to enhance P release inducing hypoxia (Zou et al., 2020). Belley et al. (2016)

reported strong correlation between bottom water dissolved oxygen concentration, oxygen penetration depth into sediments and fluxes of phosphate. To better understand the dynamics of phosphorus in coastal marine systems, it is important to identify and quantify the solid phase P fractions present in the sediments. The development of the sequential extraction schemes has allowed analysis of various phosphorus pools present in the sediment to deepen our understanding of the cycling of P in sediments (Jordan et al., 2008). Although several extraction schemes have been developed to quantify Fe and P pools in the sediments over the past three decades, however, still no single extraction scheme exist that can be used to quantify both Fe and P fractions simultaneously.

The research described in this thesis was aimed at understanding the dynamics of iron oxyhydroxide bound phosphorus (FeOOH-P) pool in sediments in response to changes in environmental conditions using Fe and P sequential extractions. A previous study has observed deep pools of iron oxyhydroxide bound phosphorous (~20 cm) linked to burrowing activity of *C. capitata*. The pools rapidly depleted on the onset of hypoxia however, the recharge mechanism of this pool is still not clear (Scicluna et al., 2015). The present study focuses on addressing the probable mechanism and timescale involved in sediment P recharge of the Gippsland Lakes. Secondly, it aimed to investigate the impact of *C. capitata* activity on Fe bound P dynamics under cyclic hypoxic/anoxic conditions. In particular, understanding the significance of the Fe bound P pool in relation to the P fluxes. Lastly, it aimed at addressing the interactions between worm irrigation activity and oxygen dynamics via investigating the biogeochemical cycling of Fe and P using a 1D model as a tool. Simulations were also performed to investigate the sensitivity of these observations to the irrigation rates, sediment carbon loading and reactive iron content.

1.1. Cycling of P in aquatic systems

Phosphorus is a key limiting nutrient for primary production in natural waters. It mostly occurs as phosphate in minerals and enter into aquatic systems through rainfall or riverine runoff (Yuan et al., 2018). Biotic and abiotic factor obstruct P along its flow path, giving rise to legacy P in the system (Simpson et al., 2019). More than 90% of the P delivered to the estuaries by river inflows is believed to be associated with suspended solids (Jordan et al., 2008). Phosphorus in the marine environment is mainly present as phosphate (PO_4^{3-}). Biological uptake, adsorption onto surfaces or precipitation with minerals and formation of CFA (carbonate fluorapatite) represent the consumption pathway for phosphate (Schulz & Zabel, 2006). Changes in biogeochemical cycles of P, through internal or external loading, adversely affect aquatic ecosystems globally. Recently, considerable efforts have been made to reduce external nutrient loading in order to control eutrophication. However, internal loading from sediments may prevent improvements in lake water quality (Søndergaard et al., 2003). The phosphorus in sediments can either be immobile P, which is not easily available acting as a sink for P or reactive P which may become available to algae/bacteria (Korppoo et al., 2012). Sedimentary phosphorus is present in either sorbed or bound form and the main sedimentary P pools are exchangeable P, P bound to Fe, Mn, Al, Ca and organic P (Petkuviene et al., 2016). Organic P represent the most dominant form of P comprising 20-25% of the total sediment P pool. It can also serve as a source of P when inorganic P is limited (Thompson & Cotner, 2018). Phosphate bound to Fe and Mn oxides is redox sensitive such that phosphorus adsorbs onto iron oxyhydroxide under oxic conditions while oxygen stress conditions can induce reduction of these compounds promoting release of P into porewater (Korppoo et al., 2012; Reed et al., 2011)). Benthic P cycling studies have

found that dynamic Fe bound P pools dominate top layers (0-3 cm) of the sediment in Fe rich sediments that can readily become bioavailable under reducing conditions (Jensen et al., 1995; Markovic et al., 2020).

In Fe-rich sediments, Fe can strongly influence the phosphorus cycling due to the adsorption capacity of iron oxides for phosphate, while reduction of Fe leads to the release of bound P (Canfield et al., 2005; Zhao et al., 2021). The biogeochemical cycling of P in such systems is linked with redox sensitive iron dynamics. Iron in aquatic system can exist in two states- Ferric (Fe (III)) or Ferrous (Fe (II)) and the change from one state to another depending upon the prevailing redox condition, impact the biogeochemical cycling of phosphorus, sulphur, carbon, nitrogen and other trace metals (Hyacinthe et al., 2006). Microbial communities respire utilising the energy released during the oxidation of organic matter in conjunction with the reduction of an oxidant for their own energy metabolism. Microbes have to compete with abiotic factors and reactions as well since both the oxidised and reduced forms of iron react spontaneously with a range of compounds. Iron reducing microorganisms can utilise Fe (III) as electron acceptor under anoxic conditions and Fe (II) can function as electron donor under both anoxic and oxic environments for iron oxidising microorganisms (Weber et al., 2006). The dissimilatory Fe (III) reduction by iron reducing microorganisms may results in formation of Fe(II) bearing minerals such as vivianite, siderite and geologically significant mixed valence iron minerals like green rust and magnetite (O'Loughlin et al., 2019). In natural environments, hydrogen sulphide is the most significant abiotic reductant for Fe (III) oxides. The release aspect of sediment P is defined by the size of the Fe bound P pool, that is, the higher the content of Fe-P pool, the larger the risk of P release (Wang et al., 2019). The release of phosphorus bound to iron oxides can therefore occur by one of the two main processes, as illustrated in Figure 1:

(1) Dissimilatory Fe oxide reduction to Fe (II) by iron reducing bacteria

(2) Chemical Fe oxide reduction to Fe (II) in sulfide presence

The presence of macro organisms in estuarine systems adds another dimensionality to understanding biogeochemical cycles, as they regulate key biogeochemical processes and are considered indicators and determinants of ecosystem health (Suzzi et al., 2022). Benthic macrofauna alter sediment biogeochemistry through burrow formation. This result in an enhanced oxygenation of surface sediment by fauna leading to the build-up of Fe bound P pool deep into the sediments. However, the Fe-P may become available on the onset of anoxia leading to an enhanced release of P from the sediment surface, which can intensify the impact of blooms.

1.2. The role of worms in sediments phosphorus cycling (respiration and irrigation)

Bioturbation is defined as all transport processes carried out by the bioturbators. Benthic fauna live in or on the sediment, and the presence, feeding and egestion of these organisms produce structures (burrows, networks and biofilms) which influence the properties of the sediment (Grabowski et al., 2011). Bioturbation has gained attention in recent years as it alters biogeochemical processes at the sediment water interface by changing the availability of nutrients and carbon for microbes or by changing abiotic conditions like redox and temperature affecting microbial reaction rates (Kristensen et al., 2012). Biogeochemical changes associated with faunal activity may include increased solute

exchange between sediment pore water and surface water, increased microbial activity through organic matter redistribution from sediment surface to deeper sediments and excretion of particle remaining at sediment water interface by worms feeding on sediment particles, bacteria and microbes within the sediment at depth (Korppoo et al., 2012). Benthic faunal impact on biogeochemical cycles may vary substantially depending up on the count, type of benthic fauna causing a change in the transport processes and reactions at sediment water interface through its activity (Quintana et al., 2007).

In iron rich sediments, bioturbation can strongly alter the P dynamics across sediment water interface by enhancing P uptake during oxygenation and P release upon anoxia. It has been documented that bioturbation improves the P retention capacity of the sediments by ventilating oxygen deeper into the anoxic sediments. The fate of P in such sediments is largely influenced by the presence of iron oxyhydroxide as P adsorption onto Fe oxides represent a major sink of P in sediments. The presence of oxygen through ventilation oxidizes the burrow walls, forming iron oxyhydroxides to which P can adsorb. This increase in iron oxide bound P may increase the P-burial but it may also lead to enhanced P release on the onset of anoxia. While studying the bioturbation impacts of benthic fauna, it was concluded that iron adsorption within burrows was the major mechanism behind labile and soluble P decrease (Chen et al., 2015). Worms through their burrowing activity enhance Fe mobilisation resulting in enhanced phosphorus retention deeper into the sediments (Danielsson et al., 2018, Korppoo et al., 2012). Benthic fauna increases the amount of iron oxyhydroxides and hence the ability of these sediments to bind phosphorus (Lewandowski et al., 2007; Norkko et al., 2012). Hupfer et al. (2019) studied the effect of bioturbation in short-term and long-term experiments. It was found that larvae density was a controlling factor for P-uptake and bioirrigation by worms resulted in sorption of SRP from the overlying water with uptake rates becoming similar to the sediments without larvae at later stages of the experiment indicating increased saturation or exhaustion of P binding sites. The amount of P released during anoxia in long-term experiment was less than the amount of P taken up during the oxic phase indicating a permanent uptake of P in the sediment. (Hupfer et al., 2019). Reactive Fe bound pools (Fe oxyhydroxide and associated P) have been observed in layers deep (15-20cm) of the sediments in Gippsland Lakes demonstrating potential of burrow formation by *C. capitata* (Scicluna et al., 2015). Worm activities tend to alter biogeochemical processes at the sediment water interface having implications for the sedimentary benthic P fluxes (Kristensen et al., 2012). Benthic fauna have also been reported to contribute to the phosphorus release from sediments through mixing and irrigation of the sediments (Leote & Epping, 2015). Bioirrigation associated solute distribution together with oxygen supply encourage remineralisation of organic matter in deeper sediment layers (Wrede et al., 2017). Gautreau et al. (2020) highlighted the effect of benthic activity on P mobilization demonstrating transfer of oxygen into burrows through ventilation leading to enhanced P uptake and anoxic conditions producing high benthic P fluxes. Based on past studies, bioturbation impacts on biogeochemical processes in relation to phosphorus cycling occurring in lakes can be illustrated through a schematic diagram (Fig. 1.1).

The quantification of benthic P uptake and fluxes is critical to understand the extent of implications of bioirrigation on sediment biogeochemistry (Kristensen et al., 2012; Roskosch et al., 2012). Considerable work has been done in past to interpret/quantify the different aspects (influences of soil mechanistic, type of reworking, type of burrows, ventilation patterns etc.) linked with bioturbation (Hölker et al., 2015; Sturdivant & Shimizu, 2017). However, the impact of bioturbators on internal

loading of phosphorus from the sediment to the surface water is yet to be clearly quantified and represents a major factor that controls lakes trophic state (Parsons et al., 2017; Wang et al., 2018). Identification and quantification of the solid phase P fractions present in the sediment represent an alternative to quantify the impacts of benthic fauna.

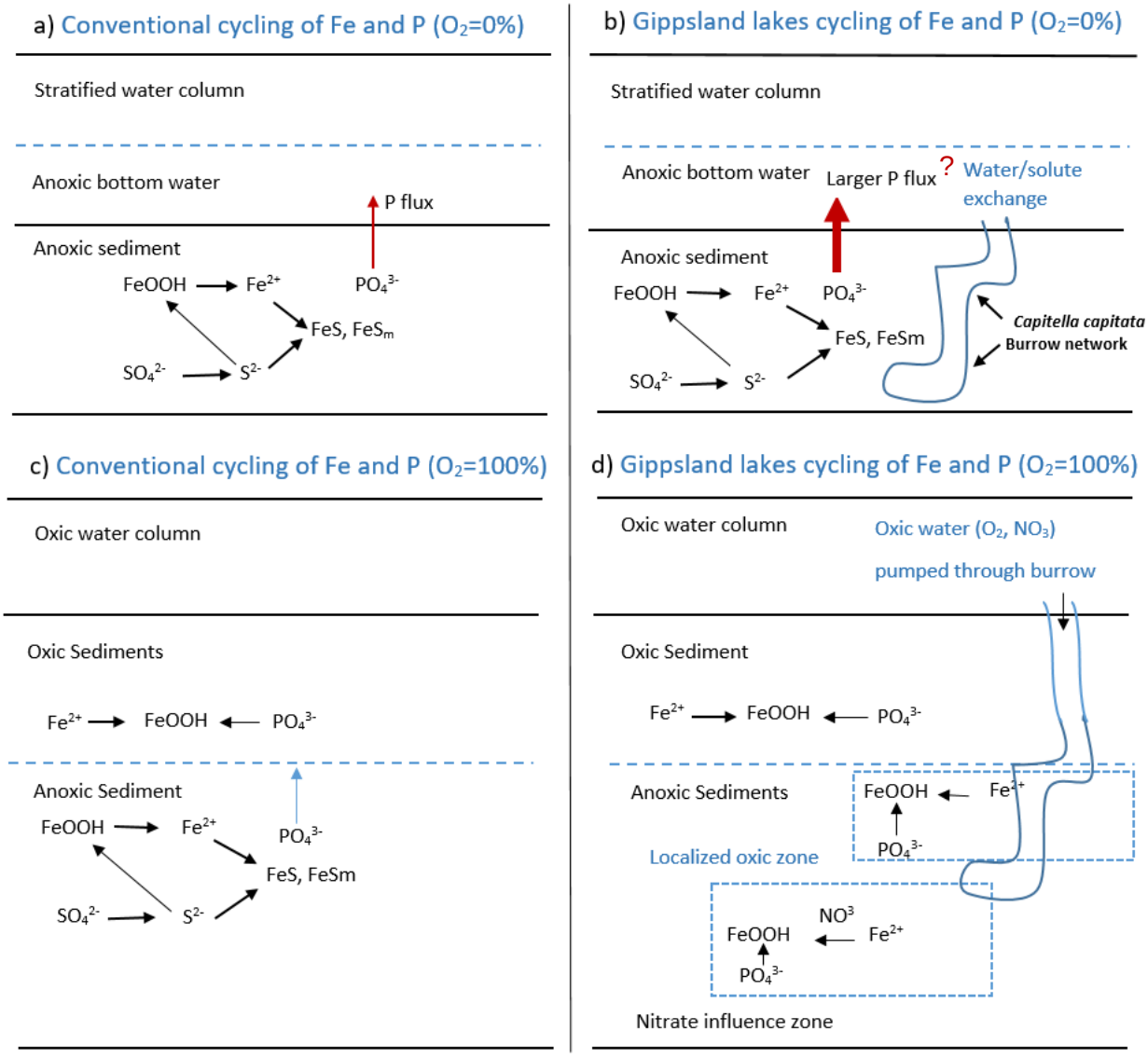

Figure 1.1. Schematic diagram illustrating the mechanism by which bioirrigation may alter cycling of Fe and P, (a) under anoxic bottom water conditions, (b) anoxic in worms presence causing bioirrigation, (c) cycling of Fe and P under oxic conditions, (d) oxic in presence of worms

1.3. Sedimentary Fe and P extractions

Sequential sediment extraction (SEDEX) is one of the most common approach to better understand the cycling of P in sediments by quantifying the various solid phase forms of iron (Fe) and phosphorous (P) in sediments. The method for the sequential extraction of different forms of sediment Fe and P originated from soil extraction. Extraction is basically a destructive approach that uses an extractant capable of breaking chemical bonds of the target substance for their identification (Rennert, 2019). The purpose of sequential extractions was to quantify discrete chemical or mineralogical compounds in series and each extraction uses specific reagents and procedures (Wang et al., 2013). The most popular example of early extraction schemes was the one proposed by Chang and Jackson in 1957. However, to date, no single standardised scheme is available for determination of Fe and P

fractionation. Since then several extraction schemes have been developed to provide more detailed insight into the speciation of Fe and P while pointing out the shortcomings of previous extraction procedures (Thompson et al., 2019). The most commonly used methods in today's literature include P extractions by Ruttenberg (1992) and Fe extractions by Poulton and Canfield (2005) (Hermans et al., 2019; Liu et al., 2020; Xiong et al., 2019). Poulton and Canfield (2005) extraction scheme for Fe and Rutternberg (1992) extraction scheme for P are the most commonly used schemes when a complete spectrum of Fe and P fractions in sediments is to be quantified. The Ruttenberg (1992) scheme quantifies five operationally-defined P fractions: exchangeable P, Iron oxyhydroxide bound P, authigenic P, $CaCO_3$-bound P and detrital P and organic P (Ruttenberg, 1992). Poulton and Canfield (2005) developed a sequential extraction procedure for Fe, which targets reactive ferrihydrite as well as poorly reactive magnetite and crystalline hematite.

I conducted a preliminary experiment on sediment slurries using the existing sequential extraction schemes to understand the different iron and phosphorus pools present in Lake King North (LKN) sediments, their dynamics and establishment of modified sequential extraction schemes for Fe and P speciation. The purpose of this experiment was to develop Fe and P sequential extraction schemes suitable for LKN sediments in order to help identify the various Fe and P pools present within the sediments. The P fraction scheme used in the laboratory experiment is based on a merger of two previous extraction methods by Ruttenberg (1992) and Psenner et al. (1988) with an additional ascorbate extraction step. The Fe extraction scheme is the same as one adopted by Hermans et al. (2021) apart from the ascorbate extraction step which was added to represent ferrihydrite as per Kostka and Luther (1994).The sequential extraction scheme used in the study for sedimentary iron and phosphorus fraction (Table 1.1).

Table 1.1. Sequential extraction schemes for P and Fe

Target P phase	**Extractant**	**Time**
Exchangeable P	1 M $MgCl_2$ (Magnesium chloride)	2 hours
Ferrihydrite	.057M Ascorbic acid/.17 sodium citrate/ .6 sodium bicarbonate	24 hours
Reactive Fe-bound P	CDB (Dithionite) buffered to pH 7.5	8 hours
SRP/NRP	1 M NaOH (Sodium hydroxide)	24 hours
Calcium phosphates	1M HCl (Hydrochloric acid)	24 hours
Organic P	1M HCl after ashing at 550 ^oC	24 hours
Target Fe phase	**Extractant**	**Time**
Ferrihydrite	.057M Ascorbic acid/.17 sodium citrate/ .6 sodium bicarbonate	24 hours
Labile Fe(III) oxides and FeS	1M HCl	4hours
Crystalline Fe oxides	CDB buffered to pH 7.5	8 hours
Magnetite	0.2 M Oxalate	6 hours
Pyrite	Nitric acid, HNO_3 (65-70%)	2 hours

Phosphorus is known to have high affinity for iron oxides and its uptake by Fe(III) has been extensively studied. The second extraction step of using ascorbate is based on Scicluna et al. (2015), considering ascorbate gives an interference free approach and provides excellent recovery. In Fe extraction, ascorbate as an extractant was used for extracting ferrihydrite in sediment extractions as ascorbate extractable Fe is known to represent the most readily bioavailable form of Fe (III) oxyhydroxides (Kostka and Luther III 1994). Ascorbate extraction was followed with HCl step as the acidic treatment can achieve complete recovery of Fe (II) from FeS and $FeCO_3$ and extraction of Fe(III) as labile iron oxides. All steps in Fe and P extractions until dithionite extraction (CDB) were carried out in a completely argon purged environment to prevent reoxidation of Fe (II) and subsequent P adsorption. The Fe and P fraction scheme used in the field data analysis of this study was based on Scicluna et al. (2015).

1.4. The Gippsland Lakes

The Gippsland Lakes are an estuarine system that contains a variety of algal species and has suffered recurring algal blooms in the past after significant rain events or rivers discharge (Cook et al., 2010). Gippsland lakes water quality depends on the competing influences of river flows and marine inputs introducing large quantities of dissolved organic matter. The system has experienced large interannual flow variations (flood and drought). Several key knowledge gaps exist around P dynamics and blooms in the system. The sediment P dynamics studied over a bloom period showed an enhanced release of P from the sediment, which was hypothesised to be driven by faunal irrigation. However, the longer term P dynamics and how this accumulates are poorly understood. Further details of these knowledge gaps and related literature are given in each chapter introduction.

1.5. Research aims, hypotheses and thesis structure

The research presented in this PhD thesis aimed at studying the estuarine biogeochemistry of phosphorus. Estuarine P dynamics can be studied through either in-situ field investigations, laboratory experiments or biogeochemical modelling. The most commonly used in-situ approach includes examining the relationship between variables representative of P loading and variables that respond to the change in conditions. The estuarine biogeochemical study through field monitoring may include either temporal monitoring, spatial monitoring or both. Laboratory experiments mimicking real field conditions under controlled environment can simplify and define complex P cycles of estuarine systems with certainty in a relatively short span of time. Modelling with adequate biogeochemical processes can help us conceptualise and test our understanding of biogeochemical processes as well as give new insights into how complex factors interact to control biogeochemical outcomes. Accordingly, this research encompasses all three approaches and the objectives were to:

(1) study the iron phosphorus dynamics within the Gippsland lakes: long-term data monitoring to investigate the sediment P dynamics over wet and dry periods

(2) investigate the influence of altering oxygen conditions and *C. capitata* activity on sediment biogeochemistry

(3) explore the interaction between bioirrigation and phosphorus release and storage within the sediment through application of a one-dimensional model

The major hypotheses driving this research were:

(1) to investigate whether P accumulation in the Gippsland Lakes sediments is derived from inflow events comprising large inputs or, alternatively, from gradual uptake over time with P acquired from water column and organic matter

(2) worm presence will lead to an enhanced P flux out of the sediment as a combined effect of bioirrigation and anoxia under cyclic hypoxic-anoxic conditions

(3) if a classical 1D model can capture faunal related factors that control the dynamics of iron oxyhydroxide associated P within the sediment

Chapter two addresses the objective (1), by monitoring the Fe and P pools present in the Gippsland lakes system to identify the factors responsible for recharge in these pools over short and long-term. The chapter gives a detailed description of the study site chosen for this research (The Gippsland Lakes). A decade long data of water quality parameters was linked with river flow to interpolate variables responsible for changes in the sediment Fe bound P fraction.

Chapter Three addresses research objective (2) using microcosms under a controlled environment. It is well known that the pumping activity of benthic fauna enhances the transport of solutes between the sediment and the overlying water. It was hypothesized that cyclic hypoxic-anoxic condition will induce stress in fauna to pump harder and the irrigation activity may play a role in enhancing sediment P release. A modified extraction scheme developed from the slurry work provided the way for sequential Fe and P extractions and water-column samples collection during the experiment for Fe and P measurements. The data analysis helped identifying the role of *C. capitata* in amplifying P cycling within the sediments.

Chapter Four examined the applicability of a classical 1D model as a tool to interpret effects of faunal activity on P cycling within the sediments. The model design, porosity profile, boundary conditions, physical parameters and environmental parameters were harmonised with laboratory experiment conditions to identify if a 1D model will be able to reproduce the laboratory outcomes. The 1D model failed to capture precise/realistic description of complex field phenomena since it lacks lateral heterogeneity and adopts relatively simple parameterizations.

In chapter Five, the key outcomes from chapter 2 & 3 were examined and combined to establish data links, constitute synthetic discussion and draw conclusions. The implications of modelling approach used in chapter 4 as well as the limitations identified for 1D model were conveyed. Additionally, reflections of this study and directions for future research work were presented.

1.6. References

Belley, R., Snelgrove, P. V., Archambault, P., & Juniper, S. K. (2016). Environmental Drivers of Benthic Flux Variation and Ecosystem Functioning in Salish Sea and Northeast Pacific Sediments. *PLOS ONE, 11*(3), e0151110. doi:https://doi.org/10.1371/journal.pone.0151110

Cai, O., Xiong, Y., Yang, H., Liu, J., & Wang, H. (2020). Phosphorus transformation under the influence of aluminum, organic carbon, and dissolved oxygen at the water-sediment interface: A simulative study. *Frontiers of Environmental Science & Engineering, 14*(3), 50. doi:https://doi.org/10.1007/s11783-020-1227-z

Canfield, D. E., Kristensen, E., & Thamdrup, B. (2005). Aquatic geomicrobiology. *Adv Mar Biol, 48*, 1-599. doi:https://doi.org/10.1016/s0065-2881(05)48017-7

Carstensen, J., Conley, D. J., Bonsdorff, E., Gustafsson, B. G., Hietanen, S., Janas, U., . . . Voss, M. (2014). Hypoxia in the Baltic Sea: Biogeochemical Cycles, Benthic Fauna, and Management. *AMBIO, 43*(1), 26-36. doi:https://doi.org/10.1007/s13280-013-0474-7

Chen, M., Ding, S., Liu, L., Xu, D., Han, C., & Zhang, C. (2015). Iron-coupled inactivation of phosphorus in sediments by macrozoobenthos (chironomid larvae) bioturbation: Evidences from high-resolution dynamic measurements. *Environmental Pollution, 204*, 241-247. doi:https://doi.org/10.1016/j.envpol.2015.04.031

Colborne, S. F., Maguire, T. J., Mayer, B., Nightingale, M., Enns, G. E., Fisk, A. T., . . . Mundle, S. O. C. (2019). Water and sediment as sources of phosphate in aquatic ecosystems: The Detroit River and its role in the Laurentian Great Lakes. *Sci Total Environ, 647*, 1594-1603. doi: https://doi.org/10.1016/j.scitotenv.2018.08.029

Cook, P. L. M., Holland, D. P., & Longmore, A. R. (2010). Effect of a flood event on the dynamics of phytoplankton and biogeochemistry in a large temperate Australian lagoon. *Limnology and Oceanography, 55*(3), 1123-1133. doi:https://doi.org/10.4319/lo.2010.55.3.1123

Danielsson, Å., Rahm, L., Brüchert, V., Bonaglia, S., Raymond, C., Svensson, O., Gunnarsson, J. (2018). Effects of re-oxygenation and bioturbation by the polychaete Marenzelleria arctia on phosphorus, iron and manganese dynamics in Baltic Sea sediments. *Boreal Environment Research, 23*, 15-23. https://www.diva-portal.org/smash/get/diva2:1181292/FULLTEXT01.pdf

Gautreau, E., Volatier, L., Nogaro, G., Gouze, E., & Mermillod-Blondin, F. (2020). The influence of bioturbation and water column oxygenation on nutrient recycling in reservoir sediments. *Hydrobiologia, 847*(4), 1027-1040. doi:https://doi.org/10.1007/s10750-019-04166-0

Grabowski, R. C., Droppo, I. G., & Wharton, G. (2011). Erodibility of cohesive sediment: The importance of sediment properties. *Earth-Science Reviews, 105*(3), 101-120. doi:https://doi.org/10.1016/j.earscirev.2011.01.008

Hartzell, J.L., Jordan, T.E. & Cornwell, J.C. (2010). Phosphorus Burial in Sediments Along the Salinity Gradient of the Patuxent River, a Subestuary of the Chesapeake Bay (USA). *Estuaries and Coasts 33*, 92-106.

doi:https://doi.org/10.1007/s12237-009-9232-2

Hallegraeff, G. M., Anderson, D.M., Belin, C. et al. (2021). Perceived global increase in algal blooms is attributable to intensified monitoring and emerging bloom impacts. *Commun Earth Environ, 2*, 117.

doi:https://doi.org/10.1038/s43247-021-00178-8

Hermans, M., Lenstra, W. K., van Helmond, N. A. G. M., Behrends, T., Egger, M., Séguret, M. J. M., . . . Slomp, C. P. (2019). Impact of natural re-oxygenation on the sediment dynamics of manganese, iron and phosphorus in a euxinic Baltic Sea basin. *Geochimica et Cosmochimica Acta, 246*, 174-196. doi:https://doi.org/10.1016/j.gca.2018.11.033

Hölker, F., Vanni, M., Kuiper, J., Meile, C., Grossart, H.-P., Stief, P., . . . Lewandowski, J. (2015). Tube-dwelling invertebrates: Tiny ecosystem engineers have large effects in lake ecosystems. *Ecological Monographs, 85*, 333–351. doi:https://doi.org/10.1890/14-1160.1

Howarth, R. W., Chan, F., Swaney, D. P., Marino, R. M., & Hayn, M. (2021). Role of external inputs of nutrients to aquatic ecosystems in determining prevalence of nitrogen vs. phosphorus limitation of net primary productivity. *Biogeochemistry, 154*(2), 293-306. doi:https://doi.org/10.1007/s10533-021-00765-z

Hupfer, M., Jordan, S., Herzog, C., Ebeling, C., Ladwig, R., Rothe, M., & Lewandowski, J. (2019). Chironomid larvae enhance phosphorus burial in lake sediments: Insights from long and short-term experiments. *Science of Total Environment*, 663, 254-264. doi:https://doi.org/10.1016/j.scitotenv.2019.01.274

Hyacinthe, C., Bonneville, S. C., & Van Cappellen, P. (2006). Reactive iron(III) in sediments: Chemical versus microbial extractions. *Geochimica et Cosmochimica Acta, 70*, 4166-4180. doi:https://doi.org/10.1016/j.gca.2006.05.018

Jensen, H. S., Mortensen, P. B., Andersen, F. Ø., Rasmussen, E. K., & Jensen, A. (1995). Phosphorus cycling in a coastal marine sediment, Aarhus Bay, Denmark. *Limnology and Oceanography, 40*, 908-917. doi:https://doi.org/10.4319/lo.1995.40.5.0908

Jordan, T. E., Cornwell, J. C., Boynton, W. R., & Anderson, J. T. (2008). Changes in phosphorus biogeochemistry along an estuarine salinity gradient: The iron conveyer belt. *Limnology and Oceanography, 53*(1), 172-184. doi:https://doi.org/10.4319/lo.2008.53.1.0172

Korppoo, M., Lukkari, K., Järvelä, J., Leivuori, M., Karvonen, T., & Stipa, T. (2012). Phosphorus release and sediment geochemistry in a low-salinity water bay of the Gulf of Finland. *Boreal Environment Research*, 17(17), 237. Retrieved from: https://helda.helsinki.fi/bitstream/handle/10138/229887/ber17-3-4-237.pdf

Kostka, J. E., & Luther, G. W. (1994). Partitioning and speciation of solid phase iron in saltmarsh sediments. *Geochimica et Cosmochimica Acta, 58*(7), 1701-1710. doi:https://doi.org/10.1016/0016-7037(94)90531-2

Kristensen, E., Penha-Lopes, G., Delefosse, M., Valdemarsen, T., Organo Quintana, C., & Banta, G. (2012). What is bioturbation? Need for a precise definition for fauna in aquatic science. *Marine Ecology Progress Series, 446*, 285-302. doi:https://doi.org/10.3354/meps09506

Leote, C., & Epping, E. H. G. (2015). Sediment–water exchange of nutrients in the Marsdiep basin, western Wadden Sea: Phosphorus limitation induced by a controlled release? *Continental Shelf Research, 92*, 44-58. doi:https://doi.org/10.1016/j.csr.2014.11.007

Lewandowski, J., Laskov, C., & Hupfer, M. (2007). The relationship between Chironomus plumosus burrows and the spatial distribution of pore-water phosphate, iron and ammonium in lake sediments. *Freshwater Biology, 52*(2), 331-343. doi:https://doi.org/10.1111/j.1365-2427.2006.01702.x

Li, J., Ianaiev, V., Huff, A., Zalusky, J., Ozersky, T., & Katsev, S. (2021). Benthic invaders control the phosphorus cycle in the world’s largest freshwater ecosystem. *Proceedings of the National Academy of Sciences, 118*(6), e2008223118. doi:https://doi.org/10.1073/pnas.2008223118

Liu, J., Krom, M. D., Ran, X., Zang, J., Liu, J., Yao, Q., & Yu, Z. (2020). Sedimentary phosphorus cycling and budget in the seasonally hypoxic coastal area of Changjiang Estuary. *Science of The Total Environment, 713*, 136389. doi:https://doi.org/10.1016/j.scitotenv.2019.136389

Markovic, S., Blukacz-Richards, A., & Dittrich, M. (2020). Speciation and bioavailability of particulate phosphorus in forested karst watersheds of southern Ontario during rain events. *Journal of Great Lakes Research, 46*. doi:https://doi.org/10.1016/j.jglr.2020.05.001

Norkko, J., Reed, D. C., Timmermann, K., Norkko, A., Gustafsson, B. G., Bonsdorff, E., . . . Conley, D. J. (2012). A welcome can of worms? Hypoxia mitigation by an invasive species. *Global Change Biology, 18*(2), 422-434. doi:https://doi.org/10.1111/j.1365-2486.2011.02513.x

O'Loughlin, E., Gorski, C., Flynn, T., & Scherer, M. (2019). Electron Donor Utilization and Secondary Mineral Formation during the Bioreduction of Lepidocrocite by Shewanella putrefaciens CN32. *Minerals, 9*, 434. doi:https://doi.org/10.3390/min9070434

Quintana, C., Tang, M., & Kristensen, E. (2007). Simultaneous study of particle reworking, irrigation transport and reaction rates in sediment bioturbated by the polychaetes Heteromastus and Marenzelleria. *Journal of Experimental Marine Biology and Ecology*, 392-406. doi:https://doi.org/10.1016/j.jembe.2007.08.015

Parsons, C., Rezanezhad, F., W. O'Connell, D., & Van Cappellen, P. (2017). Sediment phosphorus speciation and mobility under dynamic redox conditions. *Biogeosciences,* 14(14), 3585-3602. doi:https://doi.org/10.5194/bg-14-3585-2017

Petkuviene, J., Zilius, M., Lubiene, I., Ruginis, T., Giordani, G., Razinkovas-Baziukas, A., & Bartoli, M. (2016). Phosphorus Cycling in a Freshwater Estuary Impacted by Cyanobacterial Blooms. *Estuaries and Coasts, 39*(5), 1386-1402. doi:https://doi.org/10.1007/s12237-016-0078-0

Pilskaln, C., Anderson, D., McGillicuddy, D., Keafer, B. A., Hayashi, K., & Norton, K. (2014). Spatial and temporal variability of Alexandrium cyst fluxes in the Gulf of Maine: Relationship to seasonal particle export and resuspension. *Deep-sea research*, 103, 40–54. doi:https://doi.org/10.1016/j.dsr2.2012.11.001

Psenner, R., Boström, B., Dinka, M., Pettersson, K., & Puckso, R. (1988). Fractionation of phosphorus in suspended matter and sediment. *Arch Hydrobiol Beih Ergeb Limnol, 30*, 98-103. Retrieved from: https://aslopubs.onlinelibrary.wiley.com/doi/pdf/10.4319/lom.2007.5.433

Reed, D. C., Slomp, C. P., & Gustafsson, B. G. (2011). Sedimentary phosphorus dynamics and the evolution of bottom-water hypoxia: A coupled benthic–pelagic model of a coastal system. *Limnology and Oceanography, 56*(3), 1075-1092. doi:https://doi.org/10.4319/lo.2011.56.3.1075

Rennert, T. (2019). Wet-chemical extractions to characterise pedogenic Al and Fe species – a critical review. *Soil Research, 57*, 1-16. doi:https://doi.org/10.1071/SR18299

Robson, B. J. (2014). State of the art in modelling of phosphorus in aquatic systems: Review, criticisms and commentary. *Environmental Modelling & Software, 61*, 339-359. doi:https://doi.org/10.1016/j.envsoft.2014.01.012

Roskosch, A., Hette, N., Hupfer, M., & Lewandowski, J. (2012). Alteration of Chironomus plumosus ventilation activity and bioirrigation-mediated benthic fluxes by changes in temperature, oxygen concentration, and seasonal variations. *Freshwater Science, 31*(2), 269-281. doi:https://doi.org/10.1899/11-043.1

Ruttenberg, K. C. (1992). Development of a sequential extraction method for different forms of phosphorus in marine sediments. *Limnology and Oceanography, 37*(7), 1460-1482. doi:https://doi.org/10.4319/lo.1992.37.7.1460

Schulz, H., & Zabel, M. (2006). Marine Geochemistry, *2nd revised, updated and extended edition*.

Scicluna, T. R., Woodland, R. J., Zhu, Y., Grace, M. R., & Cook, P. L. M. (2015). Deep dynamic pools of phosphorus in the sediment of a temperate lagoon with recurring blooms of diazotrophic cyanobacteria. *Limnology and Oceanography, 60*(6), 2185-2196. doi:https://doi.org/10.1002/lno.10162

Simpson, Z. P., McDowell, R. W., & Condron, L. M. (2019). Phosphorus attenuation in streams by water-column geochemistry and benthic sediment reactive iron. *Biogeosciences Discuss., 2019*, 1-35. doi:https://doi.org/10.5194/bg-2019-400

Søndergaard, M., Jensen, J. P., & Jeppesen, E. (2003). Role of sediment and internal loading of phosphorus in shallow lakes. *Hydrobiologia, 506*(1), 135-145. doi:https://doi.org/10.1023/B:HYDR.0000008611.12704.dd

Sturdivant, S. K., & Shimizu, M. S. (2017). In situ organism-sediment interactions: Bioturbation and biogeochemistry in a highly depositional estuary. *PLOS ONE, 12*(11), e0187800. doi:https://doi.org/10.1371/journal.pone.0187800

Suzzi, A. L., Gaston, T. F., McKenzie, L., Mazumder, D., & Huggett, M. J. (2022). Tracking the impacts of nutrient inputs on estuary ecosystem function. *Science of The Total Environment, 811*, 152405. doi:https://doi.org/10.1016/j.scitotenv.2021.152405

Tao, W., Niu, L., Dong, Y., Fu, T., & Lou, Q. (2021). Nutrient Pollution and Its Dynamic Source-Sink Pattern in the Pearl River Estuary (South China). *Frontiers in Marine Science, 8*. doi:https://doi.org/10.3389/fmars.2021.713907

Thompson, J., Poulton, S. W., Guilbaud, R., Doyle, K. A., Reid, S., & Krom, M. D. (2019). Development of a modified SEDEX phosphorus speciation method for ancient rocks and modern iron-rich sediments. *Chemical Geology, 524*, 383-393. doi:https://doi.org/10.1016/j.chemgeo.2019.07.003

Thompson, S. K., & Cotner, J. B. (2018). Bioavailability of Dissolved Organic Phosphorus in Temperate Lakes. *Frontiers in Environmental Science*, 6, 62. doi:https://doi.org/10.3389/fenvs.2018.00062

Wang, C., Zhang, Y., Li, H., & Morrison, R. J. (2013). Sequential extraction procedures for the determination of phosphorus forms in sediment. *Limnology, 14*(2), 147-157. doi:https://doi.org/10.1007/s10201-012-0397-1

Wang, F., Cheng, P., Chen, N., & Kuo, Y.-M. (2021). Tidal driven nutrient exchange between mangroves and estuary reveals a dynamic source-sink pattern. *Chemosphere, 270*, 128665. doi:https://doi.org/10.1016/j.chemosphere.2020.128665

Wang, J., Chen, J., Guo, J., Sun, Q., & Haiquan, Y. (2018). Combined Fe/P and Fe/S ratios as a practicable index for estimating the release potential of internal-P in freshwater sediment. *Environmental Science and Pollution Research, 25*, 10740–10751. doi:https://doi.org/10.1007/s11356-018-1373-z

Wang, Z., Huang, S., & Li, D. (2019). Decomposition of cyanobacterial bloom contributes to the formation and distribution of iron-bound phosphorus (Fe-P): Insight for cycling mechanism of internal phosphorus loading. *Science of The Total Environment, 652*, 696-708. doi:https://doi.org/10.1016/j.scitotenv.2018.10.260

Weber, K., Achenbach, L., & Coates, J. (2006). Microorganisms Pumping Iron: Anaerobic Microbial Iron Oxidation and Reduction. *Nature Reviews Microbiology, 4, 752-764.* doi:https://doi.org/10.1038/nrmicro1490

Wei, X., Garnier, J., Thieu, V., Passy, P., Le Gendre, R., Billen, G., . . . Laruelle, G. G. (2022). Nutrient transport and transformation in macrotidal estuaries of the French Atlantic coast: a

modeling approach using the Carbon-Generic Estuarine Model. *Biogeosciences, 19*(3), 931-955.
doi:https://doi.org/10.5194/bg-19-931-2022

Withers, P. J. A., & Jarvie, H. P. (2008). Delivery and cycling of phosphorus in rivers: A review. *Science of The Total Environment, 400*(1), 379-395.
doi:https://doi.org/10.1016/j.scitotenv.2008.08.002

Wrede, A., Dannheim, J., Gutow, L., & Brey, T. (2017). Who really matters: Influence of German Bight key bioturbators on biogeochemical cycling and sediment turnover. *Journal of Experimental Marine Biology and Ecology, 488*, 92-101.
doi:https://doi.org/10.1016/j.jembe.2017.01.001

Xiong, Y., Guilbaud, R., Peacock, C. L., Cox, R. P., Canfield, D. E., Krom, M. D., & Poulton, S. W. (2019). Phosphorus cycling in Lake Cadagno, Switzerland: A low sulfate euxinic ocean analogue. *Geochimica et Cosmochimica Acta, 251*, 116-135.
doi:https://doi.org/10.1016/j.gca.2019.02.011

Xu, H., McCarthy, M., Paerl, H., Brookes, J., Zhu, G., Hall, N., . . . Gardner, W. (2021). Contributions of external nutrient loading and internal cycling to cyanobacterial bloom dynamics in Lake Taihu, China: Implications for nutrient management. *Limnology and Oceanography, 66*.
doi:https://doi.org/10.1002/lno.11700

Yuan, Z., Jiang, S., Sheng, H., Liu, X., Hua, H., Liu, X., & Zhang, Y. (2018). Human Perturbation of the Global Phosphorus Cycle: Changes and Consequences. *Environmental Science & Technology, 52*(5), 2438-2450.
doi:https://doi.org/10.1021/acs.est.7b03910

Zhao, Y., Wu, S., Yu, M., Zhang, Z., Wang, X., Zhang, S., & Wang, G. (2021). Seasonal iron-sulfur interactions and the stimulated phosphorus mobilization in freshwater lake sediments. *Science of The Total Environment, 768*, 144336.
doi:https://doi.org/10.1016/j.scitotenv.2020.144336

Zou, R., Wu, Z., Zhao, L., Elser, J. J., Yu, Y., Chen, Y., & Liu, Y. (2020). Seasonal algal blooms support sediment release of phosphorus via positive feedback in a eutrophic lake: Insights from a nutrient flux tracking modeling. *Ecological Modelling, 416*, 108881.
doi:https://doi.org/10.1016/j.ecolmodel.2019.108881

2. Iron phosphorus dynamics within the Gippsland Lakes: long-term data monitoring to investigate water column & sediment surface interactions

2.1. Abstract

An important ecological feature of coastal lagoons systems is their rapid response to the changes in the environment, which makes them among the most complex water systems. The uptake and release of phosphorus by the sediments in a lagoon system can significantly alter water column quality and act as a control on the formation of algal blooms. The Gippsland Lakes system has been studied in the past and is known for phosphorus release on the onset of anoxia, however, the recharge mechanism of phosphorus in the sediments is still not clear. A decade long dataset of water quality parameters and river flow was linked with the dynamics of P within the sediment to gain insights into the likely controls of P within the Gippsland Lakes sediment. The lake system typically experienced the highest inflows in winter leading to stratification and lower DO in the winter and spring although no distinct seasonal patterns were observed. Ascorbate extractable P (Asc-P), representing the FeOOH bound P pool turned out to be the most dynamic P fraction accounting for the major changes in the sediment P pool over the past decade. Even during periods of prolonged oxygenation, there was no accumulation of the sediment Asc-P fraction. Statistical analysis showed a positive association of the Asc-P fraction with bottom water TP and low bottom water DO with river inflow. This indicates that the delivery of new Fe and P is a major factor controlling the sediment phosphorus fractions in the Gippsland Lakes. These results suggest that the Gippsland Lakes respond primarily to the variations in P inputs through inflows, rather than long-term oxygenation for P build-up as previously hypothesized. The result also demonstrate that the sediment surface FRP (porewater), bottom water TP, dissolved oxygen and river inflow are key variables in the Gippsland Lakes that indicate systems response to external variables.

2.2. Introduction

Estuarine systems compared to other coastal systems have a greater risk of having harmful algal blooms (HAB) since they receive high nutrient loads from river inflows. Their shallow nature, high light penetration, salt or temperature stratification and nutrient availability result in high phytoplankton productivity (Carrasco et al., 2020). Phosphorus (P) acts as a limiting nutrient for growth in estuaries where cyanobacteria are N-fixers (Wang et al., 2021; Zhang et al., 2018). A large number of socioeconomic indicators are factors for external P loading into the water system. The P concentrations of the water system are controlled through a number of potential drivers including surface water Fe concentrations (Huser et al., 2018; Vystavna et al., 2017). The phosphorus in the water column sorbs onto ironoxyhydroxides which then 'floc' out resulting in an Fe bound P rich oxic sediment surface layer which may become available to algae/bacteria on the onset of hypoxia (Korppoo et al., 2012; Tessin et al., 2020). An increase in P flux (mostly Fe-P) from the sediment with an increase in hypoxia was found in the Changjiang estuary using sequential P extraction of sediment and kinetic diagenetic modelling (Liu et al., 2020). A global database study of estuarine systems (n=227) for sediment-water fluxes indicated highest supply of P demand by phytoplankton from the sediments in temperate latitude systems with measurements ranging from 17-100% (Boynton et al., 2017). Long-term monitoring presents an opportunity to understand sediment P response in relation to potential eutrophication related variables such as salinity, dissolved oxygen, TN:TP, temperature and chlorophyll (Chl-*a*) in aquatic systems where the relative importance of these variables is not well understood over long timescales (Giudice et al., 2018; Dove & Chapra, 2015; Randall et al., 2019).

Thamdrup showed a clear seasonal cycling of Fe in the fine-grained coastal marine sediment of Aarhus bay during 1991-1992. Solid phase analyses indicated a distribution of iron oxyhydroxide in the upper 2-4 cm. He observed that the exhaustion of the FeOOH pool in response to bottom water oxygen depletion was unlikely since the turnover time of reactive iron was estimated to be one hundred days. The increase in SO_4^{2-} reduction rate during summer was the main driver behind the compression of Fe oxide zones towards the sediment surface (Thamdrup et al., 1994). Jensen investigated seasonal variation in sedimentary P pools during the same period in Aarhus Bay and found fluxes of P associated with the labile Fe Pool. A negative correlation existed between the Fe bound P and P fluxes from the sediment. The Fe bound P pool was the most dynamic pool in the sediment showing an increase from spring to autumn after which half of the annual P release occurred (Jensen et al., 1995). In systems like the Gippsland lakes, where interannual flow variability exceeds annual variability, the dynamics and controls of sediment P has not been fully explored.

Sequential extractions are the most common approach to quantify the different sedimentary forms of Fe and P. It is generally accepted that P is stored associated with FeOOH. The Poulton and Canfield (2005) extraction scheme for Fe and the Ruttenberg (1992) extraction scheme for P are the most commonly used methods when a complete spectrum of Fe and P fractions in sediments is to be quantified. Ascorbate is known for extracting ferrihydrite in sediment extractions and ascorbate extractable Fe represents the most readily bioavailable form of Fe(III) as oxyhydroxides (Kostka & Luther, 1994). Determination of P with ascorbate as an extractant is suggested to represent

ferrihydrite with maximum sorption sites occupied by phosphate (Zhang & Lanning, 2018). Ascorbate extraction can provide useful information on the potential mobility of P species in iron rich sediments through excellent recovery and an interference-free method (Anschutz et al., 1998).

The Gippsland Lakes have suffered recurring algal blooms following bottom water anoxia and hypoxia. Extremely high sedimentary phosphorus fluxes resulting from flood events have been reported in the lake system, fuelling summer algal blooms (Cook et al., 2010). The reports on blooms and flood events for the lake system suggest an algal bloom roughly once a decade dating back to 1965 when the first bloom after a heavy rainfall season was recorded. Lake King has suffered *Nodularia spumigena* blooms in 1974, 1987, 1989, 1996, 2011 and 2022. Vertical stratification of the lake based on differences in salt concentrations allow for rapid algal growth. While previous work has captured a decrease in the sediment Asc-P pool and associated sediment P release during the last *Nodularia spumigena* bloom, the mechanism and timescale of sediment P recharge is not clear (Scicluna et al., 2015). Probable mechanisms include a gradual recharge during oxic conditions, possibly enhanced by fauna. Under this scenario, Asc P accumulates within the sediment, with P being sourced from both the water column and degradation of organic matter. We would expect to see an accumulation of Asc-P over time and in particular during oxic periods. Alternatively, Asc P accumulation may be controlled by the delivery of fresh Fe and or P. Under this scenario, we expect to see a more rapid accumulation of P, associated with inflow events, and indicators of P loading such as chl-*a* and TP in the water column. The time series presented here allows us to better understand the dynamics of P within the sediment and gain insights into the likely controls of Asc-P within the sediment.

2.3. Materials and methods

2.3.1. Study area

The Gippsland Lakes are part of Australia's largest estuary with an area over 360 square km comprising three large water bodies- Lake Wellington, Lake Victoria and Lake King. The Gippsland Lakes are connected to the ocean through an artificial entrance and receives varying degree of freshwater inflows mainly from Mitchell, Tambo, Thomson and Latrobe rivers. The Gippsland Lakes water quality depends on the competing influences of river flows, marine inputs and vertical salt stratification. The shallow system also experiences episodic flood events carrying loads of nutrients into system. The lake system has suffered algal blooms in the past after significant rain event or river discharge, which introduces large quantities of dissolved organic matter.

2.3.2. Sediment core collection

A site (37° 87' 56'' S, 147° 75' 72" E) in northern Lake King (LKN, Fig. 1) was selected for long-term monitoring as the site has been identified as the epicentre of *Nodularia spumigena* blooms in the past (Woodland & Cook, 2014). Sediment cores were collected using a 29cm x 6.6cm transparent polycarbonate cylinder from Lake King, Victoria, Australia. The cylinder was inserted directly into the sediment and the cores were capped and sealed using rubber stoppers. Four sediment cores were taken on each field trip for porosity (n = 1 core) and sediment porewater profiles plus solid phase extraction (n = 3 cores). The cores were stored at in-situ temperature during transport between the field and the laboratory. Water quality (pH, temperature, dissolved oxygen, electric conductivity and turbidity) was measured at the time of sampling using a Horiba HQ40D portable multi-probe meter.

Water quality was measured from surface to the bottom at a meter apart. The meter was allowed to sink to specific one meter distance by using the calibrated meter marks on the Horiba wire. Water samples for total nitrogen, total phosphorus, ammonium (NH_4^+), nitrate and filterable reactive phosphorus (FRP) were taken from the surface water directly. Bottom water samples were collected using a Niskin discrete depth sampler. The sampler was lowered to a few cm above the sediment surface and attached weight was released to seal the Niskin. Samples for ammonium, phosphorus and nitrate were filtered through a 0.22 μm filter, stored on ice and returned to the laboratory where the samples were analysed.

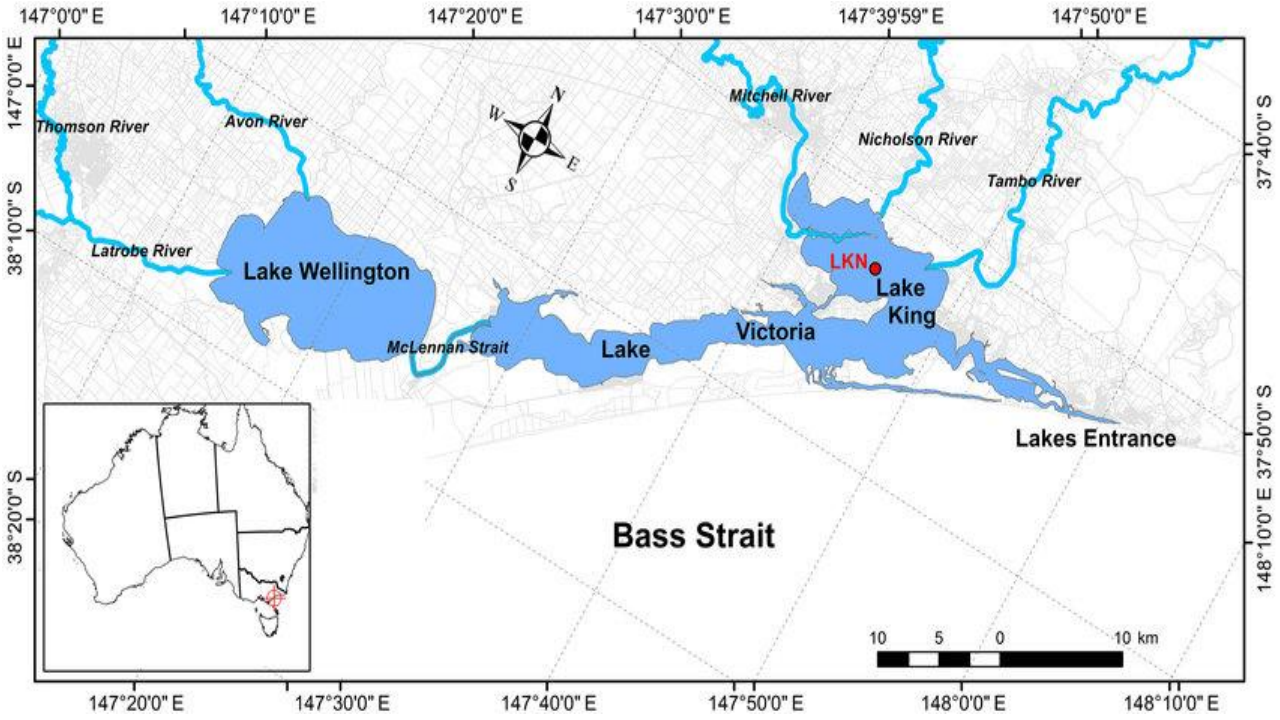

Figure 2.1. Gippsland Lakes, major tributaries and the location of Lake King North, Lake Victoria and Lake Wellington (Zhu et al., 2017)

2.3.3. Sequential extraction

Amorphous iron oxide and associated phosphorus data was collected using ascorbate as an extractant for both Fe and P in LKN sediments over the past decade by sectioning intact sediment cores at different depths. My personal input includes three years of regular sediment core sampling (October 2018- December 2021) together with interpretation and statistical analysis of the decade long data in 2021-2022. All sampling and analyses before October 2018 were performed by Water studies group members at Monash University. The cores (n =3) were sectioned at sediment depths (0–0.5, 0.5–1, 1–2, 2–3, 3–5, 5–10, 10–15, and 15–20 cm) by using a coring table. The method involves loading the core onto the coring table after removing the bottom rubber stopper and rotating the tabletop clockwise, which in turn raise the core up and then slicing the core with a scraper. The sediment sequential extraction schemes for Fe and P and subsequent analysis were performed under anoxic conditions via argon purging to understand long-term Fe and P dynamics within Gippsland lakes sediments. The extracts from all sequential extractions were passed through a 0.45 mm nylon filter. Samples for porewater FRP and Fe^{+2} were collected through centrifugation of the sediment sample at

4000 rpm for 10 min under inert argon atmosphere. The supernatant porewater was then collected using a Terumo® syringe (10ml). The supernatant is filtered through a 0.45 μm polycarbonate Millipore syringe filter into a 10ml polyethylene techno plas® tube for subsequent analysis. The solid phase Fe and P was fractionated using sequential extraction described by Scicluna et al., 2015. Each sequential extraction step aimed at retrieving a particular fraction phase of P in the sediment. The sequential extraction scheme used in the study for sedimentary iron and phosphorus fraction is summarised in Table 2.1.

Table 2.1. Sequential extraction schemes for P and Fe

Target P phase	**Extractant**	**Time**
Exchangeable P	1 M $MgCl_2$	2 hours
Ferrihydrite	.057M Ascorbic acid/.17 sodium citrate/ .6 sodium bicarbonate	24 hours
Less reactive Fe-bound P	0.5M HCL	2 hours
Calcium phosphates	Ash at 550 ^oC for 120 min and 0.5M HCL treatment	2 hours
Target Fe phase	**Extractant**	**Time**
Ferrihydrite	.057M Ascorbic acid/.17 sodium citrate/ .6 sodium bicarbonate	24 hours

2.3.4. Analytical methods

Concentrations of Fe were analysed spectrophotometrically (UV/ VIS 918 (GBC)) using the ferrozine method (Stookey, 1970). The samples were stabilised using 0.01M ferrozine (Sigma-Aldrich) and were be kept in dark before being analysed at 562 nm. Dissolved HPO_4^{2-} in all extracts was analysed using a Lachat Quikchem 8000 flow injection analyser (Protocol guidelines for APHA 4500-P was followed during the FIA analysis). Standard reference materials, sample spikes and matrix matched calibration curves ensured reliability of results in FIA sample analysis. TP and TN were analysed after persulfate digestion using standard colorimetric methods (APHA 1992). Water samples were filtered onto glass fibre filters (Whatman GF/C) and later analysed for chlorophyll-a (Chl-*a*) spectrophotometrically using a Hitachi U-2800 analyser after acetone extraction, using the method of Strickland and Parsons (1969) and the equations of Jeffrey and Humphrey (1975).

2.3.5. Statistical analyses and data sources

Principal component analysis (PCA) was used to investigate the variations in P fractionation, river inflow, surface and bottom DO, TP, TN, Chl-*a*, salinity, NH_4^+ and temperature over the monitoring timeframe and to determine which environmental components contribute more to the dynamics of phosphorus in lake sediments. Data processing was performed using GraphPad Prism version 9.0.0 for Windows, GraphPad Software, San Diego, California, USA. Mitchell river inflow data was obtained from water measurement information system (WMIS) of Environment, land, water & planning department, Victoria (https://data.water.vic.gov.au).

2.4. Results

2.4.1. LKN water column quality and sedimentary P dynamics

During the 128-month study period, the sedimentary reactive ascorbate P pool was the most dynamic and accounted for the major changes in the total P pool during the decade (Fig. 2.2e). The exchangeable $MgCl_2$ P pool represented an insignificant portion of the total P pool present in LKN sediments (Less than 2% of total P pool). Over this period, the HCl fraction was relatively stable with concentrations in the range of ~3-4 μmolg^{-1} dry sed^{-1}. Sediment porewater profiles of FRP showed a dynamics quite similar to that observed for river flow, with the highest concentrations of FRP (70 μmol L^{-1} at 0.5 cm) observed following the river inflow on 25th November 2018 leading to the highest recorded surface TP (4.74 μmol L^{-1}). The profiles of bottom water TP in LKN mirror changes in the river flow, with an increase in river flow resulting in an increase in water column TP (Fig. 2.2d). Dissolved oxygen concentrations followed a seasonal pattern with higher concentrations observed during the colder months due to increased oxygen solubility. Surface and bottom water chl-*a* concentrations remained relatively stable throughout the study period since the 2011-12 bloom (Fig. 2.2c). Temperature profiles show that the water column was cooler during the winter months (average temperature around 10^{o}C) and warmer during the summer months (average temperature around 20^{o}C). High river inflows to the Gippsland Lakes led to an increased salinity stratification within the lakes (Fig. 2.2b, 2.2d). The bottom water TN:TP remained typically in the range of 15-30 apart the 2011 bloom period and the 2018 river inflow event when the ratio depleted to <10.

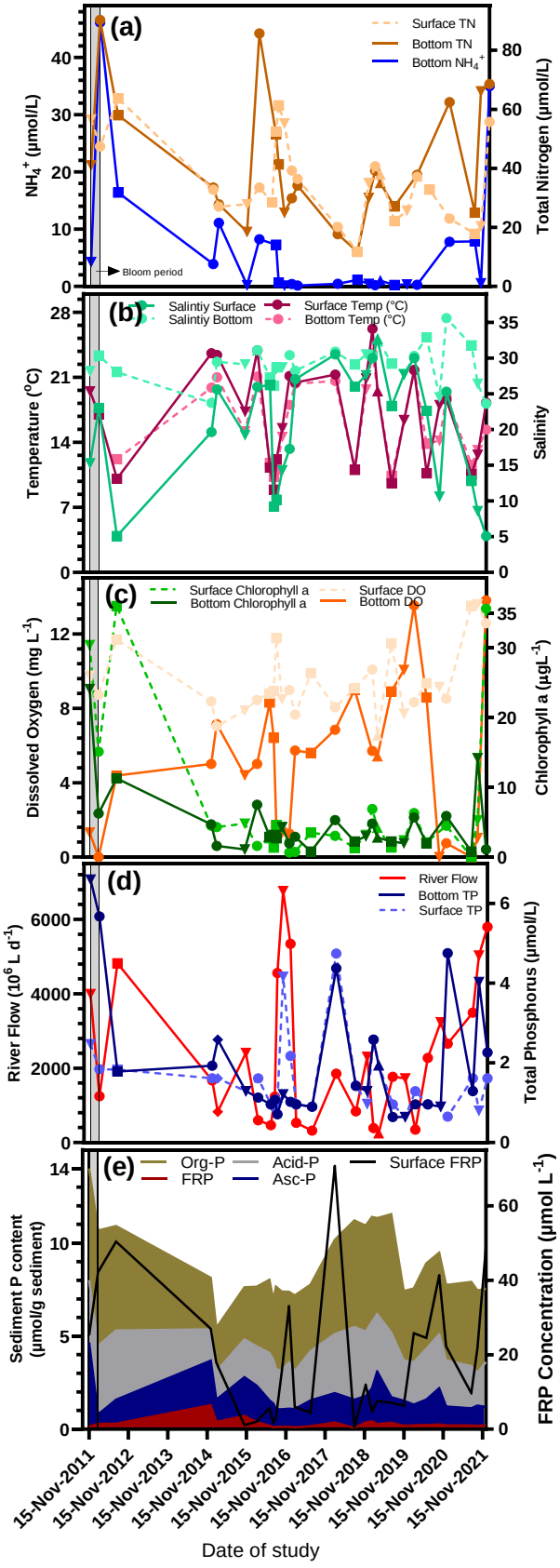

Figure 2.2. Time series of physiochemical variables (river flow in mega litres per day, water column surface (0 meters) and bottom (7 meters) total phosphorus, DO, temperature, salinity, total nitrogen and bottom water NH_4^+) and vertical P profile based on sequentially extractible P species during Nov2011 to Dec2021. Symbols ●, ▲, ■ and ▼ indicate seasons summer, autumn, winter and spring respectively.

The LKN has experienced three significant monthly river inflows during the past decade. In 2011, the flows were greater than 7000 ML d^{-1}, the flow events peaked at 6750 ML d^{-1} in 2016 and recently in 2020-2021, when LKN experienced continuous high river flow (>4500 ML d^{-1}) for more than a year. Since the last *Nodularia* bloom in 2011, when total phosphorus spiked above 6 μmol L^{-1}, the 2020-2021 bottom water column TP levels were the highest (4.75 μmol L^{-1}). Recently a considerable rise in ammonium concentration was observed. The last time, a significant rise in ammonium concentration took place was in 2016, when an increase in $NH_4^+$was accompanied by an increase in TN and bottom water chl-*a* content. The water column remained oxic during this previous event and the sedimentary P pools and bottom water TP remained relatively low during the period.

2.4.2. Fe and P uptake patterns in LKN sediments

Asc-P integrated over the top 20 cm of sediment peaked at the start of the time series at 4.5 μmol g^{-1} dry sed in 2012 during the last recorded *N. spumigena* bloom. Over the subsequent decade, the values varied between 0.9 and 2 with no clear patterns. High solid phase Ascorbate extractable Fe (Asc-Fe), integrated over the top 20 cm, was observed during the *N. spumigena* bloom in 2011-2012 and the 2015 winters. The Asc-Fe pool decreased from 43 μmol g^{-1} dry sed in winter 2015 to a concentration as low as 1.4 μmol g^{-1} dry sed in summer 2018 (Fig. 2.3a). The Asc-Fe pool sharply returned to a size of about 10 μmol g^{-1} dry sed in winter 2019. Overall, the Asc-Fe has followed a decreasing trend over the past decade with occasional winter surge. The Asc Fe:P ratios were highly variable, particularly at the sediment surface, and the values ranged between 1 to >23 for LKN sediments with an average range of about ~5-10 for most periods (Fig. 2.3b, Fig. S2). The integrated Asc-Fe to P ratio were highest during the 2015 winter corresponding to a value of ~20 and decreased to almost ~1 during the 2018 summer, which was the lowest recorded ratio during the monitoring period.

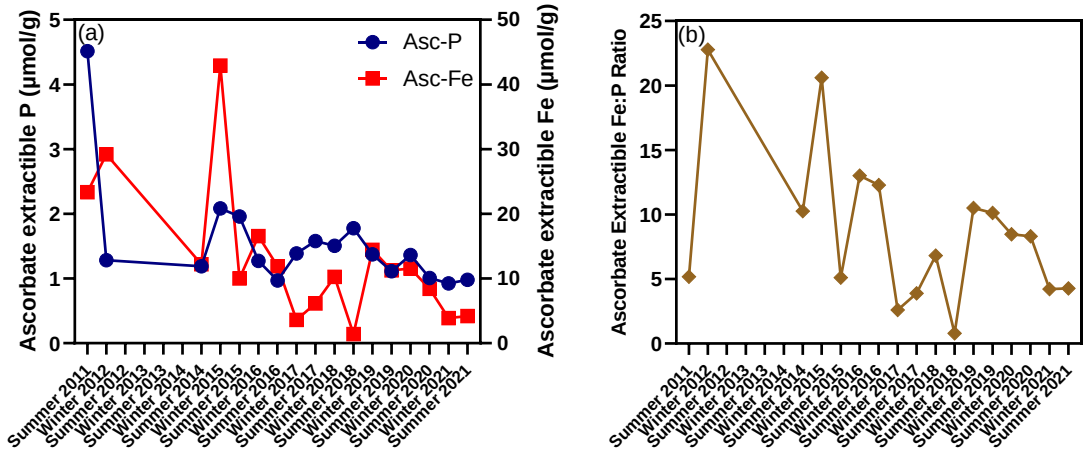

Figure 2.3. Seasonal time series plot showing, (a) Depth weighted average of ascorbate extractible Fe and P from top 20cm, (b) Profile of ascorbate extractible Fe:P ratios.

A heat map of the ascorbate extractable P shows the variation at depth of Fe bound P in LKN for the monitoring period (Fig. 2.4). Strong enrichment in Asc-P pool was observed near the sediment water interface but the Asc-P fraction at depth was quite static with concentrations ranging between 1-2 μmol g^{-1} apart from the November 2011, when deep pools of ascorbate extractable iron oxyhydroxide bound P were observed linked with the presence of *C. capitata* in these sediments (Fig. 2.4, Fig. S1). A quite variable sediment iron oxyhydroxide (Asc-Fe) pool with concentrations ranging from 1 to 40

μmol g^{-1} was observed in the top 2 cm of LKN for the past ten years. The Asc-Fe pool decreased sharply near the surface and the deeper Asc-Fe pool (below 3cm) was quite stable over the past five years with concentrations ranging between 1 to 10 μmol g^{-1} dry sed. The study shows that the Fe associated P in the top centimetre of the LKN sediment can be highly dynamic (Fig. S3).

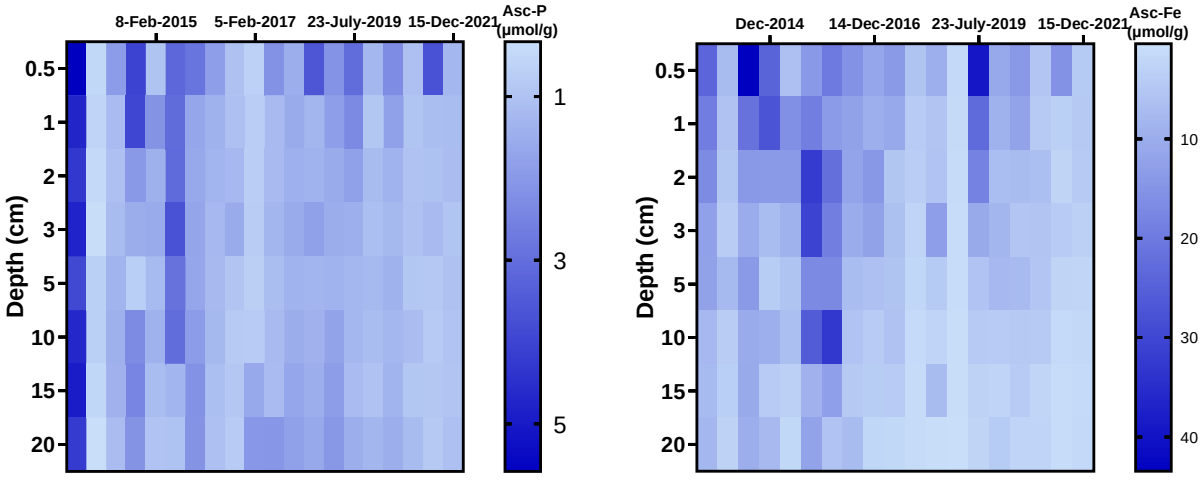

Figure 2.4. A heat map of ascorbate extractable phosphorus and iron in sediments cores from discrete depths over time. Data represents 10 years (2011-2021) sediment core extraction P & Fe output from LKN

2.4.3. Principal component analysis

The principal comment analysis showed that for Asc-P, the data variables can be reduced to 3 PC's (PC1 46.23%, PC2 25.7% and PC3 12.96%) which could explain the maximum variance in the time series data of Asc-P (Fig. 2.5). PC1 had a positive association with bottom water DO as shown through high loading and was negatively associated with Asc-P, bottom water TP and Chl-*a*. The presence of Asc-P, bottom water TP and Chl-*a* loadings in close proximity along the same PC1 indicate positive association between the variables. On the other hand, Asc-P was negatively associated with bottom water DO. PC2 explained variability between Asc-P and river flow. Asc-P was positively associated with PC2 whereas river flow was negatively associated with PC2. The nutrient variables (Chl-*a* and TP-B) and sedimentary ascorbate P pool (Asc-P) showed no clear response to inflow events. The flood events showed a negative correlation with bottom water DO suggesting inflow driven salinity stratification, which in turn leads to low DO. For the same analysis performed on Asc-Fe, two principal components were able to account for 68% of the total variance in the data (PC1 38.89%, PC2 29.14% and PC3 18.05%). Similar to Asc-P, PC1 showed a negative association between Asc-Fe and bottom water DO whereas PC2 showed a negative correlation of Asc-Fe with river flow (Fig. 2.6). The negative association of both Asc-Fe and Asc-P with bottom water DO indicate that low oxygen conditions may not necessarily lead to Fe bound P dissolution in sediments. Asc-Fe also showed a negative correlation with bottom water temperature. This indicates reduced iron reduction rates in sediments at low temperatures.

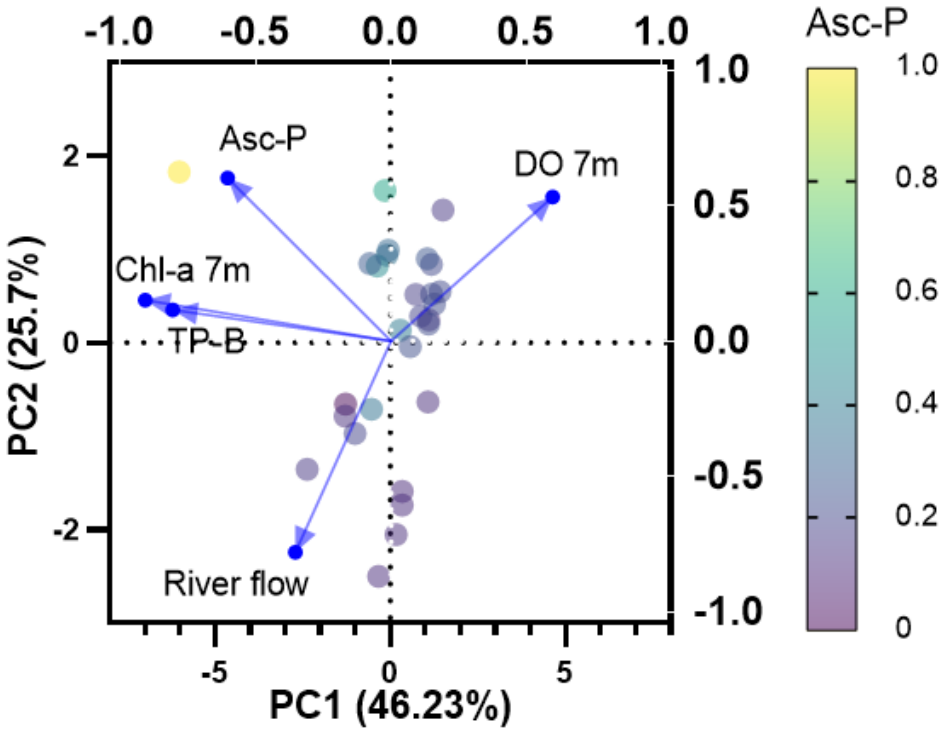

Figure 2.5. Principal component analysis (PCA) based on time series data of the ascorbate extractible phosphorus (Asc-P) and water column physiochemical variables in LKN

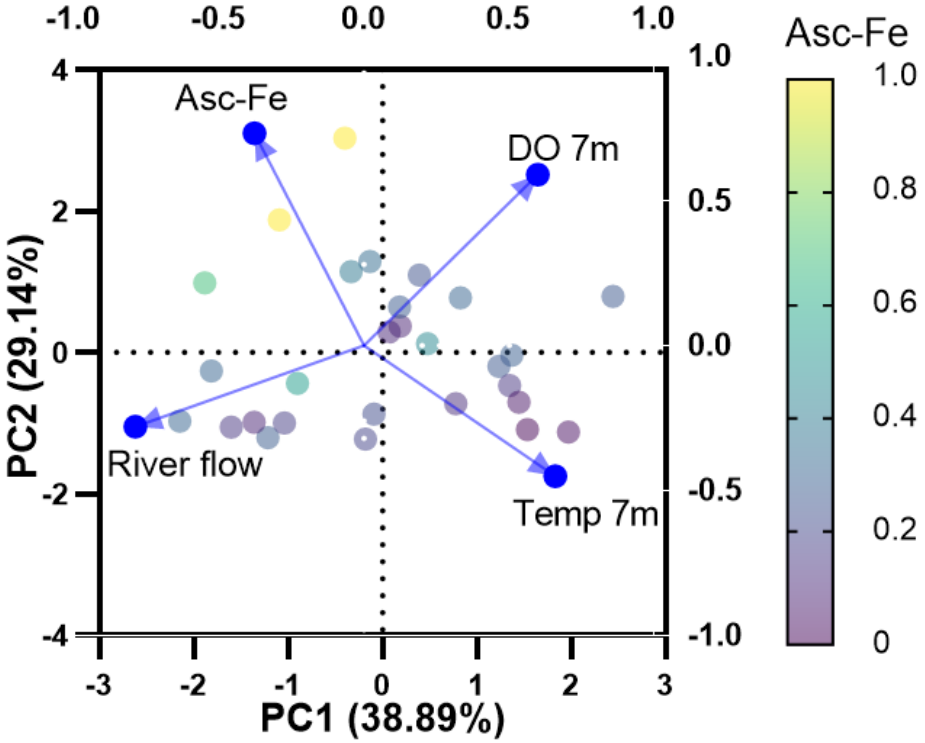

Figure 2.6. Principal component analysis (PCA) based on time series data of the ascorbate extractible iron (Asc-Fe) and water column physiochemical variables in LKN.

2.5. Discussion

2.5.2. Factors controlling Fe and P dynamics in LKN sediments

PCA analysis performed to assess factors related to the sediment Asc-P and Asc-Fe provided insight into the relative importance of two factors that control Asc-P and Asc-Fe dynamics in the LKN sediments. We had hypothesized that the highest Asc-P and Asc-Fe would be positively associated with DO because higher DO would lead to more oxidation of Fe forming more FeOOH, and P would subsequently accumulate on this. Somewhat unexpectedly, Asc-P and Asc-Fe were negatively associated with dissolved oxygen. Secondly, low DO associated with river flow, which leads to organic matter, nutrient and particle (iron) input (Fig. 2.5 and 2.6). Consistent with this, there was a very strong association of bottom water TP with Chl-*a* and Asc-P suggesting that delivery of new P and Fe to the sediment is more important in controlling iron oxyhydroxide bound P pool than longer term oxidised conditions. This is consistent with the results from other studies concerning environmental and biological parameters influence on sedimentary P dynamics. Chl-*a* was found to be positively correlated to the presence of essential nutrients (TN, NH_4–N, SRP and TP) for phytoplankton growth (Varol, 2020). Li et al. (2017) investigated the water quality parameters and biomass correlation and showed a negative association of TP, TN with DO in Honghu Lake. In another study, Chl-*a* was positively correlated with bottom water nutrient concentration. Both bottom water salinity and temperature (positively correlated) were found to be negatively associated with the Chl-*a* and high values of nutrient concentration in the bottom water (Chatterjee et al., 2013).

The PCA performed on Asc-Fe showed a negative association between the Fe fraction and bottom water temperature. Rising temperatures can cause a warmer layer of surface water while the hypolimnion warms up rather slowly, causing stratification and reduced O_2 solubility in water and increased microbial activity. The bottom water oxygen levels further decreases through enhanced oxygen consumption by degrading organic matter. The changes in wind patterns and higher inflows in winter could also affect stratification. The Gippsland Lakes typically experienced the highest inflows in winter leading to salinity driven stratification and lower DO on the winter and spring although no distinct seasonal patterns were observed. Salinity appeared to be a dominant feature for the lake water quality and is also known to exert strong influence on *Nodularia* blooms (Cook & Holland, 2012). The vertical stratification gradient from salinity promotes higher temperatures and low bottom water DO. The recent rise in ammonium concentration of the water column, suggested availability of organic matter for mineralization but inability of microbial processes to rapidly oxidise the ammonium produced due to hypoxia.

2.5.2. Sampling and analysis artefacts

Oxidation, change in temperature and sampling time artefacts can result in small Fe and P pool alterations. The cores were stored at in-situ temperature during transport and sequential extractions were performed under anoxic conditions via argon purging to avoid associated artefacts. However, the sediment core collections were performed based on weather permitted non-windy and rainy days. This might have resulted in biased low bottom water DO readings on the sampling day. The presence of Fe bound P pools under anoxic conditions in LKN can be attributed to the occasional strong winds and coastal hydrodynamic conditions supplementing DO from the overlying water. The Fe bound P pools under anoxic condition in LKN are further supported by the sedimentary Fe and P speciation. The low Fe:P ratios and the absence of considerable exchangeable P support strong adsorption of P

onto Fe oxides. Similarly, Yang et al. (2021) observed a negative correlation between bottom water DO and reactive Fe-P during the anoxic phase.

Another artefact that might affect sediment P results is the extraction of other phases of P in the Asc-P extraction. Anoxic conditions and the presence of Fe(II) and P in close proximity favours binding of P with Fe(II) to form vivianite ($[Fe_3(PO_4)_2] \cdot 8\ H_2O$).

2.5.3. Effect of hypoxia on sediment Fe-P pools

Bottom water hypoxia led to an 80% decrease in ascorbate extractible P pool of the system during the 2011 bloom. Although the system has experienced hypoxic conditions in 2016 and 2020 but reduction of iron oxyhydroxide and loss of P was quite low (~20 %). Considering the highly unfavourable conditions for Fe–P formation, the presence of Fe bound P pool under hypoxic conditions could be explained by the existence of an iron oxide phase with very high adsorption capacities as suggested by the low Fe:P ratios (Anschutz et al., 1998). The temporal porewater filterable reactive P (FRP) profiles at the LKN site also displays low concentrations of HPO_4^{2-} in the near surface sediment and an increase below ~5 cm depth. Such profiles are characteristic of iron rich sediments where presence of iron oxyhydroxide layer at the sediment water interface suppress the diffusive flux of HPO_4^{2-} through adsorption (Jilbert et al., 2011). The deviation from the paradigm that oxygen controls Fe bound P release has been exhibited in North American lakes, where extremely low P release from anoxic sediments has been observed. These low level of P releases have been explained by the resistance of iron oxides to reduction or redox insensitive binding mechanisms (Hupfer & Lewandowski, 2008). In black sea sediments, Dijkstra et al. (2014) also observed the presence of iron oxyhydroxide bound P in cores analysed under strictly anoxic conditions.

2.5.4. Do the dynamics of P within the LKN sediment reflect legacy P presence?

An important aspect of our result that deserve considerable attention in context of Fe bound P dynamics was the absence of reactive legacy P in the system. Randall et al. (2019) observed legacy P build up in sediments as a function of decade long nutrient loading contributing to the algal bloom in lake through enhanced P release. The legacy P in sediments is mainly associated with iron oxyhydroxide phases, which can experience reductive dissolution under anoxic conditions (Liu et al., 2014). Legacy P contributed to the surface enrichment in Lake Lairewa and was a large potential source for internal loading (Waters et al., 2021). Since the last bloom in 2011, the Gippsland lakes have not shown an increase in the reactive P pool of the sediment. Sustained bottom water oxygenation during the 2017-2019 period was associated with only a slight increase in the total sedimentary P content. In fact, reactive Fe and associated P had no apparent trend over the past decade and the current P concentrations correspond to some of the lowest recorded for the site. Despite long-term oxygenation and lower FRP concentrations at the surface, the relatively stable reactive Fe bound P pool in LKN sediments suggest an approach to steady state equilibrium with regard to water column. This implies either a reduction in magnitude and frequency of inflows or inflows introducing virtually no P into the lake (reduced external loading) over longer timeframes. Edlund et al. (2017) showed depletion of sediment active legacy pool in southern Lake of Woods and suggested seasonality of P loading as new drivers.

2.5.5. Role of variability in inflows (external P loading)

LKN has experienced an algal bloom roughly once a decade with *Nodularia spumigena* blooms being reported in 1974, 1987, 1989, 1996, 1997, 2011 and 2022 over the past five decades (Stephens et al., 2004; Scicluna et al., 2015). Over the past decade, high inflow events have been recorded in 2011, 2016 and 2021. The high flow event in 2011 resulted in increased salinity stratification, high bottom water TP, bottom water anoxia from late austral spring to summer and a bloom of *Nodularia spumigena* from November 2011 until February 2012 (Scicluna et al., 2015). The deep pools of iron associated P rapidly decreased on the onset of anoxia the following summer. Cook et al. (2010) also suggested that the high nutrient loads entering the Gippsland Lakes are responsible for the algal blooms. Contrary to 2011-12, the high river inflow of 2016 was not able to produce the bloom effect. This behaviour can be explained by the sediment surface FRP variation. The FRP concentrations of ~40–70 μmol L^{-1} at 0.5 cm correspond to the highest diffusive P fluxes observed in the system during the 2011-12 bloom period compared to ~15–30 μmol L^{-1} at 0.5 cm observed during the 2016 period. This suggest lack of P delivery and labile organic matter remineralisation at the surface during the 2016 inflow event marked by the absence of enhanced iron oxyhydroxide bound P pool. The ascorbate extractable P pools in 2011 were about 5 μmol g^{-1} dry sed to a depth of 20 cm whereas P pools of less than 1 μmol g^{-1} dry sed were present in 2016. The bottom water hypoxia in summer following the 2016 flow event resulted in the release of less than half of the ascorbate bound P pool from the surface sediment compared to an 80% reduction during 2011-12 bloom (Fig. 2.2a). The February 2018 concentrations represent another occasion when sediment surface FRP reached closer to 50 μmol L^{-1} following a medium inflow event. Completely oxic conditions at the sediment water interface during the period and an increase in sedimentary P content up to 25% suggest that the higher FRP concentrations were linked to the delivery of fresh P through inflows. This further supports the notion that the external P loading as part of inflow event control condition in Gippsland Lakes through formation of temporary P pool and the release of P upon the onset of anoxia.

The present FRP (>50 μmol L^{-1}) and bottom water TP (>4 μmol L^{-1}) concentrations from November 2021 until March 2022 are also some of the highest recorded in the study probably translating from the resent 2019-2020 Victorian bushfires. However, the sedimentary P pools have remained relatively stable. Considering the sediment water interface is completely oxygenated, the conditions should have led to an increase in sediment Fe-P pool. Unlike the 2011 short span inflow event, which allowed sedimentary P uptake, the persistence of the current inflow event might be the reason for this behaviour. A *Nodularia* bloom is currently (May 2022) affecting the Gippsland Lakes. The data here suggests that the bloom seems to have been fed by the river flows and not the sediment, however further analysis of loads data is needed, which is beyond the scope of this thesis given submission timelines.

2.6. Conclusions

The present study gives an insight into the likely controls of Asc-P within the sediment. The study shows that the high flow events that have been reported in the past and during the current monitoring period have a significant impact on LKN water quality and nutrient load lead to the formation/reduction of iron oxyhydroxide bound P pool. Extended periods of oxygenation and delivery of P to the system result in a thicker Fe oxide bearing P layer and stable Fe bound P pool. A reduction in nutrients entering the lake could prove critical in controlling the water quality of the lake.

Bottom water total phosphorus and dissolved oxygen are key variables that correlate with sediment phosphorus dynamics. Monitoring and undertaking further research on the sediment surface water interactions of the lake could prove critical in improving the findings of the current study and predicting the long-term behaviour of the lake.

2.7. References

Anschutz, P., Zhong, S., Sundby, B., Mucci, A., & Gobeil, C. (1998). Burial efficiency of phosphorus and the geochemistry of iron in continental margin sediments. *Limnology and Oceanography, 43*(1), 53-64. doi:https://doi.org/10.4319/lo.1998.43.1.0053

Boynton, W. R., Ceballos, M., Bailey, E. M., Hodgkins, C. L. S., Humphrey, J. L., & Testa, J. M. (2017). Oxygen and Nutrient Exchanges at the Sediment-Water Interface: a Global Synthesis and Critique of Estuarine and Coastal Data. *Estuaries and Coasts, 41*, 301-333. doi:http://dx.doi.org/10.1007/s12237-017-0275-5

Carrasco Navas-Parejo, J. C., Corzo, A., & Papaspyrou, S. (2020). Seasonal cycles of phytoplankton biomass and primary production in a tropical temporarily open-closed estuarine lagoon — The effect of an extreme climatic event. *Science of The Total Environment, 723*, 138014. doi:https://doi.org/10.1016/j.scitotenv.2020.138014

Chatterjee, A., Klein, C., Naegelen, A., Claquin, P., Masson, A., Legoff, M., Leynaert, A. (2013). Comparative dynamics of pelagic and benthic micro-algae in a coastal ecosystem. *Estuarine, Coastal and Shelf Science, 133*, 67–77. doi:https://doi.org/10.1016/j.ecss.2013.08.015

Cook, P., & Holland, D. (2012). Long term nutrient loads and chlorophyll dynamics in a large temperate Australian lagoon system affected by recurring blooms of cyanobacteria. *Biogeochemistry, 107*, 261-274 doi:https://doi.org/10.1007/s10533-010-9551-1

Cook, P. L. M., Holland, D. P., & Longmore, A. R. (2010). Effect of a flood event on the dynamics of phytoplankton and biogeochemistry in a large temperate Australian lagoon. *Limnology and Oceanography, 55*(3), 1123-1133. doi:https://doi.org/10.4319/lo.2010.55.3.1123

Giudice, D., Zhou, Y., Sinha, E., & Michalak, A. M. (2018). Long-Term Phosphorus Loading and Springtime Temperatures Explain Interannual Variability of Hypoxia in a Large Temperate Lake. *Environmental Science & Technology, 52*(4), 2046-2054. doi:https://doi.org/10.1021/acs.est.7b04730

Dijkstra, N., Kraal, P., Kuypers, M. M. M., Schnetger, B., & Slomp, C. P. (2014). Are Iron-Phosphate Minerals a Sink for Phosphorus in Anoxic Black Sea Sediments? *PLOS ONE, 9*(7), e101139. doi:https://doi.org/10.1371/journal.pone.0101139

Dove, A., & Chapra, S. C. (2015). Long-term trends of nutrients and trophic response variables for the Great Lakes. *Limnology and Oceanography, 60*(2), 696-721. doi:https://doi.org/10.1002/lno.10055

Edlund, M. B., Schottler, S. P., Reavie, E. D., Engstrom, D. R., Baratono, N. G., Leavitt, P. R., Paterson, A. M. (2017). Historical phosphorus dynamics in Lake of the Woods (USA–Canada) — does legacy phosphorus still affect the southern basin? *Lake and Reservoir Management, 33*(4), 386-402.

doi:https://doi.org/10.1080/10402381.2017.1373172

Hupfer, M., & Lewandowski, J. (2008). Oxygen Controls the Phosphorus Release from Lake Sediments – a Long-Lasting Paradigm in Limnology. *International Review of Hydrobiology, 93*(4-5), 415-432. doi:https://doi.org/10.1002/iroh.200711054

Huser, B. J., Futter, M. N., Wang, R., & Fölster, J. (2018). Persistent and widespread long-term phosphorus declines in Boreal lakes in Sweden. *Sci Total Environ, 613-614*, 240-249. doi:https://doi.org/10.1016/j.scitotenv.2017.09.067

Jeffrey, S. W., & Humphrey, G. F. (1975). New spectrophotometric equations for determining chlorophylls a, b, c1 and c2 in higher plants, algae and natural phytoplankton. *Biochemie und Physiologie der Pflanzen, 167*(2), 191-194. doi:https://doi.org/10.1016/S0015-3796(17)30778-3

Jensen, H. S., Mortensen, P. B., Andersen, F. Ø., Rasmussen, E. K., & Jensen, A. (1995). Phosphorus cycling in a coastal marine sediment, Aarhus Bay, Denmark. *Limnology and Oceanography, 40*, 908-917. doi: https://doi.org/10.4319/lo.1995.40.5.0908

Jilbert, T., Slomp, C. P., Gustafsson, B. G., & Boer, W. (2011). Beyond the Fe-P-redox connection: preferential regeneration of phosphorus from organic matter as a key control on Baltic Sea nutrient cycles. *Biogeosciences, 8*(6), 1699-1720. doi:https://doi.org/10.5194/bg-8-1699-2011

Korppoo, M., Lukkari, K., Järvelä, J., Leivuori, M., Karvonen, T., & Stipa, T. (2012). *Phosphorus release and sediment geochemistry in a low-salinity water bay of the Gulf of Finland,* 17, 237-251. Retrieved from: https://helda.helsinki.fi/bitstream/handle/10138/229887/ber17-3-4-237.pdf

Kostka, J. E., & Luther, G. W. (1994). Partitioning and speciation of solid phase iron in saltmarsh sediments. *Geochimica et Cosmochimica Acta, 58*(7), 1701-1710. doi:https://doi.org/10.1016/0016-7037(94)90531-2

Liu, J., Hu, Y., Yang, J., Abdi, D., & Cade-Menun, B. J. (2014). Investigation of soil legacy phosphorus transformation in long-term agricultural fields using sequential fractionation, P K-edge XANES and solution P NMR spectroscopy. *Environmental Science and Technology, 49*(1), 168-176.

doi:https://doi.org/10.1021/es504420n

Liu, J., Krom, M. D., Ran, X., Zang, J., Liu, J., Yao, Q., & Yu, Z. (2020). Sedimentary phosphorus cycling and budget in the seasonally hypoxic coastal area of Changjiang Estuary. *Science of The Total Environment, 713*, 136389. doi:https://doi.org/10.1016/j.scitotenv.2019.136389

Poulton, S. W., & Canfield, D. E. (2005). Development of a sequential extraction procedure for iron: implications for iron partitioning in continentally derived particulates. *Chemical Geology, 214*(3), 209-221. doi:https://doi.org/10.1016/j.chemgeo.2004.09.003

Randall, M. C., Carling, G. T., Dastrup, D. B., Miller, T., Nelson, S. T., Rey, K. A., . . . Aanderud, Z. T. (2019). Sediment potentially controls in-lake phosphorus cycling and harmful cyanobacteria in shallow, eutrophic Utah Lake. *PLOS ONE, 14*(2), e0212238. doi:https://doi.org/10.1371/journal.pone.0212238

Ruttenberg, K. C. (1992). Development of a sequential extraction method for different forms of phosphorus in marine sediments. *Limnology and Oceanography, 37*(7), 1460-1482. doi:https://doi.org/10.4319/lo.1992.37.7.1460

Scicluna, T. R., Woodland, R. J., Zhu, Y., Grace, M. R., & Cook, P. L. M. (2015). Deep dynamic pools of phosphorus in the sediment of a temperate lagoon with recurring blooms of diazotrophic cyanobacteria. *Limnology and Oceanography, 60*(6), 2185-2196. doi:https://doi.org/10.1002/lno.10162

Stephens, A., Biggins, N. and Brett, S. (2004). *Algal Bloom Dynamics in the Estuarine Gippsland Lakes.* Publication SR4, EPA Victoria, Scientific report.

Stookey, L. L. (1970). Ferrozine---a new spectrophotometric reagent for iron. *Analytical Chemistry, 42*(7), 779-781. doi:https://doi.org/10.1021/ac60289a016

Strickland, J. D. H., & Parsons, T. R. (1969). A Practical Handbook of Seawater Analysis. Fisheries Research Board of Canada Bulletin 167. . *The Quarterly Review of Biology, 44*(3), 327-327.

doi:https://doi.org/10.1086/406210
Tessin, A., März, C., Kędra, M., Matthiessen, J., Morata, N., Nairn, M., . . . Peeken, I. (2020). Benthic phosphorus cycling within the Eurasian marginal sea ice zone. *Philosophical Transactions of the Royal Society A: Mathematical, Physical and Engineering Sciences, 378*(2181), 20190358.
doi:https://doi.org/10.1098/rsta.2019.0358
Thamdrup, B., Fossing, H., & Jørgensen, B. B. (1994). Manganese, iron and sulfur cycling in a coastal marine sediment, Aarhus bay, Denmark. *Geochimica et Cosmochimica Acta, 58*(23), 5115-5129.
doi:https://doi.org/10.1016/0016-7037(94)90298-4
Varol, M. (2020). Spatio-temporal changes in surface water quality and sediment phosphorus content of a large reservoir in Turkey. *Environmental Pollution, 259*, 113860.
doi:https://doi.org/10.1016/j.envpol.2019.113860
Vystavna, Y., Hejzlar, J., & Kopáček, J. (2017). Long-term trends of phosphorus concentrations in an artificial lake: Socio-economic and climate drivers. *PLOS ONE, 12*(10), e0186917.
doi:https://doi.org/10.1371/journal.pone.0186917
Wang, M., Zhang, H., Du, C., Zhang, W., Shen, J., Yang, S., & Yang, L. (2021). Spatiotemporal differences in phosphorus release potential of bloom-forming cyanobacteria in Lake Taihu. *Environmental Pollution, 271*, 116294.
doi:https://doi.org/10.1016/j.envpol.2020.116294
Woodland, R. J., & Cook, P. L. (2014). Using stable isotope ratios to estimate atmospheric nitrogen fixed by cyanobacteria at the ecosystem scale. *Ecol Appl, 24*(3), 539-547.
doi:https://doi.org/10.1890/13-0947.1
Waters, S., Webster-Brown, J. G., & Hawes, I. (2021). The release of legacy phosphorus from deforestation-derived sediments in shallow, coastal lake Forsyth/Te Roto o Wairewa. *New Zealand Journal of Marine and Freshwater Research, 55*(3), 446-465.
doi:https://doi.org/10.1080/00288330.2020.1804408
Zhang, J.-Z., & Lanning, N. T. (2018). Ascorbic acid as a reductant for extraction of iron-bound phosphorus in soil samples: a method comparison study. *Communications in Soil Science and Plant Analysis, 49*(17), 2155-2161.
doi: https://doi.org/10.1080/00103624.2018.1499751
Zhang, S., Wang, W., Zhang, K., Xu, P., & Lu, Y. (2018). Phosphorus release from cyanobacterial blooms during their decline period in eutrophic Dianchi Lake, China. *Environ Sci Pollut Res Int, 25*(14), 13579-13588.
doi:https://doi.org/10.1007/s11356-018-1517-1

2.8. Supplementary information

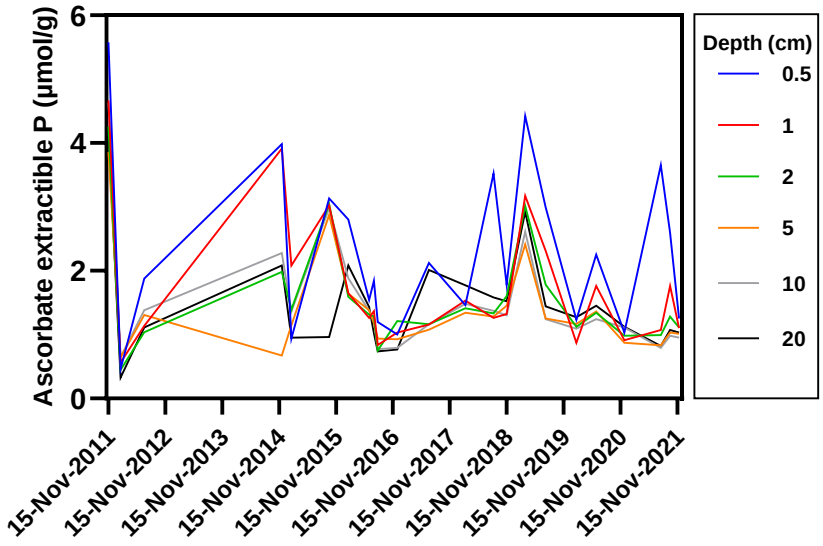

Figure. S1. Profiles of sequentially extractable phosphorus in sediments cores from discrete depths over time. Data represents 10 years (2011-2021) sediment core extraction P output from LKN

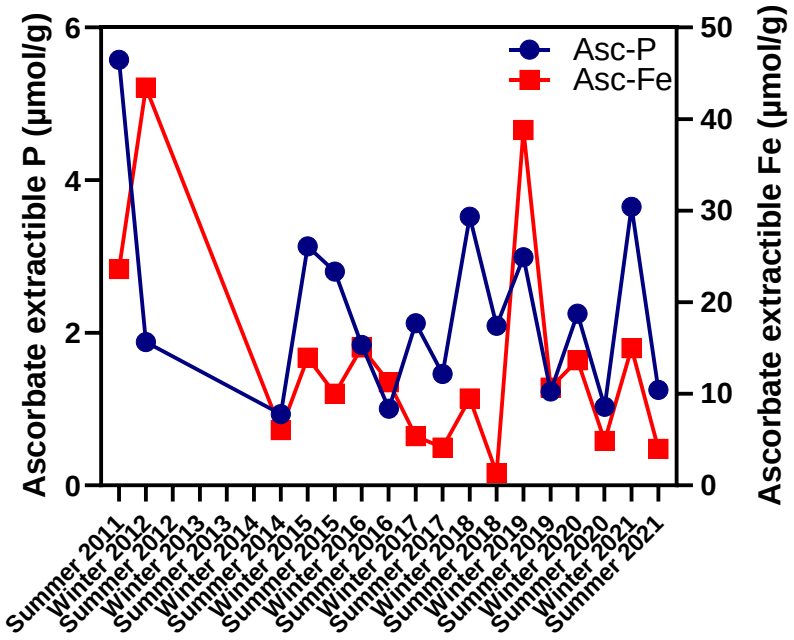

Figure. S2. Seasonal time series plot showing depth weighted average of Asc-Fe and Asc-P in top 0.5cm

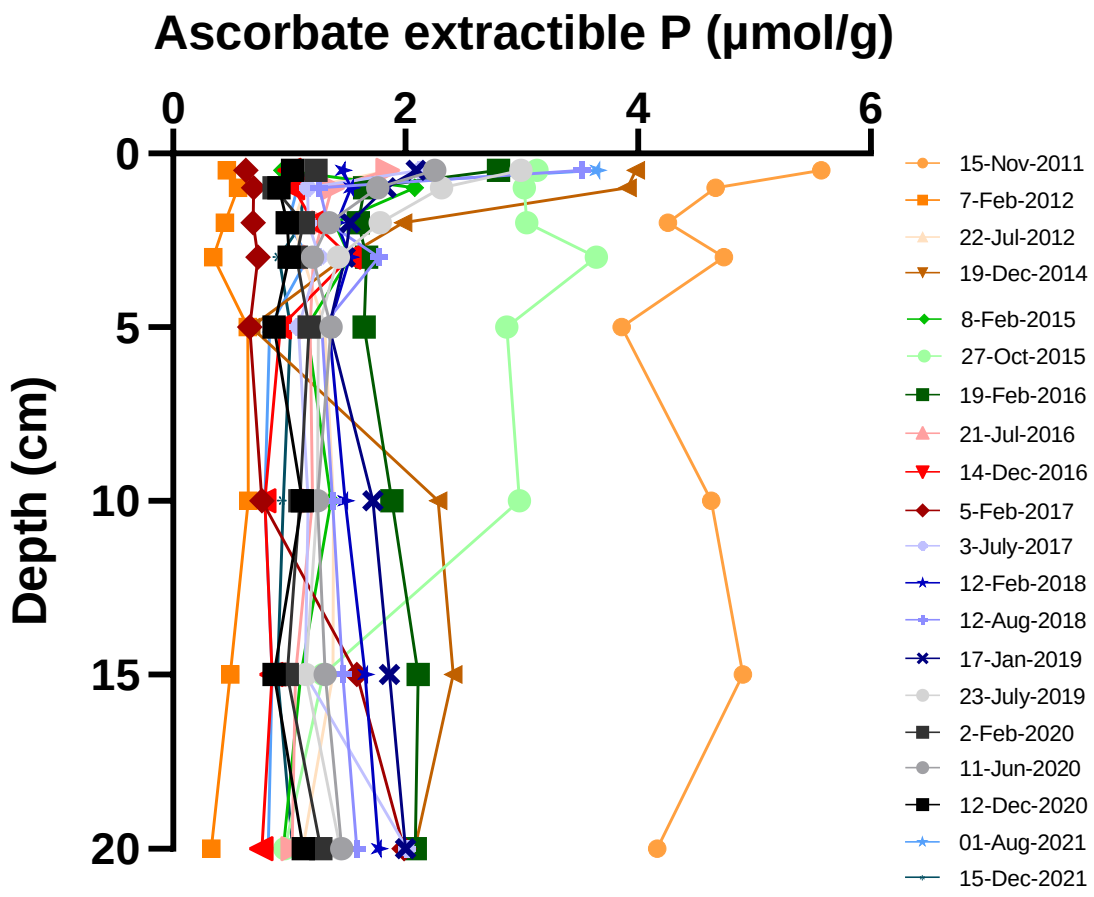

Figure. S3. Profiles of sequentially extractable phosphorus in sediments cores from discrete depths over time. Data represents 10 years (2011-2021) sediment core extraction P output from LKN.

Date	Nov -11	Feb -12	Jul-12	Dec -14	Feb -15	Oct-15	Feb -16	Jun -16	Oct-16	Dec -16	Feb -17	Feb -18	Aug -18	Nov -18	Jan-19	Mar -19	Jul-19	Nov -19	Feb -20	Jun -20	Oct-20	Dec -20	Aug -21	Sep -21	Dec -21
FRP	0.15	0.29	0.30	1.29	0.39	0.72	0.38	0.19	0.13	0.13	0.10	0.36	0.07	0.37	0.42	0.27	0.35	0.18	0.21	0.23	0.26	0.20	0.20	0.17	0.21
Asc-P	4.66	0.79	1.58	3.68	1.58	2.80	2.34	1.55	1.07	1.10	1.08	1.94	1.58	1.78	2.20	3.10	1.72	1.53	1.32	1.59	2.19	1.21	1.12	1.27	1.19
Acid-P	8.01	14.0	4.47	10.6	5.31	10.9	5.36	3.10	4.82	4.45	4.10	3.14	3.59	3.12	5.11	10.1	5.49	11.2	5.24	10.9	5.77	11.4	6.18	11.3	5.19	11.5	3.70	3.60	4.32	5.08	3.70	3.39	3.03	3.61
Org-P	1	7	1	8.13	5.44	7.62	7.65	8.03	7.39	7.38	7.18	7	1	3	1	4	5	7.42	7.55	8.90	9.48	7.75	7.91	7.45	7.53
0.5m FRP	25.1	8	42.1	6	50.4	0	27.0	0	17.8	8	1.12	2.00	5.67	15.2	0	33.0	0	6.00	70.6	5	0.50	11.9	0	4.80	7.60	7.10	6.30	25.8	0	24.5	0	41.3	0	22.2	0	21.7	0	48.9	0
River Flow	399	124	481	167		241			676	533		185		230			176	172		227	323	265	349	502	579
TP 0.5m	2.47	1.84	1.83	1.61	1.61	1.29	1.61	0.96	4.16	2.17	0.96	4.74	1.43	0.97	2.58	1.94	0.96	0.64	1.29	0.96	0.90	0.65	1.61	0.80	1.61
TP-B	6.60	5.67	1.78	1.93	2.58	1.29	1.13	0.96	1.21	1.02	0.96	4.37	1.42	1.29	2.58	1.94	0.64	0.64	0.96	0.96	0.90	4.75	1.29	4.03	2.26
DO 0.5m	9.77	8.73	11.7	0	8.37	7.04	7.88	8.45	8.80	8.50	8.98	7.66	8.06	9.07	10.0	9	6.52	11.5	0	7.71	8.33	9.35	9.15	8.52	13.5	1	13.5	9	12.5	7
DO 7m	1.32	0.00	4.38	5.01	7.15	4.40	5.01	8.31	1.31	1.26	5.73	6.85	9.00		5.71	5.42	8.90	10.0	6	13.5	3	8.58	0.00	0.75	0.00	1.03	13.8	0
Cha a 0.5m	30.4	0	15.1	0	36.0	0	4.50	4.30	4.80	1.60	2.70	4.30	0.66	0.74	3.05	1.31	3.20	6.90	4.20	1.37	2.40	6.30	2.10		4.50	0.00	5.30	14.2	35.6	0
Cha a 7m	24.1	0	6.25	11.3	0	4.70	1.60	1.10	7.50	2.90	4.29	1.97	2.92	5.32	2.24	3.00	4.80	2.80	2.23	2.00	5.70	2.00		5.90	0.80	0	1.10
0.5m Temp (°C)	19.5	0	17.0	0	10.0	7	23.6	0	23.4	0	17.3	0	23.9	0	11.3	0	15.5	3	21.1	5	20.4	5	21.3	0	11.0	4	20.8	8	26.2	3	19.5	1	9.60	16.3	9	21.8	1	10.6	6	18.0	2	18.6	0	10.5	7	12.6	8	18.2	6
7m Temp(°C)				12.2	0	19.9	0	21.0	0	15.2	0	21.1	0	11.8	0	14.5	9	18.0	5	20.3	2	20.6	0	11.0	7	19.7	1	23.6	1	19.5	2	10.3	8	16.4	3	21.7	4	13.8	5	14.2	0	18.9	5	11.5	6	13.1	8	15.3	7
Salintiy 0.5m	15.2	7	23.0	1		19.6	6	25.6	2	19.2	4	25.9	9	26.2	2	14.3	0	17.2	8	27.0	4	30.5	0	26.0	0	27.6	0	30.0	0	32.5	0	23.3	0	27.7	0	30.0	0	22.6	0	10.6	0	25.3	0	12.8	0		
Salintiy 7m	28.1	8	30.3	4	28.0	5	23.7	1	29.4	9	29.1	3	31.1	0	27.2	8	28.7	0	30.4	0	28.2	2	30.9	0	29.1	0	30.5	0	30.4	0	32.7	4	29.2	0	27.8	0	30.3	0	32.9	0	24.5	0	35.6	0	31.8	0	26.4	0	23.6	2
7m NH4+ (uM)	4.29		46.1	1	16.4	0	3.90	11.1	0	0.23	8.23		0.16	0.41	0.17	0.46	1.13	0.47	0.23	1.00	0.24	0.36	0.29			7.79	7.86	0.57	35.0	0
0.5m TN	56.6	0	47.4	0	63.7	0	32.8	0	27.0	0	27.8	0	33.5	0	28.5	0	55.2	9	39.2	9	36.4	0	20.1	6	11.8	4	35.0	0	40.7	0	37.8	6	22.1	0	25.7	0	37.1	2	32.8	0	23.0	0	17.8	5	20.4	3	55.7	1
7m TN	41.0	8	90.3	0	58.0	0	33.5	0	27.8	0	18.5	0	85.7	0			25.0	0	29.8	6	34.2	0	17.6	8	11.7	4	30.0	0	39.2	0	35.0	0	27.1	0			37.8	3			62.4	3	25.0	0	66.1	4	68.5	7

Figure. S4. Data represents 10 years (2011-2021) sediment core extraction P output from LKN and time series of physiochemical variables.

Table S1. (a) PC1, PC2 and PC3 loadings, (b) contribution of variables

a

Variable	PC1	PC2	PC3
Asc-P	-0.60	0.60	-0.36
River Flow	-0.35	-0.77	-0.47
TP-B	-0.80	0.11	0.39
DO 7m	0.59	0.53	-0.33
Cha a 7m	-0.90	0.15	-0.14

b

Variable	PC1	PC2	PC3
Asc-P	0.16	0.28	0.20
River Flow	0.05	0.47	0.35
TP-B	0.28	0.01	0.24
DO 7m	0.15	0.22	0.17
Cha a 7m	0.35	0.02	0.03

3. Influence of altering oxygen conditions and Capitella capitata activity on sediment biogeochemistry

3.1. Abstract

The low oxygen (O_2) concentrations and the presence of benthic fauna have been reported as the primary factors responsible for internal loading of phosphorus from the sediments and consequentially algal blooms. Both factors are often linked to enhance dissimilatory iron reduction and subsequently the availability of bound phosphorus at sediment water interface. However, the amount of P uptake/release in presence of benthic fauna under varying oxygen conditions remains questionable. The present study aimed at quantifying the impact of *Capitella capitata* activity on sedimentary P flux under altering oxygenation conditions. An experimental approach was used to test varying oxygen conditions and the role of benthic fauna in microcosms. The presence of *C. capitata* led to the introduction of oxygenated pore water into anoxic regions of the sediment in oxic treatment through burrow formation. In the presence of *C. capitata*, the Fe-bound P pool was two times higher in the oxic (100 %) treatment compared to oxic treatment without worms during an initial incubation. Upon altering oxygenation of the water column, a five times lower Fe-bound P pool was observed in treatment with worms under altering oxic (10 %) and anoxic conditions compared to treatment with worms under oxic (100 %) condition. The remarkably lower total P pool, reduction induced color change (brown to black) and higher P flux (1166 μmol m^{-2} d^{-1}) from the sediment in treatment with worms under altering oxic (10 %) and anoxic condition could only be explained through an enhanced bioirrigation and sediment respiration effect. Using ascorbate extraction, a fivefold decrease in content of amorphous iron oxyhydroxide bound P was observed in treatment with worm under oxic (10 %) and anoxic condition compared to a one-third decrease in crystalline content from CDB extraction. The results highlight the potential of bioirrigating fauna in altering sediment biogeochemistry. Thus, the study shows that the emergence of benthic fauna can induce enhanced P uptake under completely oxic conditions, however, the establishment of low oxygen conditions at sediment water interface can produce larger P effluxes with fauna.

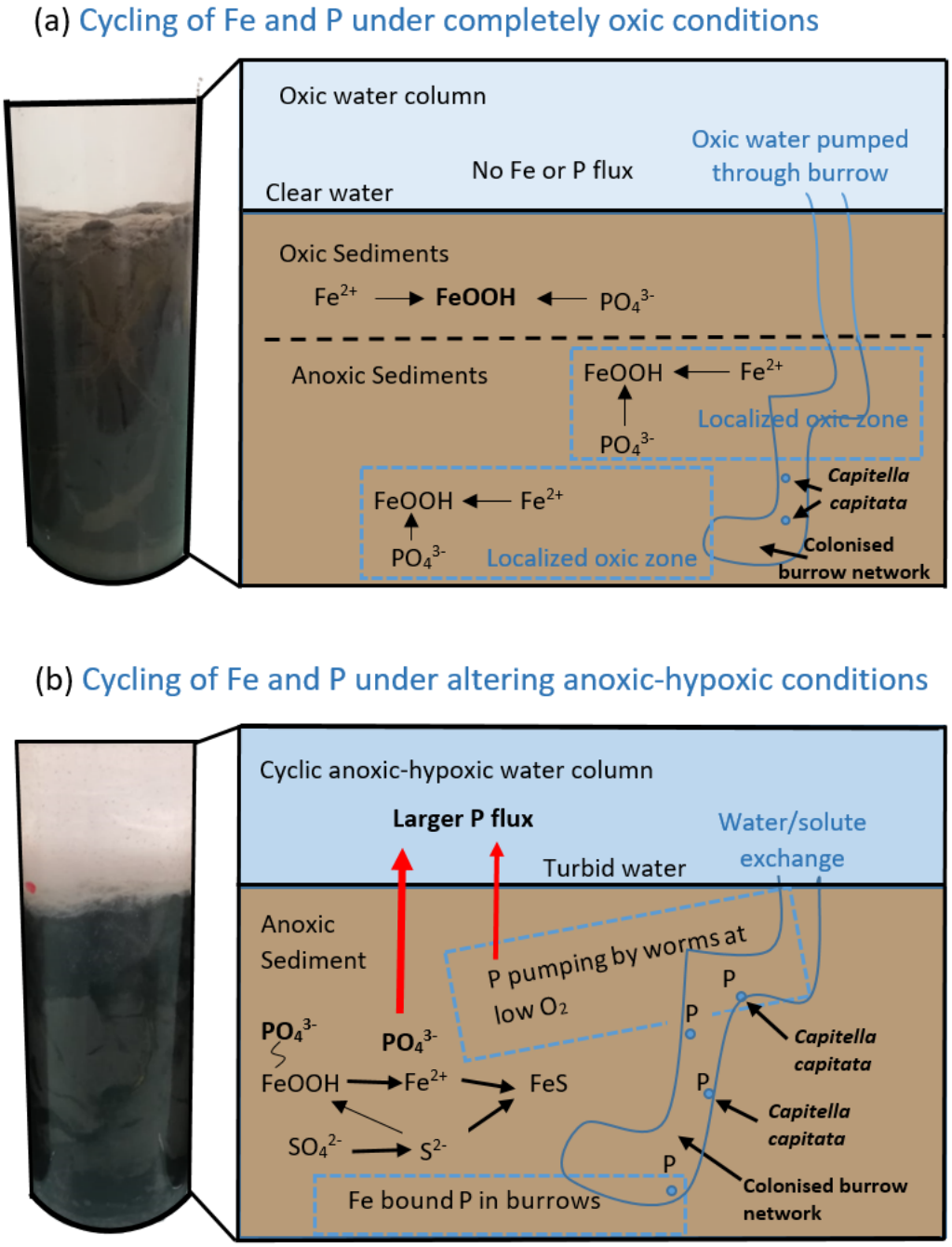

Graphical abstract

3.2. Introduction

Estuarine systems around the world may experience periods of seasonal algal bloom leading to bottom water deoxygenation. The internal P loading from sediments in lakes and estuaries as part of bottom water hypoxia/anoxia have been shown to release trapped sediment phosphorus acting as an important control on the formation and perseverance of algal blooms. (Biddanda et al., 2018; Howarth et al., 2011). Redox sensitive iron dynamics control phosphate adsorbed to iron (III) compounds under oxic conditions while anoxia lead iron (III) reduction to iron (II) subsequently returning both iron and sorbed phosphate into solution (Korppoo et al., 2012; Reed et al., 2011). As a result, dissolution of Fe-oxides upon the onset of hypoxia or anoxia and release of associated P acts as a major source of bioavailable-P that fuels primary productivity (Watson et al., 2017). The role of benthic fauna activity in sediment P dynamics adds complexity to the understanding of sedimentary biogeochemical cycles.

Bioirrigation refers to the enhanced exchange of solutes across sediment water interface caused by benthic fauna for feeding and respiratory purposes (Kristensen et al., 2012). Bioirrigation activities enhance the sediment phosphorus binding capacity through increased oxygen penetration due to pumping action of worms and diffusion of inorganic nutrients leading to a formation of iron oxyhydroxides bound P on the exposed burrow walls. The hypoxia can then lead to a more pronounced release of P from the sediments. The pumping activity of bioturbators reinforces the transport of solutes between sediment and water generating iron oxyhydroxides by transporting oxygen into the area surrounding the burrows and increase P retention (Carstensen et al., 2014; Danielsson et al., 2018). Hupfer et al. (2019) used microcosms to quantify the Fe bound P pool dynamics under controlled conditions. He showed that the accumulation of P on sediment surface and in burrows was mainly in the form of Fe bound P pool, acting as hotspots for dissolution once conditions are set reducing. Uptake and release of phosphorus associated with iron oxides within sediments has previously been studied in Gippsland Lakes system and deep dynamic pools (extended to > 20cm) of phosphorus developed from polychaete *C. capitata* burrowing activity were observed. However, the Fe bound P pools quickly disappeared on the onset of anoxia (Scicluna et al., 2015).

The impact of benthic fauna on internal loading of phosphorus from the sediment to the surface water is yet to be clearly quantified and may be an important factor that controls lakes trophic state (Parsons et al., 2017; Wang et al., 2018). Experiments conducted on benthic fauna under varying oxygen conditions have shown that the most fauna could survive intermittent or short-term hypoxia while only a few fauna were tolerant to the formation of anoxia (Riedel et al., 2012). Fauna are also known to ventilate their burrows more often when the oxygen concentration is relatively low in the overlying water, but very low levels (below 0.5 mg/L) or absence of oxygen can inhibit bioirrigation activity and lead to mortality (Nogaro et al., 2008; Norkko et al., 2012; Sturdivant et al., 2012). The benthic fauna sensitivity and tolerance to oxygen regime are key characteristics for their survivability and activity. This suggest an enhance burrow ventilation for some fauna than for others under some specific oxygen conditions. The enhanced ventilation and mixing caused by the benthic fauna is known to contribute to the phosphorus release from sediments (Leote & Epping, 2015).

Zhu et al. (2016) simulated that the benthic fauna strongly influence the sediment nutrient fluxes through bioirrigation activities acting as a sink for P upon oxygenation and as a significant source of P on the onset of anoxia, thus enhancing algal blooms in the Gippsland Lakes. He showed that the oxygen regime in the lakes is variable (Zhu et al., 2017). The Gippsland Lakes are a coastal lagoon

system that tends to experience seiche and tidal effect due to strong wind forcing and mixed semidiurnal tides leading to cyclic changes of oxygen conditions at the SWI. *C. capitata* worms have previously been shown to play a role in the accumulation of P within the Gippsland Lakes sediment under oxic conditions (Scicluna et al., 2015). They have also shown remarkable ability to survive hypoxic-anoxic conditions and produce burrow structures deep into the sediments (Chareonpanich et al., 1994; Rosenberg et al., 2001). It is well known that some fauna can show increased activity under low oxygen conditions (Herreid, 1980). Based on these observations, I hypothesise that *C. capitata* worms may play a role in enhancing sediment P release under cyclic hypoxic-anoxic conditions. My aim was 1) to measure how much the presence of *C. capitata* alters sediment biogeochemistry and water chemistry under oxic, anoxic or cyclic hypoxic/anoxic conditions and 2) to investigate the significance of Fe bound P pool in relation to the sedimentary P fluxes. In this study, laboratory experiments were performed to investigate the impacts of varying oxygen condition on P dynamics across the sediment water interface on microcosms prepared from LKN sediment cores. The changes of P fluxes over time and microcosm Fe and P fractions at the end of the experiment were measured.

3.3. Materials and methods

3.3.1. Microcosms

Sediment cores were collected using a 29cm x 6.6cm transparent polycarbonate cylinder from Lake King North (LKN) of Gippsland Lakes, Victoria, Australia (37° 52’ 32’’ S, 147° 45’ 26” E). This site has previously been studied in detail by Scicluna et al. 2015 to investigate the uptake and release of phosphorus associated with iron oxides within the sediments. Field sampling was similar to the methods adopted in chapter 2. The polycarbonate cylinder was inserted directly into the sediment and the cores were capped and sealed using rubber stoppers. The cores were stored at in-situ temperature during transport between the field and the laboratory. To measure water quality (pH, temperature, dissolved oxygen, electric conductivity and turbidity) at the time of sampling, a Horiba multi-probe meter was used. Six sediment cores collected from the Gippsland Lakes (LKN) were sieved through a 500 μm mesh sieve and repacked into 24 microcosms (small core liners (L = 12 cm, D = 4 cm)). The sediments were carefully homogenised before packing them into core liners (microcosms). *C. capitata* used in the experiment were retrieved after sieving sediments cores collected from another site, Patterson Lakes in SE Melbourne (38° 03’ 59.7’’ S, 145° 08’ 16.7” E) using an Ekman grab sampler. *C. capitata* were added at a density of ~2700 individual’s m^{-2}.

3.3.4. Principal experimental design

Alternating oxygen concentrations

Twenty-four microcosms were set up to explore the impact of *C. capitata* and oxygen concentrations on sediment biogeochemistry. Before experiments commenced all microcosms were pre-incubated for a period of 30 days with 128 μM P addition at the start. Aerators were used to provide oxic conditions during the initial incubation. Phosphorus concentrations were measured regularly (every second day) in the overlying water during the pre-incubation and the cores were examined for burrowing activity in the sediment. Six out of total 24 sediment core microcosms (3 with, 3 without worms) were sectioned (profiles: 0-0.5, 0.5-1, 1-3 and 3-7 cm) to obtain initial Fe and P concentrations in the sediments at the end of initial incubation.

Six scenarios were tested with three microcosms per condition (Supplementary Fig. S6). The experimental design can be summarised as follows: (1) 6 cores (3 with, 3 without worms) incubated under 0%/10% oxic condition on an alternating cycle of 24hours each for a period of 32 days. We hypothesise that worms presence will lead to enhanced P flux out of the sediment. (2) 6 cores (3 with, 3 without) incubated under 0%/100% oxic condition on an alternating cycle of 24 hours each for a period of 32 days. It was hypothesised that this would have much less P loss due to worms bioirrigation effect, as the cores will more rapidly re-oxidise. (3) 3 cores (with worm) incubated under 10% constant oxic condition and 3 cores (with worm) incubated under completely oxic incubation (100%) for a period of 32 days. It was hypothesised that this would have no P loss due to an enhanced worms bioirrigation effect, as the cores will remain oxidised.

Stable oxygen concentrations

In a separate experiment, the effect of anoxia and stable oxygen condition on *C. capitata* activity and sediment biogeochemistry were investigated by pre-incubating 15 microcosms under oxic condition for a period of 21 days with 720 μM P addition at the start. Aerators were used to provide oxic conditions during the initial incubation. 6 cores (3 with, 3 without worms) were then incubated under anoxic conditions and 9 cores with worms were incubated under constant 10%, 47% and 100% oxic conditions (3 for each treatment) for a period of 22 days. It was hypothesized that anoxia will result in an initially high P flux resulting from combined effect of anoxic conditions and bioirrigation but P flux will be greatly reduced with worms mortality. Sediment cores were sectioned (profiles: 0-0.5, 0.5-1, 1-3 and 3-7 cm) to obtain final Fe and P concentrations in the sediments at the end of the experiment.

3.3.4. Sequential extraction

The sediment sequential extraction schemes for Fe and P and subsequent analysis were performed under anoxic condition via argon purging. The extracts were passed through a 0.45 mm nylon filter from all sequential extractions. The P fraction scheme used in this study is based on two previous extraction methods (Psenner et al., 1988; Ruttenberg, 1992) with slight modification (Table. 3.1). The solid phase Fe was fractionated using sequential extraction described by Hermans et al. (2019).

Table 3.1. The sequential extraction scheme used in the study for sedimentary Fe and P fractionation.

Target P phase	**Extractant**	**Time**
Exchangeable P (MG-P)	1 M $MgCl_2$	2 hours
Ferrihydrite bound P (amorphous Fe-P or Asc-P)	.057M Ascorbic acid/.17 sodium citrate/ .6 sodium bicarbonate	24 hours
Reactive Fe-bound P (Crystalline Fe-P or CDB-P)	CDB buffered to pH 7.5	8 hours
SRP/NRP	1 M NaOH	24 hours
Calcium phosphate (HCl-P)	1M HCl	24 hours
Organic P	1M HCl , after ashing at 550^{o}C	2 hours
Target Fe phase	**Extractant**	**Time**
Ferrihydrite (Iron oxyhydroxide)	.057M Ascorbic acid/.17 sodium citrate/ .6 sodium bicarbonate	24 hours
Labile Fe(III) oxides or oxyhydroxides and FeS	1M HCl	4hours
Crystalline Fe oxides	CDB buffered to pH 7.5	8 hours
Magnetite	0.2 M Oxalate	6 hours

Pyrite	HNO_3 (65-70%)	2 hours

3.3.4. Analytical methods and statistical analyses

Concentrations of Fe were analysed spectrophotometrically (UV/ VIS 918 (GBC)) using the ferrozine method (Stookey, 1970), except for the Fe in CDB extracts. The samples were stabilised using 0.01M ferrozine (Sigma-Aldrich) and were be kept in dark before being analysed at 562 nm. Dissolved HPO_4^{2-} in all extracts, except CDB, was analysed using a Lachat Quikchem 8000 flow injection analyser (Protocol guidelines for APHA 4500-P was followed during the FIA analysis). Phosphorus and iron concentrations in the CDB extracts were determined by ICP-OES (Thermo *iCAP* 7000 series). Standard reference materials, sample spiking technique and matrix matched calibration curves ensured reliability of results in FIA and ICP sample analysis.

The mean and standard deviation of the three replicate of each treatment were carried out by descriptive statistics. After 32 days of experimental incubation, the effects of treatments on P effluxes were determined using a one-way RM-ANOVA to detect differences among treatments with time as the repeated factor (day 10-22). If differences were determined, Tukey's test was also used to define which treatments differed. All statistical analyses were performed using GraphPad Prism version 9.0.0 for Windows, GraphPad Software, San Diego, California, USA.

3.4. Results

3.4.1. Core pre-incubation

C. capitata started burrowing within the first few hours of their emplacement on sediment surface. The initial oxic incubation was continued for 30 day and the formation of yellow red iron oxides deep into the sediment were observed over this period (Fig. 3.1a). There was an uptake of ~70% P from the overlying water during the first 2 days owing to the rapid colonization by worms and a total uptake of 112.5 μM P during the oxic incubation (Fig. 3.1b).

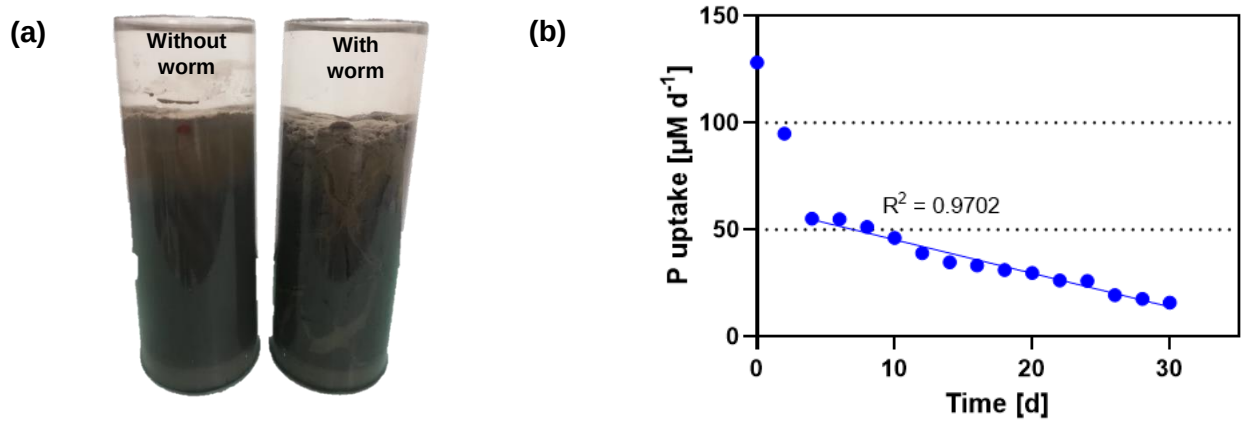

Figure 3.1. Initial incubation (a) worms presence as opposed to cores without worm indicating iron bound P pool development deep into the sediment (b) P uptake during the initial 30 days period.

The oxic incubation showed enrichment of iron oxyhydroxide near the sediment water interface with a strong influence from burrowing activity (Asc-Fe ~36 μmol g^{-1} dry sed +worms and ~23 μmol g^{-1} dry sed -worms). The iron oxyhydrooxide pool decreased quickly with depth in the sediment (Fig. 3.2a). Asc-P within the sediment was consistently higher in the worm treatments with the largest difference being observed at the surface of the sediment (14.5 μmol g^{-1} dry sed vs 6.1 μmol g^{-1} dry

sed) and the lowest difference at 5cm (1.9 μmol g^{-1} dry sed vs 1.5 μmol g^{-1} dry sed, Fig. 3.2b). A high proportion of Asc-P (> 63%) at the sediment surface in worm treatments contrary to without worm treatments (~47%), characterize the excessive formation of freshly precipitated Fe(III) oxyhydroxides by worms and subsequent P adsorption onto it. The CDB-P and Fe fractions that targets more crystalline Fe oxides and bound P varied relatively little with depth and did not show the pronounced difference observed in the Asc P fraction. All incubation with worms showed a decrease in pore water filterable reactive (FRP) profile, mirroring an increase in Asc-P pool (Fig. 3.2e). This is consistent with the hypothesis that bioirrigation would lead to an enhanced iron bound phosphorus formation through introduction of oxygenated overlying water into the sediment. The exchangeable P ($MgCl_2$ extractable) was quite low ranging between 0.3-0.7 μmol g^{-1} dry sed and 0.2-1 μmol g^{-1} dry sed in worm treated and untreated cores. Mean concentrations of $MgCl_2$, HCl and NaOH extractable P comprised only a small fraction of the total extractable P pool (supplementary Fig. S1).

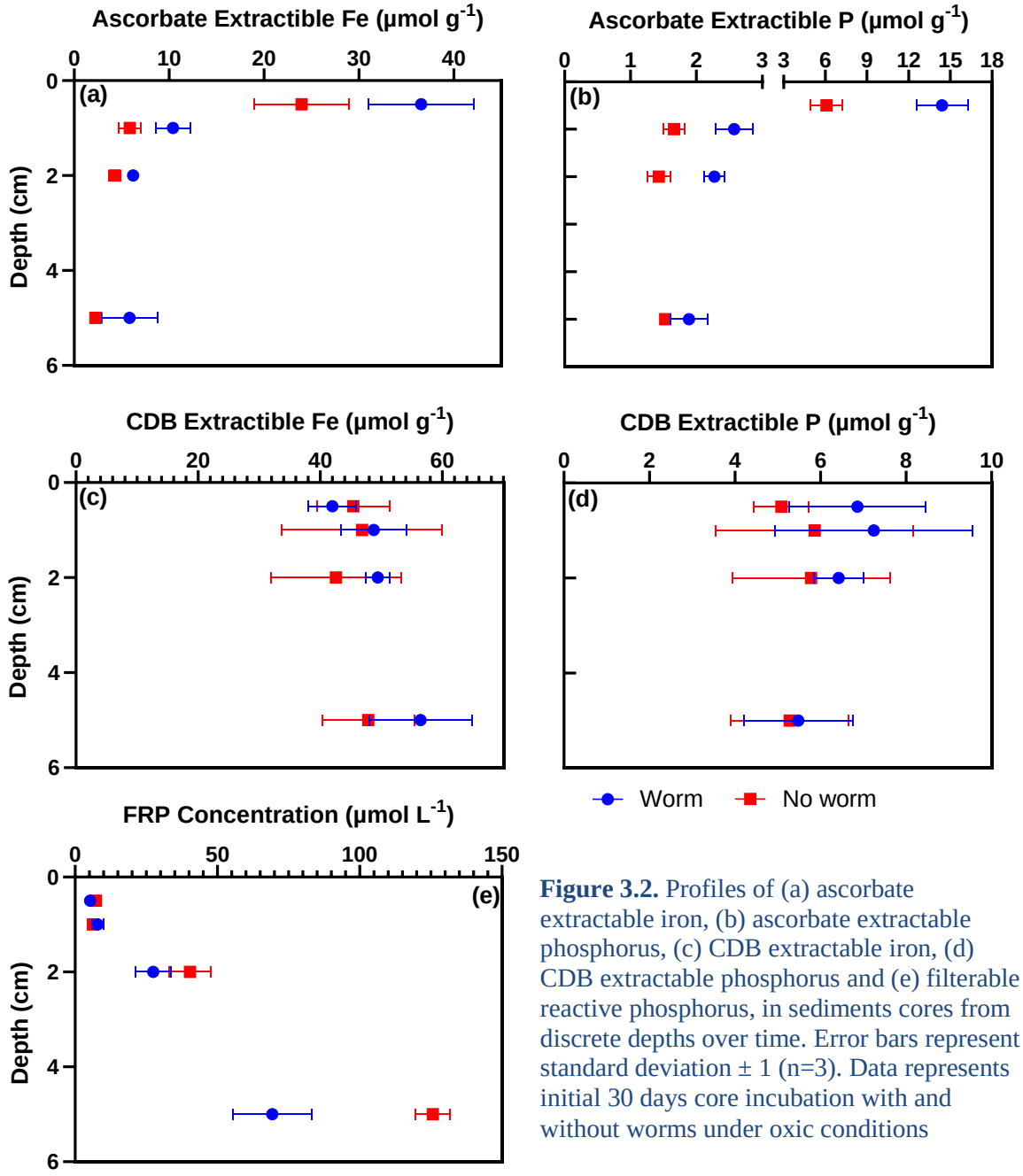

Figure 3.2. Profiles of (a) ascorbate extractable iron, (b) ascorbate extractable phosphorus, (c) CDB extractable iron, (d) CDB extractable phosphorus and (e) filterable reactive phosphorus, in sediments cores from discrete depths over time. Error bars represent standard deviation ± 1 (n=3). Data represents initial 30 days core incubation with and without worms under oxic conditions

3.4.2. Phosphorus efflux experiments

In altering oxygen concentration treatments, the only treatment that resulted in a sustained efflux of P from the sediment was the 10/0 + worms treatment (Fig. 3.3). Within this treatment, a fouling (turbidity and sediment particles stuck to the core walls) was observed, and dead *C. capitata* were observed at the surface of the sediment on day 18. The P fluxes increased significantly for oxygen condition 10/0 +W treatment during 10-20 days of the experiment. This increase in P flux was significantly higher compared to all other treatments with and without worms (one-way RM-ANOVA, oxygen condition 10/0 +W treatment, $p < 0.0001$). The P production rates declined after day 20 in 10/0 +worms treatment, suggesting exhaustion of P binding sites or worm mortality. The P fluxes followed an alternating pattern of P negative and positive fluxes owing to the release of P upon the onset of anoxia and sediment re-oxidizing upon exposure to oxygen. In stable oxygen

concentration treatments, only anoxic treatments with and without worms resulted in initially high efflux of P from the sediment (Fig. 3.6). The maximum efflux of P was observed for anoxic +W which was nearly two times the amount of P flux observed in anoxic -W.

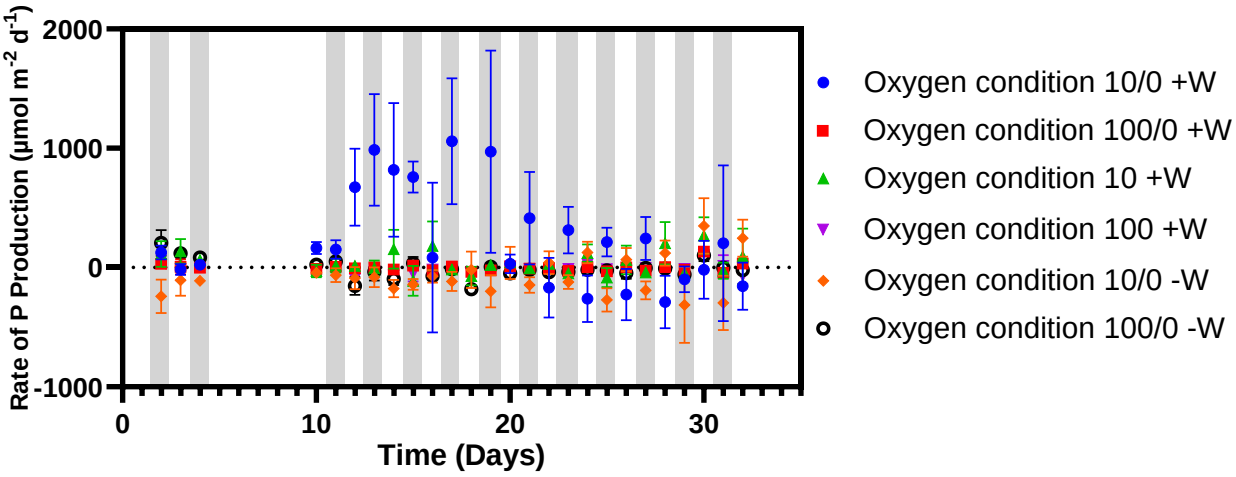

Figure 3.3. Comparison of P uptake/release during the 32 days incubation of cores with and without the addition of worms subjected to constant and oscillating oxygen conditions. The number 0, 10 and 100 indicate oxygen condition with 0 being completely anoxic while +W indicate worm presence and -W absence. A forward slash symbol between numbers indicate altering of oxygen condition every 24 housrs.

FRP concentrations in sediments generally increased with depth for all treatments. The presence of very little FRP at the surface and lowest FRP at the bottom in +worm 100 and +worm 100/0 treatment together with low phosphorus enrichment in overlying water suggest worm activity enhanced P retention capacity in sediments through oxygenation and rapid cycling of phosphorus at sediment water interface. By contrast, Pore water mean FRP concentration increased from 27 μmol L^{-1} to ~50 μmol L^{-1} in +worms 10% and +worms 10/0 incubations (Fig. 3.4a). The exchangeable P pool ($MgCl_2$ extractable) increased from 0.5 μmol g^{-1} dry sed to ~0.9 μmol g^{-1} dry sed for all other treatments except completely oxic and 100/0W, corresponding to the release of P from iron oxyhydroxides (Fig. 3.4b). The Asc-P concentration was highest in 100% oxic treatment with worms, reaching up to 14 μmol g^{-1} dry sed at surface, while 10/0 treatment with worms had the lowest concentration of 2 μmol g^{-1} dry sed at the surface. At the conclusion of the experiment, the mean Asc-P for the 100% oxic treatment with worms was same as mean Asc-P (~5.2 μmol g^{-1} dry sed) for initial incubation. The mean Asc-Fe increased to 19 μmol g^{-1} dry sed as opposed to 14 μmol g^{-1} dry sed at start, validating unavailability of additional P for P binding sites. The sequential CDB-P step, comprised a uniform pool of P throughout the profile, the only exception being the 100W treatment where an increase in CDB-Fe pool was accompanied by an increase in CDB-P pool. The NaOH and HCl extractable P pool showed little to no change with mean concentrations ranging between 0.15-0.3 μmol g^{-1} dry sed for NaOH-P and 0.9-2 μmol g^{-1} dry sed for HCl-P fraction (supplementary Fig. S2). The total P content in completely oxic treatment with worms were distinctly higher near the surface than all other treatments with worms (Fig. 3.5).

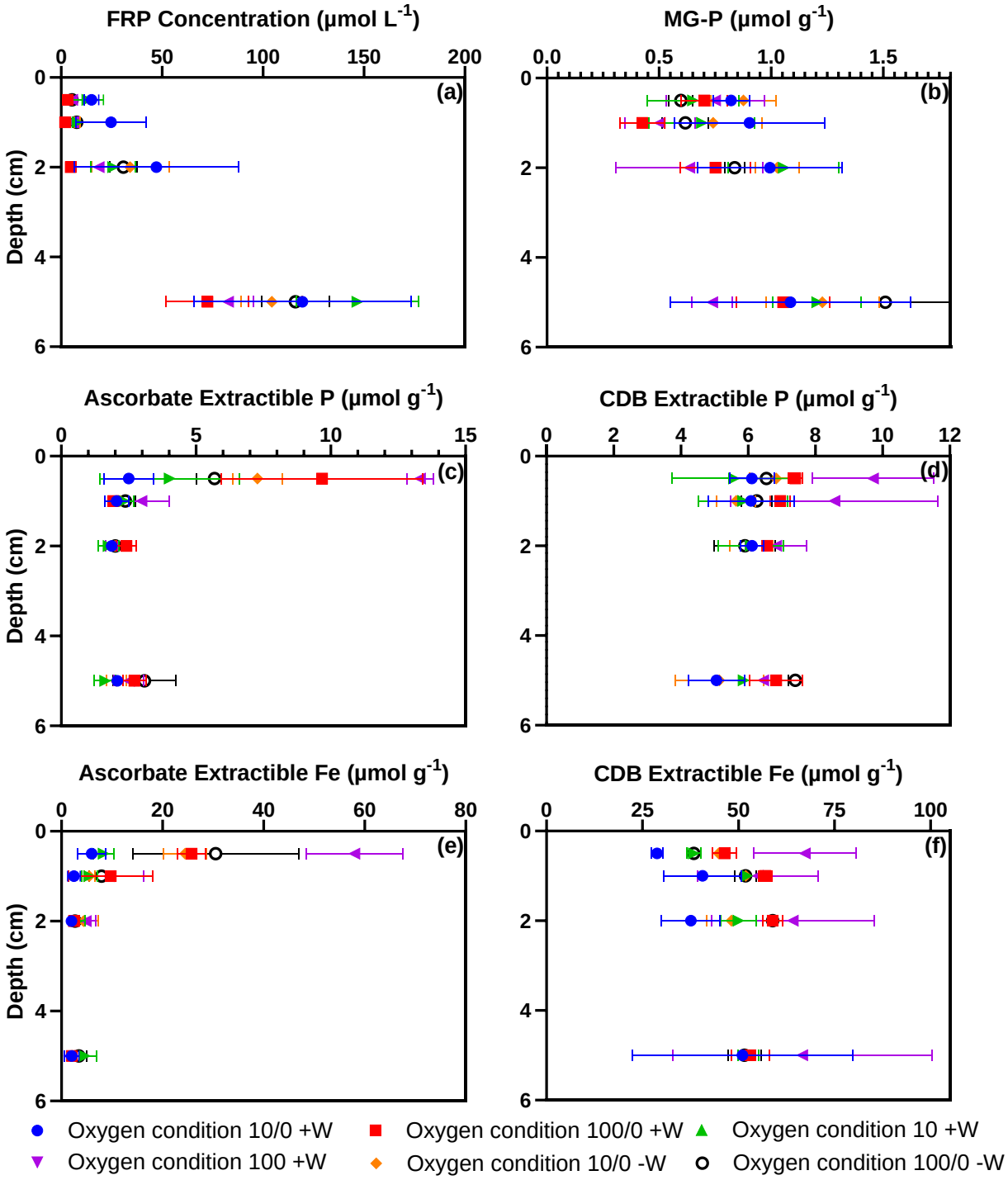

Figure 3.4. Profiles of (a) filterable reactive phosphorus, (b) exchangeable phosphorus (c) ascorbate extractable phosphorus, (d) CDB extractable phosphorus (e) ascorbate extractable iron, and (f) CDB extractable iron in sediments cores from discrete depths over time. Error bars represent standard deviation ± 1 (n=3). Data represents 32 days core incubation output with and without addition of worms under varying oxic conditions

An increase in Asc-Fe fraction accompanied by an increase in Asc-P during the oxic incubation and a decrease in Asc-Fe leading to a decrease in Asc-P during anoxia support the notion that ascorbate extractable fraction gave a good estimate of the changes in iron bound P pool (Fig. 3.4c,d). The correlation between Asc-P and Asc-Fe confirms the role of FeOOH in P adsorption and the efficacy of ascorbate step (supplementary information, Fig. 3). A mass balance for the sediment and water

column showed that the enhanced water column P-flux accounted for >75% of the decrease in ascorbate P pool in +worms 10/0 incubation. The CDB-P and Fe fractions represented a significant proportion of the total Fe and P pool, with a concentration range of ~5-6 μmol P g^{-1} dry sed and ~40-60 μmol Fe g^{-1} dry sed throughout the sediment profile (Fig. 3.4e,f).

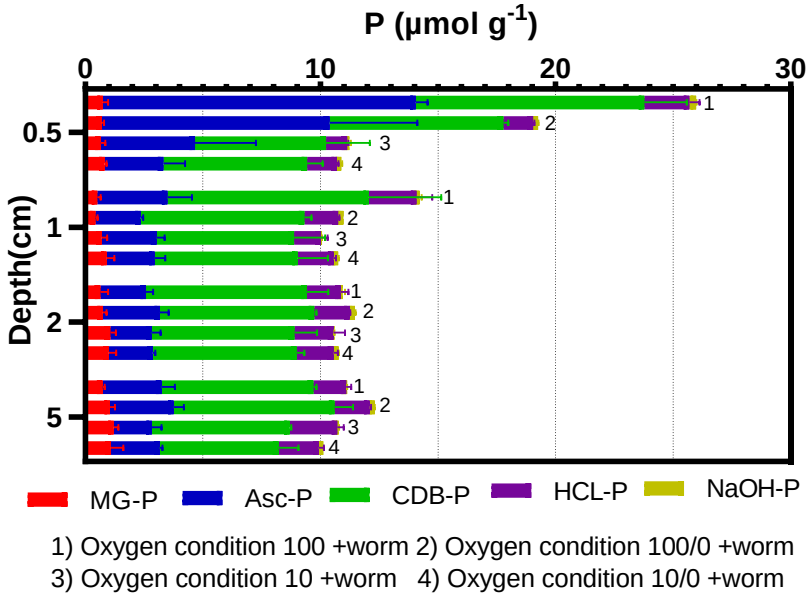

Figure 3.5. Impact of varying oxic conditions (with and without worms) on five sequential extraction fractions of phosphorus (P μmol g-1) in sediment core samples taken at end of experiment as depth profile

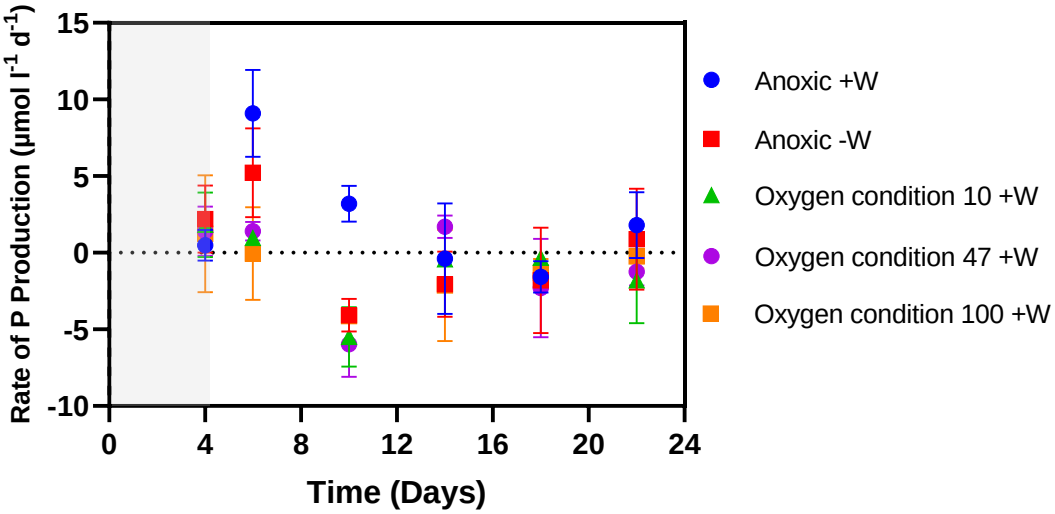

Figure 3.6. Rate of P uptake/release during the 22 days incubation of cores with worms under anoxia and with worms stable oxygen conditions. The numbers 10, 47 and 100 indicate the oxygen condition. +W indicate presence of worms and –W absence.

3.5. Discussion

3.5.1. The mechanism for enhanced P release by worms (respiration and irrigation)

It has been shown that the redox sensitive iron dynamics keep phosphorus sorbed to iron (III) compounds under oxic conditions while anoxia led to iron reduction, returning both iron and sorbed phosphate into solution (Korppoo et al., 2012; Reed et al., 2011). The presence of *C. capitata* in the current study has led to the construction of burrows and successive oxygenation of these galleries together with phosphorus addition resulted in an enhanced uptake of P by Fe oxyhydroxides during the initial oxic incubation. The low mean concentration of FRP within the deeper pore water of +worm sediments at the end of initial incubation support existence of heterogeneous oxic regions incorporating P sorbed onto Fe(III) oxides. The continuation of low FRP and the persistence of similar Asc-P pool in +worms 100% and 100/0 incubation following the initial worm incubation indicate the absence of P for stimulating adsorption. The case is further supported by an increased Fe oxide pool, more yellowish brown coloured oxic zone and high Fe:P ratios, indicating the presence of P-binding sites. This is consistent with the literature that bioirrigation improves the P retention capacity of sediments through enhanced iron bound phosphorus burial under oxic conditions (Lewandowski et al., 2007; Norkko et al., 2012).

Conversely, oscillating hypoxic-anoxic conditions produced high P-flux from the sediment in +worms 10/0 incubation. This is consistent with the expectation that anoxia will result in reductive dissolution of Fe oxides and build-up of P in porewater. It is likely hypoxia will intensify *C. capitata* activity for transporting oxygen into the sediment and consequently pumping out P into the overlying water. *C. capitata* has the ability to adapt well to oxygen depletion by relying solely on anaerobic metabolism but individuals normally die within several days of being exposed to anoxic conditions (Gamenick et al., 1998). A fourfold decrease in Asc-Fe and associated P pool and presence of more FRP in porewater observed in +worms 10/0 is therefore an effect of enhanced bioirrigation and respiration. The high P flux and absence of Fe^{2+} in pore water/overlying water suggests that the Fe released is ultimately bound in sulfidic form. The hypothesis is supported by the observed color change from brown to black and increase in Fe^{2+} to Fe^{3+} ratios in HCl-Fe extractable step (supplementary Fig. S4). Scicluna et al. (2015) observed a similar effect where colonization of sediments by *C. capitata* induced a rapid development of a deep dynamic P pool, which exhausted rapidly over seasonal hypoxia releasing P into overlying water column.

A remarkably similar P production rate was observed in a separate experiment where the cores (+worms) initially incubated under oxic conditions were exposed to anoxia. However, the P production rate declined immediately afterward as opposed to +worms 10/0 treatment suggesting worms died rendering reduced bioirrigation effect (supporting Fig. S6). Based on the outcomes of the experiments the impact of worms on sediment biogeochemistry in response to oxygen dynamics can be summarised into following three categories:

Bioirrigation acting as a sink for P (Increased sediment/water interface resulting from burrowing activity causing enhanced organic matter degradation and subsequent rapid iron bound phosphorus burial under oxic conditions).

Anoxia acting as a source for P (Anoxic conditions dissolving iron oxyhydroxides and rapid release of P through combined ventilation and upward diffusion factor, following up with *C. capitate* mortality and equilibrium establishment between porewater and overlying water)(Fig. 3.6).

Altering anoxic-hypoxic conditions in conjunction with bioirrigation acting as an enhanced source for P (Altering anoxic-hypoxic conditions allowing for the continuation of iron oxide reduction and P release during anoxia and upward transport of porewater P via bioirrigation and diffusion. The survivability of worm increases under cyclic anoxic-hypoxic conditions thereby enhancing the bioirrigation effect and associated mineralization of organic matter, re-oxidation of reduced species and upward transport of solutes) (Supplementary Fig. S5, S6).

3.5.2. Relative efficacy of the Asc vs CDB approaches

The ascorbate (Asc-Fe) extraction is known to extract fresh ferrihydrite and represents the most readily bioavailable form of Fe(III) as oxyhydroxides (Kostka & Luther, 1994; Raiswell et al, 2010). The citrate dithionite bicarbonate (CDB) step represent the most commonly used sequential fractionation to determine the most reactive Fe oxides and bound P (Gleyzes et al., 2002). However, the application of ascorbate extraction for oxyhydroxide bound P is quite limited in the literature. Unlike Fe fractionation, where ascorbate and CDB steps are frequently used to extract the amorphous and crystalline Fe oxide phases, a single widely acceptable approach for determination of labile P fractionation does not exist. Considering ascorbate gives an interference free approach and provides excellent recovery, it was recommended as an optimal method for Fe bound P extraction from sediment samples by Zhang and Lanning (2018) & Anschutz et al. (1998).

In this study, Asc-P/Fe extractions showed an excellent agreement between iron oxidation/reduction as well as subsequent P sorption/desorption. The rapid increase or decrease in Asc-P pool at surface and at depth for all treatments consequent to altering conditions shows accumulation/dissolution of iron bound P (Fig. 3.5, Supplementary Fig. S3). The fraction gave a good approximation of the ferrihydrite besides associated P pool and that CDB extracts too much Fe and P representing crystalline iron oxides and associated P. The CDB-P step was not as effective in representing the rapidly changing sediment biogeochemistry due to dissimilatory iron reduction and iron oxyhydroxide formation over shorter time scales. The ascorbate step followed up with CDB step in P extractions provide a good estimation for iron bound phosphorus dynamics in sediment pool.

3.5.3. The sediment mass balance

An evaluation of the changes in P pools induced by *C. capitata* were made through a mass balance approach by using the overlying water FRP and solid phase labile P data. If the Asc-P extraction gives a good approximation of the P associated with easily reduced iron oxyhydroxides, FRP in overlying water should mirror 1:1 changes in the sediment Asc-P pool. To obtain an estimate of total P input per unit sediment area, the concentration of P removed from the system (112.25 μM) was divided by the total sediment surface area (m^2). Considering the density (2.65 g/ml) for solid phase and the calculated porosity (0.89), the Sediment amorphous iron bound P content for each depth were derived from the Asc-P extraction data by multiplying the average Asc-P at each depth in μmol g^{-1} with bulk density (g m^{-3}). The Asc-P in each slice (μmol m^{-3}) was than multiplied by the depth of each slice (m) to obtain the integrated P (μmol m^{-2}). The natural Asc-P pool background of the sediment before the addition of P was subtracted from the integrated pool to determine the Total Asc-P inventory in the

sediment. A comparison of the total P uptake by the sediment and total Asc-P inventory in the sediment showed a ~69% recovery of P in Asc-P pool. Thus, the ascorbate P pool gave a good approximation of the P uptake during the oxic incubation.

To counter check the argument, the release of phosphorus during the 10/0 +worms treatment was compared with decrease in Asc-P pool of sediment. The Asc-P pool decreased >60% during the experiment and the mass balance showed a recovery of 76% of the decrease in the Asc pool in overlying water. About ~45% of this decrease came from the top 0.5cm of the sediment indicating the presence of highly reactive iron bound P pool on the sediment water interface. Incorporating the CDB-P fraction data into the equation lead to a recovery of >93% suggesting dissolution of more crystalline iron bound P. The strong agreement between the two independent quantities gives confidence in Asc-P extraction as an important step in sequential extraction scheme. The range of P flux (-0.5 to 1166 μmol m^{-2} d^{-1}) in intact sediment cores with and without worms shows the dependence of phosphorus fluxes on oxygen conditions and fauna presence. The diffusive P flux (1166 μmol m^{-2} d^{-1}, Supplementary Fig. S5) directed from the sediment into the overlying water corresponds to some of the highest fluxes estimated in literature (1180 μmol m^{-2} d^{-1} ; Berezina et al. (2019), 1300 μmol m^{-2} d^{-1}; Pitkänen et al, (2001) & 1199 μmol m^{-2} d^{-1} ; Boardman et al., (2010)). Artificially created anoxia in cores from Gulf of Finland resulted in P effluxes in the range of ~1200 μmol m^{-2} d^{-1} to the overlying water (Korppoo et al., 2012). Similarly, a source of P delivery resulted in P effluxes of about ~1200-2000 μmol m^{-2} d^{-1} higher than those before the inflow (Astrid Hylén1, 2021).

3.5.4. C. capitata effects on biogeochemical processes and relevance for estuarine systems

In context of the Gippsland Lakes, the findings of this work reveal that the presence of *C. capitata* can accelerate the uptake and release of P from the sediments. The rate by which *C. capitata* ventilate their burrows may vary considerably depending upon the oxygen condition at the sediment water interface. Under oxic conditions, bioirrigation activity by *C. capitata* coupled with the availability of P at the sediment water interface facilitates P binding to the iron oxyhydroxides. In contrast, bioirrigation coupled with large Fe bound P pool supports high P fluxes from the sediments. The wind forcing and tidal effects. Sensitivity of the *C. capitata* to varying oxygen condition was clearly shown by the difference in P fluxes between ~200 μmol m^{-2} d^{-1} during stable 10% oxygen condition and ~1150 μmol m^{-2} d^{-1} during artificially created cyclic 10% oxic and completely anoxic condition. Completely anoxic conditions may prevent extended P release from the sediment to the overlying water through *C. capitata* mortality; it is believed that the strong winds and tidal effect can support varying oxygen condition at sediment water interface resulting in extended P release from sediments in coastal lagoon systems like Gippsland Lakes.

The findings within this study demonstrate that the activity of benthic fauna is an important factor influencing nutrient cycling in aquatic systems. While many studies have concluded P fluxes to be primarily related to oxygen condition, the present study suggest that the availability of Fe and P, oxygen condition at the sediment water interface and the benthic fauna specie are critical to the sedimentary P uptake or release. The large-scale effect of benthic fauna on phosphorus dynamics is known to be dependent on the benthic community under consideration and their abundance (Zhang et al., 2010).

3.6. Conclusions

Our result shows that the P flux from sediment is related to the oxygen condition, availability of iron oxyhydroxide bound P and benthic fauna bioirrigation. The present study shows that the ascorbate and the more aggressive CDB can be utilised in succession to investigate the amorphous and less reactive Fe bound P fractions respectively. We conclude that the benthic fauna strongly influence the sediment nutrient fluxes through bioirrigation activities acting as a significant source of P on the onset of anoxia and sink of P upon oxygenation. Anoxia may lead to a high initial P flux but the extent of P release from the sediments is influenced by the survivability of worms under anoxic/hypoxic conditions. Further experimental studies investigating the bioirrigation effect of benthic fauna must focus on intact sediment cores to evaluate dependency on sediment characteristics and approach longer timescales to consider conversion of iron oxyhydroxide bound P fractions.

3.7. References

Anschutz, P., Zhong, S., Sundby, B., Mucci, A., & Gobeil, C. (1998). Burial efficiency of phosphorus and the geochemistry of iron in continental margin sediments. *Limnology and Oceanography, 43*(1), 53-64. doi:https://doi.org/10.4319/lo.1998.43.1.0053

Berezina, N., Maximov, A., & Vladimirova, O. (2019). The influence of benthic invertebrates on the phosphorus flux at the sediment-water interface in the easternmost Baltic Sea. *Marine Ecology Progress Series, 608*, 33-43. doi:https://doi.org/10.3354/meps12824

Biddanda, B. A., Weinke, A. D., Kendall, S. T., Gereaux, L. C., Holcomb, T. M., Snider, M. J., . . . Ruberg, S. A. (2018). Chronicles of hypoxia: Time-series buoy observations reveal annually recurring seasonal basin-wide hypoxia in Muskegon Lake – A Great Lakes estuary. *Journal of Great Lakes Research, 44*(2), 219-229.

doi:https://doi.org/10.1016/j.jglr.2017.12.008

Boardman, M. Robb. (2010). Role of sediments in nutrient cycling. *Department of water*, Western Australia.
Retrieved from: https://www.water.wa.gov.au/__data/assets/pdf_file/0013/3172/100174.pdf

Carstensen, J., Conley, D. J., Bonsdorff, E., Gustafsson, B. G., Hietanen, S., Janas, U., . . . Voss, M. (2014). Hypoxia in the Baltic Sea: Biogeochemical Cycles, Benthic Fauna, and Management. *AMBIO, 43*(1), 26-36.

doi:https://doi.org/10.1007/s13280-013-0474-7

Chareonpanich, C., Montani, S., Tsutsumi, H., & Nakamura, H. (1994). Estimation of Oxygen Consumption of a Deposit-feeding Polychaete *Capitella* sp. I. *Fisheries science, 60*(3), 249-251.

doi:https://doi.org/10.2331/fishsci.60.249

Danielsson, Å., Rahm, L., Brüchert, V., Bonaglia, S., Raymond, C., Svensson, O., Gunnarsson, J. (2018). Effects of re-oxygenation and bioturbation by the polychaete Marenzelleria arctia on phosphorus, iron and manganese dynamics in Baltic Sea sediments. *Boreal Environment Research, 23*, 15-23.
Retrieved from: https://www.diva-portal.org/smash/get/diva2:1181292/FULLTEXT01.pdf

Gamenick, I., Vismann, B., Grieshaber, M., & Giere, O. (1998). Ecophysiological differentiation of *Capitella capitata* (Polychaeta). Sibling species from different sulfidic habitats. *Marine Ecology Progress Series, 175*, 155-166. doi:https://doi.org/10.3354/meps175155

Gleyzes, C., Tellier, S., & Astruc, M. (2002). Fractionation studies of trace elements in contaminated soils and sediments: a review of sequential extraction procedures. *TrAC Trends in Analytical Chemistry, 21*(6), 451-467. doi:https://doi.org/10.1016/S0165-9936(02)00603-9

Hermans, M., Lenstra, W. K., van Helmond, N. A. G. M., Behrends, T., Egger, M., Séguret, M. J. M., . . . Slomp, C. P. (2019). Impact of natural re-oxygenation on the sediment dynamics of manganese, iron and phosphorus in a euxinic Baltic Sea basin. *Geochimica et Cosmochimica Acta, 246*, 174-196.

doi:https://doi.org/10.1016/j.gca.2018.11.033

Herreid, C. F. (1980). Hypoxia in invertebrates. *Comparative Biochemistry and Physiology Part A: Physiology, 67*(3), 311-320.

doi:https://doi.org/10.1016/S0300-9629(80)80002-8

Howarth, R., Chan, F., Conley, D. J., Garnier, J., Doney, S. C., Marino, R., & Billen, G. (2011). Coupled biogeochemical cycles: eutrophication and hypoxia in temperate estuaries and coastal marine ecosystems. *Frontiers in Ecology and the Environment, 9*(1), 18-26. doi:https://doi.org/10.1890/100008

Hupfer, M., Jordan, S., Herzog, C., Ebeling, C., Ladwig, R., Rothe, M., & Lewandowski, J. (2019). Chironomid larvae enhance phosphorus burial in lake sediments: Insights from long and short-term experiments. *Science of The Total Environment, 663*, 254-264.

doi:https://doi.org/10.1016/j.scitotenv.2019.01.274

Hylén Astrid, S. J. v. d. V., 3,4, Mikhail Kononets1, Mingyue Luo, Elin Almroth-Rosell, and Per O. J. Hall. (2021). Deep-water inflow event increases sedimentary phosphorus release on a multi-year scale. *Biogeosciences, 18*, 2981-3004.

doi:https://doi.org/10.5194/bg-18-2981-2021

Korppoo, M., Lukkari, K., Järvelä, J., Leivuori, M., Karvonen, T., & Stipa, T. (2012). Phosphorus release and sediment geochemistry in a low-salinity water bay of the Gulf of Finland. *Boreal Environment Research, 17*(3-4), 237–251. Retrieved from: https://helda.helsinki.fi/bitstream/handle/10138/229887/ber17-3-4-237.pdf

Kostka, J. E., & Luther, G. W. (1994). Partitioning and speciation of solid phase iron in saltmarsh sediments. *Geochimica et Cosmochimica Acta, 58*(7), 1701-1710. doi:https://doi.org/10.1016/0016-7037(94)90531-2

Kristensen, E., Penha-Lopes, G., Delefosse, M., Valdemarsen, T., Organo Quintana, C., & Banta, G. (2012). What is bioturbation? Need for a precise definition for fauna in aquatic science. *Marine Ecology Progress Series, 446*, 285-302. doi:https://doi.org/10.3354/meps09506

Leote, C., & Epping, E. H. G. (2015). Sediment–water exchange of nutrients in the Marsdiep basin, western Wadden Sea: Phosphorus limitation induced by a controlled release? *Continental Shelf Research, 92*, 44-58.

doi:https://doi.org/10.1016/j.csr.2014.11.007

Lewandowski, J., Laskov, C., & Hupfer, M. (2007). The relationship between Chironomus plumosus burrows and the spatial distribution of pore-water phosphate, iron and ammonium in lake sediments. *Freshwater Biology, 52*(2), 331-343. doi:https://doi.org/10.1111/j.1365-2427.2006.01702.x

Nogaro, G., Mermillod-Blondin, F., Montuelle, B., Boisson, J.-C., & Gibert, J. (2008). Chironomid larvae stimulate biogeochemical and microbial processes in a riverbed covered with fine sediment. *Aquatic Sciences, 70*(2), 156-168. doi:https://doi.org/10.1007/s00027-007-7032-y

Norkko, J., Reed, D. C., Timmermann, K., Norkko, A., Gustafsson, B. G., Bonsdorff, E., Conley, D. J. (2012). A welcome can of worms? Hypoxia mitigation by an invasive species. *Global Change Biology, 18*(2), 422-434. doi:https://doi.org/10.1111/j.1365-2486.2011.02513.x

Parsons, C., Rezanezhad, F., W. O'Connell, D., & Van Cappellen, P. (2017). Sediment phosphorus speciation and mobility under dynamic redox conditions. *Biogeosciences, 14*(14), 3585-3602.

doi:https://doi.org/10.5194/bg-14-3585-2017

Pitkänen, H., Lehtoranta, J., & Räike, A. (2001). Internal nutrient fluxes counteract decreases in external load: the case of the estuarial eastern Gulf of Finland, Baltic Sea. *Ambio, 30*(4-5), 195-201.

doi:https://doi.org/10.1579/0044-7447-30.4.195

Psenner, R., Boström, B., Dinka, M., Pettersson, K., & Puckso, R. (1988). Fractionation of phosphorus in suspended matter and sediment. *Arch Hydrobiol Beih Ergeb Limnol, 30*, 98-103. https://aslopubs.onlinelibrary.wiley.com/doi/pdf/10.4319/lom.2007.5.433

Raiswell, R., Vu, H. P., Brinza, L., & Benning, L. G. (2010). The determination of labile Fe in ferrihydrite by ascorbic acid extraction: Methodology, dissolution kinetics and loss of solubility with age and de-watering. *Chemical Geology, 278*(1), 70-79. doi:https://doi.org/10.1016/j.chemgeo.2010.09.002

Reed, D. C., Slomp, C. P., & Gustafsson, B. G. (2011). Sedimentary phosphorus dynamics and the evolution of bottom-water hypoxia: A coupled benthic–pelagic model of a coastal system. *Limnology and Oceanography, 56*(3), 1075-1092. doi:https://doi.org/10.4319/lo.2011.56.3.1075

Riedel, B., Zuschin, M., & Stachowitsch, M. (2012). Tolerance of benthic macrofauna to hypoxia and anoxia in shallow coastal seas: A realistic scenario. *Marine Ecology Progress, 458*, 39-52. doi:https://doi.org/10.3354/meps09724

Rosenberg, R., Nilsson, H. C., & Diaz, R. J. (2001). Response of Benthic Fauna and Changing Sediment Redox Profiles over a Hypoxic Gradient. *Estuarine Coastal and Shelf Science, 53*, 343-350.

doi:https://doi.org/10.1006/ecss.2001.0810

Ruttenberg, K. C. (1992). Development of a sequential extraction method for different forms of phosphorus in marine sediments. *Limnology and Oceanography, 37*(7), 1460-1482. doi:https://doi.org/10.4319/lo.1992.37.7.1460

Scicluna, T. R., Woodland, R. J., Zhu, Y., Grace, M. R., & Cook, P. L. M. (2015). Deep dynamic pools of phosphorus in the sediment of a temperate lagoon with recurring blooms of diazotrophic cyanobacteria. *Limnology and Oceanography, 60*(6), 2185-2196. doi:https://doi.org/10.1002/lno.10162

Stookey, L. L. (1970). Ferrozine---a new spectrophotometric reagent for iron. *Analytical Chemistry, 42*(7), 779-781. doi:https://doi.org/10.1021/ac60289a016

Sturdivant, S. K., Díaz, R. J., & Cutter, G. R. (2012). Bioturbation in a Declining Oxygen Environment, in situ Observations from Wormcam. *PLOS ONE, 7*(4), e34539. doi:https://doi.org/10.1371/journal.pone.0034539

Wang, J., Chen, J., Guo, J., Sun, Q., & Haiquan, Y. (2018). Combined Fe/P and Fe/S ratios as a practicable index for estimating the release potential of internal-P in freshwater sediment. *Environmental Science and Pollution Research, 25,* 10740–10751. doi:https://doi.org/10.1007/s11356-018-1373-z

Watson, A. J., Lenton, T. M., & Mills, B. J. W. (2017). Ocean deoxygenation, the global phosphorus cycle and the possibility of human-caused large-scale ocean anoxia. *Philosophical Transactions of the Royal Society A: Mathematical, Physical and Engineering Sciences, 375*(2102), 20160318.

doi:https://doi.org/10.1098/rsta.2016.0318

Zhu, Y., Hipsey, M. R., McCowan, A., Beardall, J., & Cook, P. L. M. (2016). The role of bioirrigation in sediment phosphorus dynamics and blooms of toxic cyanobacteria in a temperate lagoon. *Environmental Modelling & Software, 86*, 277-304. doi:https://doi.org/10.1016/j.envsoft.2016.09.023

Zhu., McCowan, A., & Cook, P. (2017). Effects of changes in nutrient loading and composition on hypoxia dynamics and internal nutrient cycling of a stratified coastal lagoon. *Biogeosciences, 14*, 4423-4433. doi:https://doi.org/10.5194/bg-14-4423-2017

Zhang, J.-Z., & Lanning, N. T. (2018). Ascorbic acid as a reductant for extraction of iron-bound phosphorus in soil samples: a method comparison study. *Communications in Soil Science and Plant Analysis, 49*(17), 2155-2161.

doi:https://doi.org/10.1080/00103624.2018.1499751

Zhang, L., Gu, X.-z., Fanl, C., Shang, J., Shen, Q., Wang, Z., & Shen, J. (2010). Impact of different benthic animals on phosphorus dynamics across the sediment-water interface. *Journal of environmental sciences, 22 11*, 1674-1682.

doi:https://doi.org/ 10.1016/S1001-0742(09)60305-3

3.8. Supplementary information

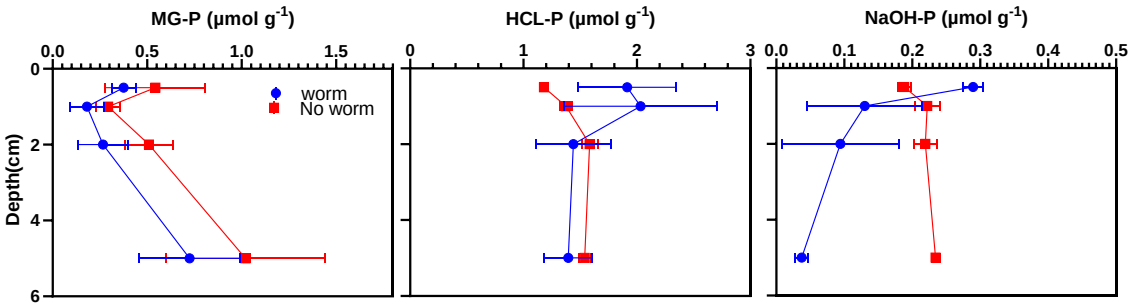

Figure S1. Profiles of (a) exchangeable phosphorus, (b) HCL extractable phosphorus, and (c) NaOH extractable P in sediments cores from discrete depths over time. Error bars represent standard deviation ± 1 (n=3).

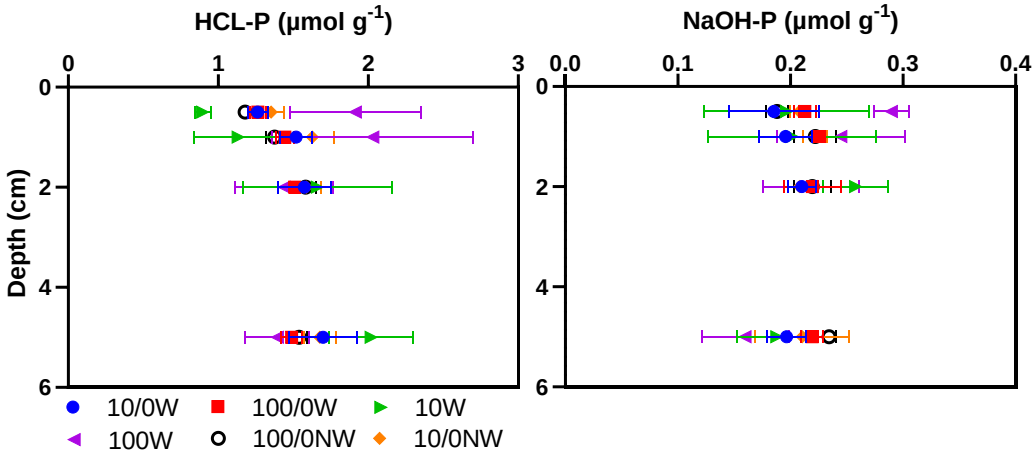

Figure S2. Profiles of acid and base extractable phosphorus in sediments cores from discrete depths over time. Error bars represent standard deviation ± 1 (n=3). Data represents 32 days core incubation output with and without addition of worms under varying oxic conditions

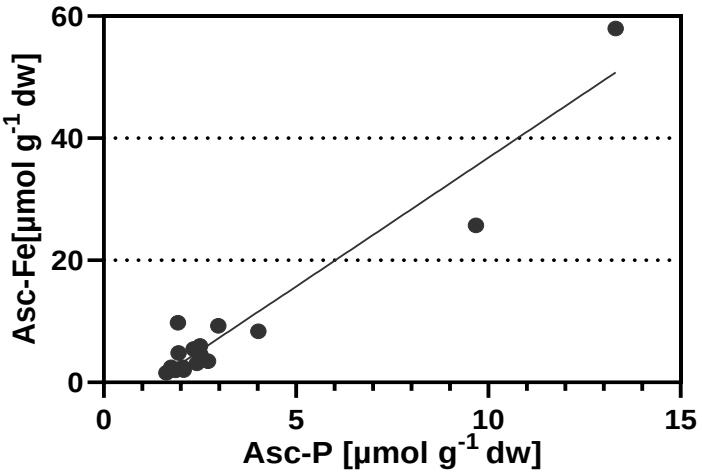

Figure S3. Relation between ascorbate extractable iron (Asc-Fe) and ascorbate extractable P (Asc-P) of oxidized as well as of anoxic sediments in P uptake experiments at all depths (Regression line: n=16, r2=0.92).

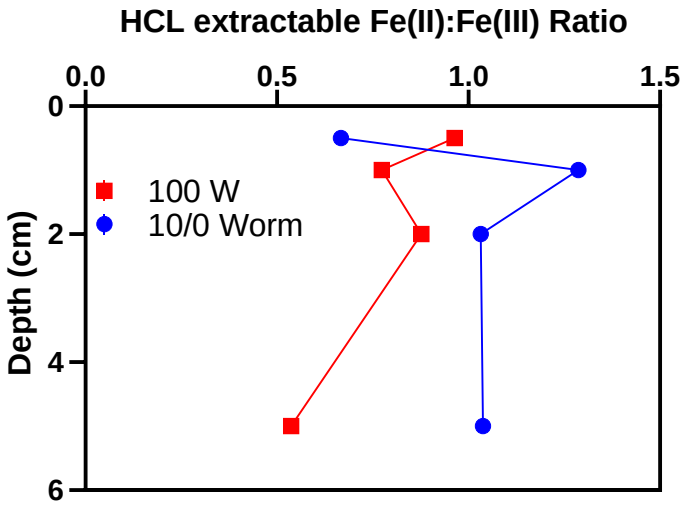

Figure S3. HCL extractable F(II):Fe(III) ratios indicating the change in iron monosulfide (FeS) formation in sediment cores.

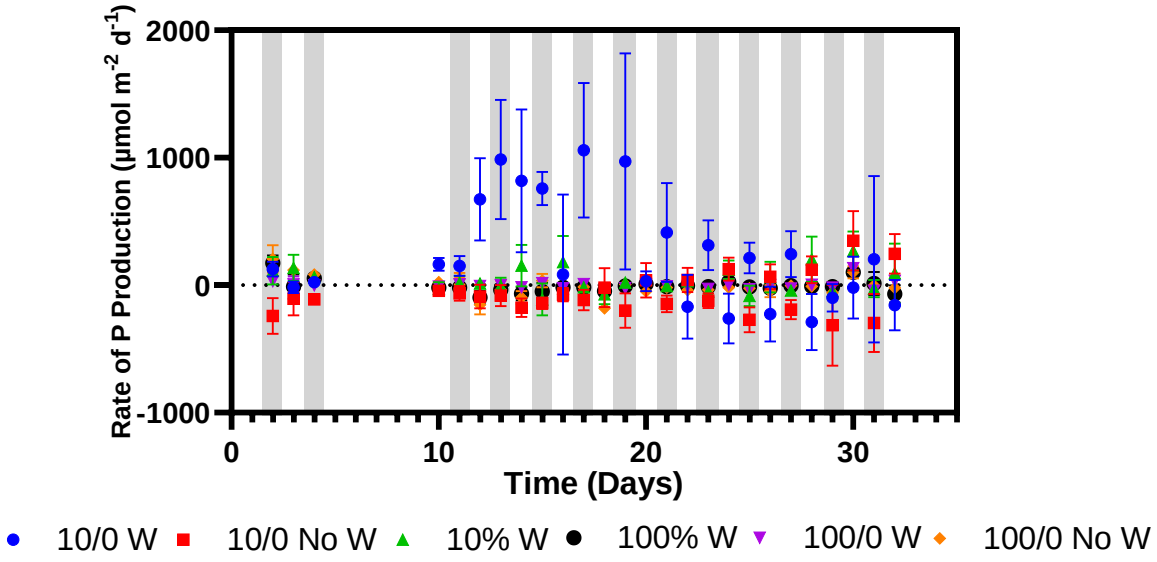

Fig. S5. Comparison of P uptake/release during the 32 days incubation of cores with and without the addition of worms subjected to constant and recurrent oxygen conditions

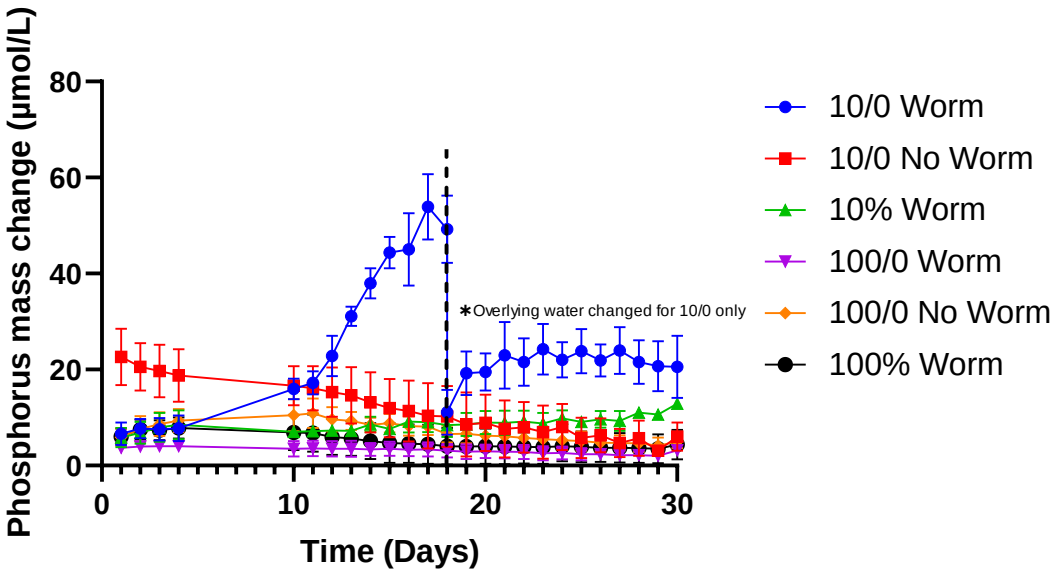

Fig. S6. Impact of *C. capitata* on P release from the sediments during the 30 days incubation of cores with worms under altering anoxic/hypoxic condition compared to uninhabited and oxic controls

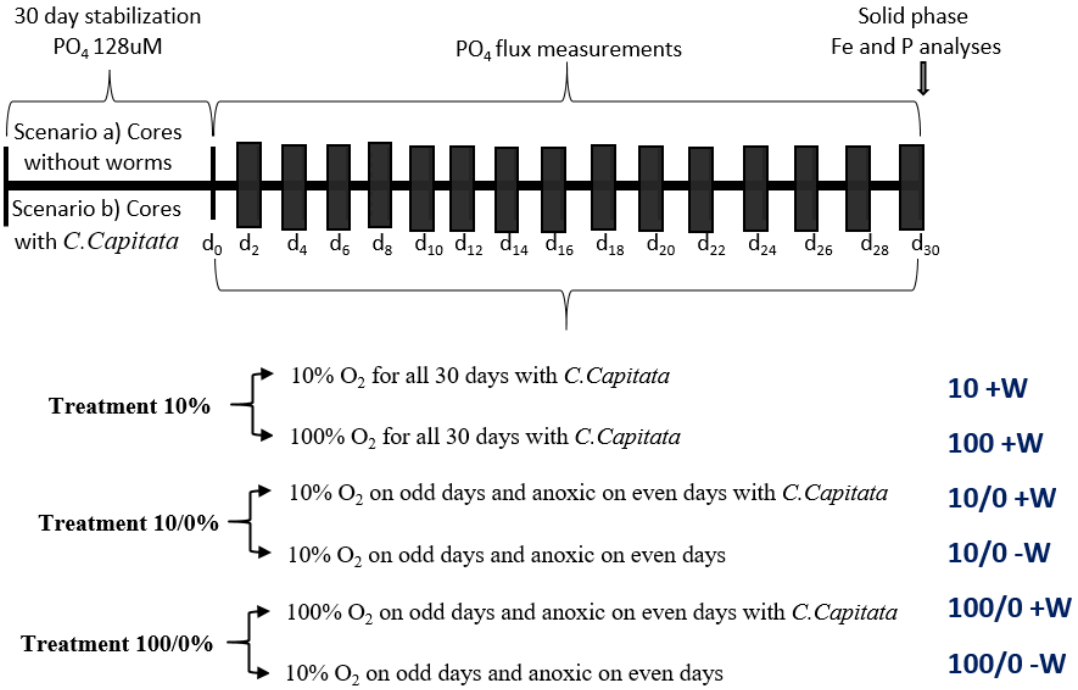

Fig. S7. A schematic view of the treatments performed on microcosms with and without worms

4. Application of a one-dimensional model to explore the interaction between bioirrigation and phosphorus release and storage within the sediment

4.1. Abstract

Bioirrigation defined as all transport processes of solute imposed by benthic fauna is a crucial factor controlling Fe and P cycling in the sediments. Benthic fauna activity in turn rely on environmental conditions and can result in enhanced solute fluxes occurring at sediment water interface through vigorous pumping. To better understand how bioirrigation impact sediment P cycling under oscillating oxic/hypoxic conditions, a mechanistic reactive 1D transport model was applied. First, the model was calibrated to simulate baseline scenarios representative of the environmental conditions experienced by sediment cores in the laboratory experiments. Second, the key role of bioirrigation in influencing sedimentary P effluxes was analysed in a series of oscillating oxygen condition scenarios that included scenarios without benthic fauna as control. The model results showed that bioirrigation controlled the concentration of phosphorus in the water column. As expected a much larger FeOOH bound P pool was observed in baseline scenario with bioirrigation compared to simulation without benthic fauna activity. The mean P fluxes were nearly 3 times higher than the fluxes observed during the real experimental incubations. Unlike laboratory experiments where peak P fluxes were observed during the anoxic cycle, anoxia had no effect on P fluxes in model simulations. Overall, failure to mimic experimental data demonstrate that the current implementation of the model is not enough to explain some of the bioirrigation effects observed. The behaviour of benthic fauna needed to be studied in detail before implementing their behaviour into the model to assess impact on sediment biogeochemistry.

4.2. Introduction

Benthic fauna are an important driving factor influencing oxygen consumption across sediment water interface and their presence can alter the processes occurring at the sediment water interface (Zhang et al., 2021). The impact of benthic fauna activities on sediment biogeochemistry are complex as fauna have specific solute transport, reworking or bio-mixing attributes and their effects on sediments are unique (Quintana et al., 2007). Benthic fauna increase the amount of iron oxyhydroxides by ventilating oxygen deeper into the anoxic sediments and hence improves the P retention capacity of the sediments (Lewandowski et al., 2007; Norkko et al., 2012; Quintana et al., 2018). Miatta and Snelgrove (2021) observed that faunal richness as opposed to environmental variables could explain the maximum variance in benthic fluxes occurring at the sediment surface. Hypoxic conditions, on the other hand, limit benthic faunal activity and are often associated with enhanced phosphate fluxes from the sediment (Belley et al., 2016; Berezina et al., 2019; Sturdivant et al., 2012). In general, the effect of faunal activity depends on a combination of factors including species community, individual behaviour, the sediment matrix and the depth at which they occur (Borger et al., 2019).

Models are valuable tools built by integrating existing knowledge of appropriate sedimentary biogeochemical processes and their interactions. The principle motive of developing models is to use customised scenario to study biogeochemical response of sediments to the changes within the sediment or in the overlying bottom water conditions (Paraska et al., 2014). The transport processes occurring at the sediment water interface are influenced to a varying degree by fauna depending upon their behaviour. A transport-reaction model postulated on average sediment microenvironment produced a good agreement between model predicted and observed porewater profiles for marine sediments (Aller, 1980, 1982). Kanzaki et al. (2019) showed oxygen and organic loading as important drivers of sediment mixing by luring fauna deeper into the sediments. Simulations performed with hypoxia tolerant organisms showed fauna activity deep into the sediments despite oxygen depletion while fauna with little to low oxygen tolerance could not go below ~4 cm into the sediments. An insight into the response of sediments to hypoxic and reoxygenation conditions through modelling showed phosphorus cycling in sediments was dominated by aerobic iron oxyhydroxide formation coupled with dissimilatory iron reduction. Since bioirrigation was not included in the model simulations due to negligible importance of bioirrigation at the study site, no accumulation of Fe-associated P below ~3 cm was observed, even after five years of oxic conditions in the water column (Reed et al., 2011). A diagenetic model used to stimulate P mobility showed bioirrigated sediments to be 50% more efficient at retaining P. The simulations showed a direct contribution of bioirrigation in enhanced P burial and reduced diffusive PO_4^{3-} fluxes from the sediments (Dale et al., 2016). Bioirrigation was responsible for transfer of oxygen deeper into the anoxic sediment, reoxidising subsurface metals (Kristensen et al., 2018). Quintana et al. (2018) investigated the impact of species activity on sedimentary fluxes and found different contrasting behaviour of species in various environments. The study suggested considering specie local distribution and specie specific effects e.g. survival, bioirrigation coefficient while estimating their environmental implications in the system. Zhu et al. (2016) used a simple 0 dimensional sediment model within their larger model framework to simulate bioirrigation enhanced P fluxes out of the sediment in the Gippsland Lakes. While the approach allowed to simulate *Nodularia* bloom dynamics, it did not capture the mechanistic insight into the interaction between bioirrigation and environmental conditions.

The Gippsland Lakes is part of Australia's largest estuarine systems stretching over 360 square km defined by three large water bodies- Lake Wellington, Lake Victoria and Lake King. Delivery of the majority of the lakes freshwater inflow comes from the Mitchell, Tambo, Thomson and Latrobe Rivers. The lake system experiences seasonal and interannual variability for river flow discharges. High flow events have been recorded in year 2011, 2016 and 2021, leading to stratification and lower bottom water DO. The lake system has experienced hypoxia associated problems such as enhanced P release from the sediment leading to prolongation of the existing bloom in the past (Zhu et al., 2016). A large toxic *Nodularia spumigena* bloom occurred in the lakes and persisted for three months from November 2011 to January 2012. It was reported that bottom water hypoxia following dinoflagellate bloom in summer and flood event in winter, resulted in the release of sediment P to support the bloom development (Zhu et al., 2017). Eutrophication and hypoxia have shown a positive feedback mechanism where hypoxia enhances eutrophication and subsequently P efflux from the sediment (Liu et al., 2019). Eutrophication driven hypoxia has even more severe implications for coastal lagoon systems as compared to lakes (Rabalais et al., 2014). Phosphorus is a key nutrient in Gippsland lakes as change in the bottom water total inorganic phosphate and hypoxia have been positively associated.

Quantitative understanding of phosphorus biogeochemical cycling subject to transient redox conditions is lacking in the Gippsland Lakes. Limited knowledge of the role of benthic fauna in regulating biogeochemical fluxes at the sediment-water interface for the Gippsland Lakes impedes understanding of sediment biogeochemistry and process quantification. Biogeochemical models are now able to capture complex biogeochemical feedbacks with success and provide an alternative way of studying the nutrient cycling in sediments. Zhu et al. (2016) used a 3-D coupled hydrodynamic-biogeochemical/ecological model to show that the oxygen regime in the Gippsland lakes is variable. There is likely to be an interaction between this, the faunal activity and resulting P fluxes since without bioirrigation implementation the model underestimated P concentrations in bottom water of the Gippsland Lakes. Through creation of sedimentary feedback in response to altering environmental conditions, a reactive transport model provides an alternative way for understanding the phosphorus dynamics in the Gippsland Lakes by applying different oxygen and irrigation perspectives and using observational database. A reactive one-dimensional model was used to assess the potential role of worms in altering sediment biogeochemistry. In this paper, we have made use of biogeochemical parameters observed at the start of lab experiment as input for the reactive transport model that has been modified to account for changes in Fe, P and C fluxes and allows picking homogeneous starting profile. The transient features like bioirrigation profile parameters, overlying water P concentrations and overlying water O_2 concentrations were analysed using the model. My aim was to use data from laboratory experiments under controlled conditions and investigate the ability of model as a tool to simulate 1) the extent to which the presence of worms enhances the accumulation of P within the sediment associated with FeOOH, (2) the interactions between worm irrigation activity and oxygen concentrations in controlling the flux of dissolved P across the sediment water interface and (3) the sensitivity of these observations to irrigation rates, sediment carbon loading and reactive iron content.

4.3. Materials and methods

4.3.1. Reactive transport model (RTM) formulation

In the current study an existing RTM model was modified to incorporate phosphorus based processes and reactions. The RTM is a one-dimensional diagenesis model to simulate the fluxes across sediment water interface and depth profiles of solutes and solid species, following the standard formulation of marine sediment models (Boudreau, 1997; Meysman et al., 2005). The model simulates based on the following generic mass balance equations for solutes and solids respectively (Boudreau, 1997; van de Velde & Meysman, 2016):

$$Solutes: \quad \varphi \frac{\partial C_i^{PW}}{\partial t} = \frac{\partial}{\partial z}\left[\varphi D_i \frac{\partial C_i^{PW}}{\partial z} - \varphi u C_i^{PW}\right] + \alpha\varphi\left(C_i^0 - C_i\right) + \sum_k w_{i,k} R_k \qquad \text{Eq. (1)}$$

$$Solids: \quad (1-\varphi)\frac{\partial C_i^S}{\partial t} = \frac{\partial}{\partial z}\left[(1-\varphi) D_b \frac{\partial C_i^S}{\partial z} - (1-\varphi) v C_i^S\right] + \sum_k w_{i,k} R_k \qquad \text{Eq. (2)}$$

In above equations, C_i^{PW} and C_i^S refer to the concentrations of solutes and solids respectively. φ is the porosity, (1- φ) is the solid volume fraction, t is the time, z is the sediment depth, D_i is the effective diffusion coefficient, C_i^0 is the overlying water solute concentration and u and v are the sedimentation velocities of the porewater and solid volume fraction respectively. D_b refers to the rate of diffusion of solids due to bioturbation, α is the solute bioirrigation coefficient, $w_{i,k}$ is the stoichiometric coefficient of species i in reaction k (see Table 4.1), and R_k refers to the reaction rate of reaction k (see Table 4.2). The model considers the transport and reaction of 16 species (8 solid, 8 solute) in the upper 10cm of the sediment (supplementary Table S2). List of constants included in the reactive transport model is given in table S1.

Solutes are subject to transport by diffusion, advection and bioirrigation. Diffusion coefficients are corrected for temperature and salinity using R package marelac (Soetaert et al., 2010) and adjusted for tortuosity following Boudreau. (1997). Advection accounts only for burial, which is assumed to be constant both with time and depth. No other advection (e.g. due to surface pressure differentials) or dispersion is considered, on the basis that the sediments are always assumed to be cohesive (non-permeable). Bioirrigation is implemented using a non-local exchange coefficient α (Brigolin et al., 2017; Dale et al., 2013; Tarhan et al., 2021; van de Velde & Meysman, 2016; Zhao et al., 2020). The coefficient α decreases exponentially with depth (because the faunal count and activity tend to decrease into the sediment), which is represented by a sigmoidal relationship as a function of depth x (in cm) as follows:

$$\alpha = \frac{\alpha^0 \exp\left(-\frac{(x-10)}{1.25}\right)}{1+\exp\left(-\frac{(x-10)}{1.25}\right)} \qquad \text{Eq. (3)}$$

Solid species are affected by bioturbation, which is implemented as a diffusion term in equation 4, where D_b represents a "biodiffusion" coefficient (Boudreau, 1998; van de Velde & Meysman, 2016; Zhao et al., 2020) and an advection term to represent burial. Similar to bioirrigation, bioturbation coefficient D_b decreases exponentially with depth following a sigmoidal function of depth x (in cm) as follows:

$$D_b = \frac{D_b^0 \exp\left(-\frac{(x-10)}{1.25}\right)}{1+\exp\left(-\frac{(x-10)}{1.25}\right)} \qquad \text{Eq. (4)}$$

4.3.2. Model setup

The grid size in the model was set uneven over a 10 cm depth of the sediment domain with higher resolution near the sediment water interface. The model employed non-uniformity among grid layers with a higher resolution near the sediment water interface.

The solute concentrations for species at the sediment water interface were assigned a fixed flux value with $C=C^0$ (overlying water concentrations) for solutes and a constant flux boundary was imposed for solids. Organic fluxes and iron oxyhydroxide fluxes were estimated as a percentage of sediment flux-2.5% OM^f and 1% $FeOOH^f$. At lower boundary conditions, the solute concentrations for all species were time invariable and were defined as zero concentration gradient. The Redfield ratio of 106:1 was used as the C/P ratio of the organic matter. In laboratory experiments, dissolved Fe^{2+} effluxed from the sediment is rapidly deposited at the sediment surface, such that Fe is essentially conserved in the sediment (Iftikhar et al., unpublished data). To reproduce this effect, the surface flux of $FeOOH^f$ includes a term equal to the Fe^{2+} efflux (see Table 4.1).

Table 4.1. List of steady state boundary conditions used for simulations in the reactive transport model

Species	UBC*	Value	LBC*	Value	Unit
Solids					
OM_f	Organic Flux	0	No gradient	0	μmol cm^{-2} y^{-1}
OM_s	Organic Flux	0	No gradient	0	μmol cm^{-2} y^{-1}
FeOOH	Fixed Flux	$-F_{Fe2+}$	No gradient	0	μmol cm^{-2} y^{-1}
FeOOH.P	Coupled Flux	0	No gradient	0	μmol cm^{-2} y^{-1}
O_4					
FeS	Fixed Flux	0	No gradient	0	μmol cm^{-2} y^{-1}
FeS_2	Fixed Flux	0	No gradient	0	μmol cm^{-2} y^{-1}
Solutes					
O_2	Fixed Flux	0.28	No gradient	0	μmol cm^{-3}
CO_2	Fixed Flux	2.2	No gradient	0	μmol cm^{-3}
H_2O	Fixed Flux	52500	No gradient	0	μmol cm^{-3}
H^+	Fixed Flux	1000	No gradient	0	μmol cm^{-3}
PO_4^{2-}	Fixed Flux	0.005	No gradient	0	μmol cm^{-3}
SO_4^{2-}	Fixed Flux	28.2	No gradient	0	μmol cm^{-3}
HS^-	Fixed Flux	0	No gradient	0	μmol cm^{-3}
Fe^{2+}	Fixed Flux	0	No gradient	0	μmol cm^{-3}

* UBC: Upper boundary condition; LBC: Lower boundary condition.

$-F_{Fe2+}$ is the surface flux of Fe^{2+} calculated by the model. This term ensures that all Fe remains in the system, consistent with laboratory experiments. See section 3.2

The homogeneous starting pool meant that initial reduction rates are even everywhere in the sediment. The initial conditions at the upper boundary were set oxic with the solid phase representing 2.5 % reactive C and 1 % reactive Fe in the sediment. The sedimentation rate for solute and solid state was kept at 0 for all simulations. The model was not designed to incorporate mortality of worms under anoxic or prolong hypoxic conditions. Therefore, bioirrigation and bioturbation parameters are constant.

A reasonable range of parameter values for temperature (10 ^oC), pressure (1 bar), salinity (35 ppt) and porosity (0.8) was established in accordance with the literature available on the Gippsland Lakes. List of environmental and transport parameters used in the model is given in table S3.

The aerobic respiration, dissimilatory iron reduction and sulfate reduction represent the three mineralisation pathways for the fast and slow decaying organic matter fractions. The reaction set also

includes the formation of iron sulfide and pyrite, the reoxidation of reduced compounds, the crystallization of iron compounds and P adsorption reaction. "Orthophosphate" is modelled as a single specie, which we call PO_4^{3-}, which represents the various equilibrium species, HPO_4^{2-} etc. The variable Fe.store determines the fraction of dissolved Fe that was irrigated out of the sediment and subsequently gets deposited at the surface as FeOOH. The model assumed that Fe is oxidised by dissolved oxygen in the bottom water and it appears at the surface as FeOOH. The parameter Fe.store was set to 1 ensuring complete deposition of effluxed iron to the top layer as FeOOH. The model considers two reactive pools of iron oxyhydroxide bound P representing amorphous and well crystalline species. Fe-P_f is the P bound to amorphous FeOOH and Fe-P_s is the P bound to crystalline FeOOH. Chi-bought (χ^0) is the ratio of adsorbed or co-precipitated P with ironoxyhydroxides when available. The ratio is set to 0.3 by default and is called FeP.on in the model. χ is the actual ratio of bound P to FeOOH at any given point (which is always $\leq \chi^0$). For simplicity, we have assumed that the processes such as nitrification and denitrification have a negligible effect on phosphorus fluxes. To reduce model complexity, manganese reduction and methanogenesis were also excluded from the reaction set. The full set of 15 reactions is given in Table 4.2. The rate expressions for these reactions follow the standard kinetic rate laws and are given in Table 4.3.

Table 4.2. List of kinetic reactions included in the reactive transport model

No.	Name	Equation	Ref.†
	Primary redox reactions		
R1	Aerobic respiration	$^{*}OM_f + O_2 \rightarrow CO_2 + (1/106)PO_4^{3-} + H_2O$	a
R2	Aerobic respiration	$OM_s + O_2 \rightarrow CO_2 + (1/106)PO_4^{3-} + H_2O$	a
R3	Iron reduction	$OM_f + 4FeOOH + 8H^+ \rightarrow CO_2 + 4Fe^{2+} + (1/106)PO_4^{3-} + 7H_2O$	b, c
R4	Iron reduction	$OM_s + 4FeOOH + 8H^+ \rightarrow CO_2 + 4Fe^{2+} + (1/106)PO_4^{3-} + 7H_2O$	b, c
R5	Sulphate reduction	$OMf + 0.5SO_4^{2-} + 0.5H^+ \rightarrow CO_2 + 0.5HS^- + (1/106)PO_4^{3-} + H_2O$	a, b
R6	Sulphate reduction	$OMs + 0.5SO_4^{2-} + 0.5H^+ \rightarrow CO_2 + 0.5HS^- + (1/106)PO_4^{3-} + H_2O$	a, b
	Secondary reactions		
R7	Sulphide oxidation	$HS^- + 2O_2 \rightarrow SO_4^{2-} + H^+$	b, c
R8	Iron oxidation	$Fe^{2+} + 0.25O_2 + 1.5H_2O \rightarrow FeOOH + 2H^+$	b
R9	Iron reduction by sulphide	$HS^- + 8FeOOH + 15H^+ \rightarrow SO4^{2-} + 8Fe^{2+} + 12H_2O$	c
R10	Iron sulphide formation	$Fe^{2+} + HS^- \rightarrow FeS + H^+$	b, c
R11	Iron sulphide Dissolution	$FeS + 2O_2 \rightarrow Fe^{2+} + SO_4^{2-}$	a, d
R12	Pyrite formation	$FeS + 0.25SO_4^{2-} + 0.75HS^- + 1.25H^+ \rightarrow FeS_2 + H_2O$	c
R13	Pyrite Dissolution	$2FeS_2 + 7O_2 + 2H_2O \rightarrow 2Fe^{2+} + 4SO_4^{2-} + 4H^+$	a
R14	FeOOH stabilization	$FeOOH^f + \chi^0 Fe\text{-}P^f \rightarrow FeOOH^s + \chi^0 Fe\text{-}P^s$	a
R15	P adsorption to FeOOH	$FeOOH^f + \chi PO_4^{2-} \rightarrow FeOOH^f + \chi Fe\text{-}P^f$	e

***** OM is in the form $(CH_2O)(PO_4^{3-})_{1/106}$. The term *f* stands for fast and *s* stands for slow.

† **References**: a: Reed et al. (2011); b: Faber et al. (2012); c: van de Velde and Meysman (2016); d: (Berg, 2003)

Table 4.3. List of kinetic expressions included in the reactive transport model

No.	Name	Equation	Ref.†
Primary redox reactions			
R_{min}^{f}	Mineralisation of fast OM	$(1-\varphi)K_f[\mathrm{OM}_f]$	a
R_{min}^{s}	Mineralisation of slow OM	$(1-\varphi)K_s[\mathrm{OM}_s]$	a
R1	Aerobic respiration	$R_{min}^{f}\cdot\frac{[\mathrm{O_2}]}{K_{\mathrm{O_2}}+[\mathrm{O_2}]}$	a
R2	Aerobic respiration	$R_{min}^{s}\cdot\frac{[\mathrm{O_2}]}{K_{\mathrm{O_2}}+[\mathrm{O_2}]}$	a
R3	Iron reduction	$R_{min}^{f}\cdot\frac{K_{\mathrm{O_2}}}{K_{\mathrm{O_2}}+[\mathrm{O_2}]}\cdot\frac{[\mathrm{FeOOH}^f]}{K_{\mathrm{FeOOH}}+[\mathrm{FeOOH}^f]}$	a, b
R4	Iron reduction	$R_{min}^{s}\cdot\frac{K_{\mathrm{O_2}}}{K_{\mathrm{O_2}}+[\mathrm{O_2}]}\cdot\frac{[\mathrm{FeOOH}^s]}{K_{\mathrm{FeOOH}}+[\mathrm{FeOOH}^s]}$	a, b
R5	Sulphate reduction	$\Psi R_{min}^{f}\cdot\frac{K_{\mathrm{O_2}}}{K_{\mathrm{O_2}}+[\mathrm{O_2}]}\cdot\frac{[\mathrm{FeOOH}^f]}{K_{\mathrm{FeOOH}}+[\mathrm{FeOOH}^f]}\cdot\frac{[(\mathrm{SO_4^{2-}})^f]}{K_{\mathrm{SO_4^{2-}}}+[(\mathrm{SO_4^{2-}})^f]}$	a, c
R6	Sulphate reduction	$\Psi R_{min}^{s}\cdot\frac{K_{\mathrm{O_2}}}{K_{\mathrm{O_2}}+[\mathrm{O_2}]}\cdot\frac{[\mathrm{FeOOH}^s]}{K_{\mathrm{FeOOH}}+[\mathrm{FeOOH}^s]}\cdot\frac{[(\mathrm{SO_4^{2-}})^s]}{K_{\mathrm{SO_4^{2-}}}+[(\mathrm{SO_4^{2-}})^s]}$	a, c
Secondary reactions			
R7	Sulphide oxidation	$\varphi K_{\mathrm{SO}}[\mathrm{O_2}][\mathrm{HS^-}]$	a, c
R8	Iron oxidation	$\varphi K_{\mathrm{IO}}[\mathrm{O_2}][\mathrm{Fe^{2+}}]$	a, c
R9	Iron reduction by sulphide	$(1-\varphi)K_{\mathrm{IRS}}[\mathrm{FeOOH}][\mathrm{HS^-}]$	a, d
R10	Iron sulphide Formation	$\varphi K_{\mathrm{ISF}}[\mathrm{Fe^{2+}}][\mathrm{HS^-}]$	c
R11	Iron sulphide Dissolution	$(1-\varphi)K_{\mathrm{ISD}}[\mathrm{O_2}][\mathrm{FeS}]$	b
R12	Pyrite Formation	$(1-\varphi)K_{\mathrm{PF}}[\mathrm{HS^-}][\mathrm{FeS}]$	c
R13	Pyrite Dissolution	$(1-\varphi)K_{\mathrm{PD}}[\mathrm{O_2}][\mathrm{FeS_2}]$	b
R14	FeOOH stabilization	$(1-\varphi)K_{\mathrm{Fe.S}}[\mathrm{FeOOH}]$	a
R15	P adsorption to FeOOH	$\varphi k_{sorption}[\mathrm{PO_4^{3-}}]\frac{\chi^0[\mathrm{FeOOH}^f]-[Fe-P^f]}{\chi^0[\mathrm{FeOOH}^f]}$	E

† References: a: van de Velde and Meysman (2016); b: Reed et al. (2011); c: Faber et al. (2012); d: Berg et al. (2003); e: (Wang et al., 2003)

4.3.3. Model solution

A numerical solution to equations (1) and (2) was implemented using the programming language R (version) via the free software RStudio (version). The model solved 16 state variables (chemical species) using the method of Soetaert and Meysman (2012). Briefly, the spatial derivatives of the partial differential equations were expanded over the grid using the R package ReacTran (Soetaert & Meysman, 2012). The resulting ordinary differential equations were then integrated using the stiff

solver vode from R package deSolve (Soetaert et al., 2010).

4.3.4. Description of simulations run on model

The model was set up to simulate the phosphorus fluxes observed in the laboratory incubation experiments performed on sediment cores from the Gippsland Lakes. The model was initially spun-up for two baseline scenarios that were representative of the conditions encountered by the sediment cores during the laboratory studies. Both scenario simulations were performed for 30 days under oxic conditions with 128 μM P addition (as was undertaken in the lab experiment). In the scenario with the presence of *C. capitata*, the parameters D_b and α take the value of 28 cm^2yr^{-1} and 46.5 yr^{-1} and bioturbation and irrigation rates were kept zero for the other scenarios assuming the absence of *C. capitata*. The model was then applied across a range of bottom water dissolved O_2 concentrations from completely anoxic (0 mM) to oxic (0.28 mM) on outputs from the two scenarios. The experimental design involves simulation run for 30 days under stable oxygen conditions 10 % and 100 % on outputs from both scenario and simulation run for 30 days under altering oxygen conditions 10/0% and 100/0% on outputs from both scenarios. The conditions were altered every 24 hours and the parameters D_b and α take the value of zero during 0% cycle. All treatments involving *C. capitata* are indicated with a prefix W and those without worms with a prefix N. Treatments with their bioirrigation turned off during the altering days are represented with a letter S at the end. A detailed description of the treatments performed on the two scenarios is given in the form of a time series (Figure 4.1).

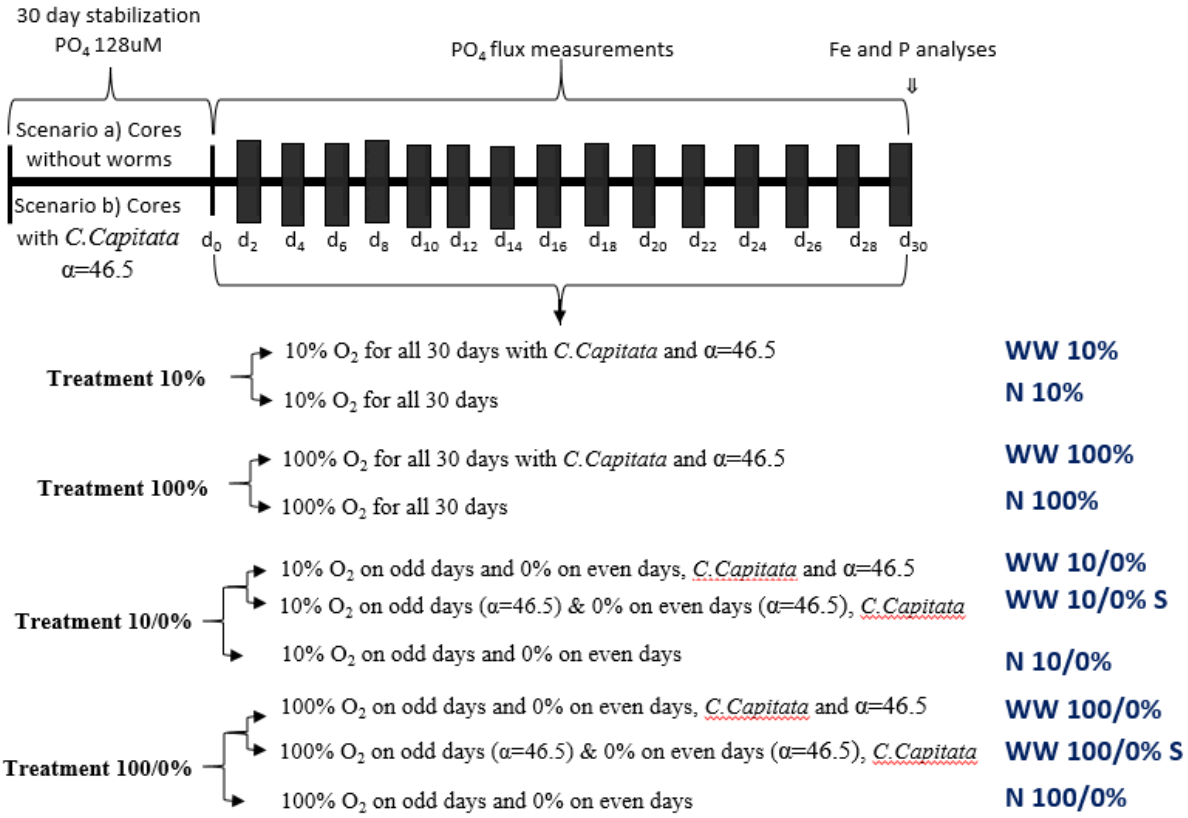

Figure 4.1. A schematic view of the simulations performed on a) bioturbed and b) non-bioturbed sediments

4.3.5. Model sensitivity analyses

The sensitivity of the model to sediment iron content, bioirrigation rate and sediment organic carbon content was investigated as follows, The sensitivity of sedimentary P pools and associated P fluxes to $FeOOH^f$ availability was investigated by performing simulations, where the iron concentrations were varied between 0.04 %, 0.22 % and 0.53 % corresponding to 7.16, 41 and 95 μmol Fe g^{-1} dry sediment respectively (Fig. 4.6). In each simulation, $FeOOH^f$ concentration after pre-incubation was 179 μmol Fe g^{-1} dry sediment. The sensitivity of the model to irrigation was tested for the *C. capitata* based scenario only. Since irrigation rates have not been observed in the Gippsland Lakes before, simulations performed with the irrigation rate turned on varied between average irrigation rate to some of the highest reported in literature. In each simulation, the initial irrigation rate for pre-incubation was kept at 46.5 yr^{-1} to have the same starting conditions.

The model simulations were also repeated at a higher initial organic carbon concentration (1 and 5%, C = 833 and 4166 μmol C g^{-1} dry sediment for fast decaying fraction respectively) to observe P flux sensitivity relative to the amount of organic matter loading.

4.4. Description and interpretation of model outputs

4.4.1. Model baseline simulations

Consistent with the hypotheses that worms will play a role in P accumulation, there was an uptake of ~20% more P from the water column in +worms treatment compared to –worms treatment as indicated by the larger total P pool for +worms treatment (Fig. 4.2a). After the initial large influx of P, the diffusive P flux decreased slowly over the 30-day period in –worm treatment suggesting saturation of P binding sites. In +worms treatment, irrigation fluxes were into the sediment for the initial 3 days and then led to release of P from the sediment till the end of experiment. The amorphous enrichment FeP^f after 30 days of baseline simulation run was nearly 35 times more than the crystalline Fe bound P pool (FeP^s) in both treatments (Fig. 4.2e, 4.2f).

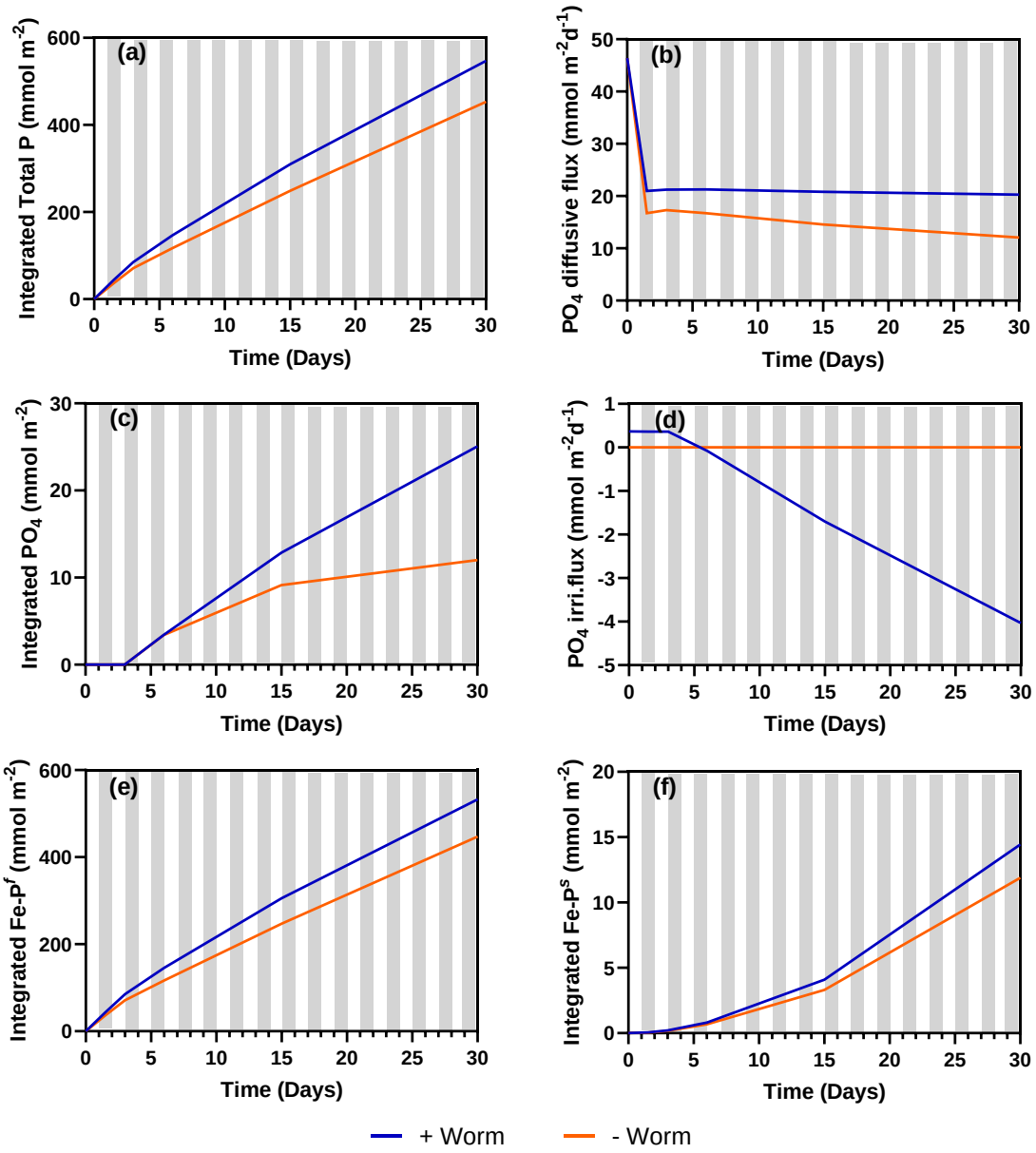

Figure 4.2. P uptake/release during the 30 day baseline incubation of cores in presence of worms (+ worms) and absence of worms (- worms) subjected to oxic conditions. Bioirrigation coefficient α equals 46.5, carbon loading 1% and $FeOOH^f$ 1%. Negative value means out of the sediment.

4.4.5. Model experimental simulations

There was very little variation in PO_4^{3-} fluxes over the entire 30 day period for all treatments with worms except for W10/0% S treatment which had irrigation off during the anoxic even days (Fig. 4.3b, 4.3d). The W10/0% S was the only treatment to show sharp variation in uptake and release of PO_4^{3-} on altering days suggesting an uptake upon oxygenation and release due to anoxia. The iron oxyhydroxide bound P pool was initially high in all treatments > 500 mmol m^{-2} and steadily decreased during the course of the experiment to 400-450 mmol m^{-2}. Similar to the P fluxes, the W10/0% S also showed slightly different behaviour for Fe bound P pool (FeP^f), initially decreasing quickly as compared to other treatments and then stabilizing in the range of 450 mmol m^{-2} (Fig. 4.3e). There was a decrease in iron reduction rate over time in W10/0% S treatment as compared to other treatments (Supplementary material, Table S4). The changes in the Fe bound P pool (FeP^f) mirrored

the integrated PO_4^{3-} pool, which goes up when the Fe bound P pool goes down. The irrigation flux rate was always much larger than the organic matter degradation rate resulting in much large irrigation fluxes so, on balance, PO_4^{3-} is always leaving the system (Fig. 4.3d). The integrated PO_4^{3-} pool was roughly stable in all simulations except the W10/0% S treatment.

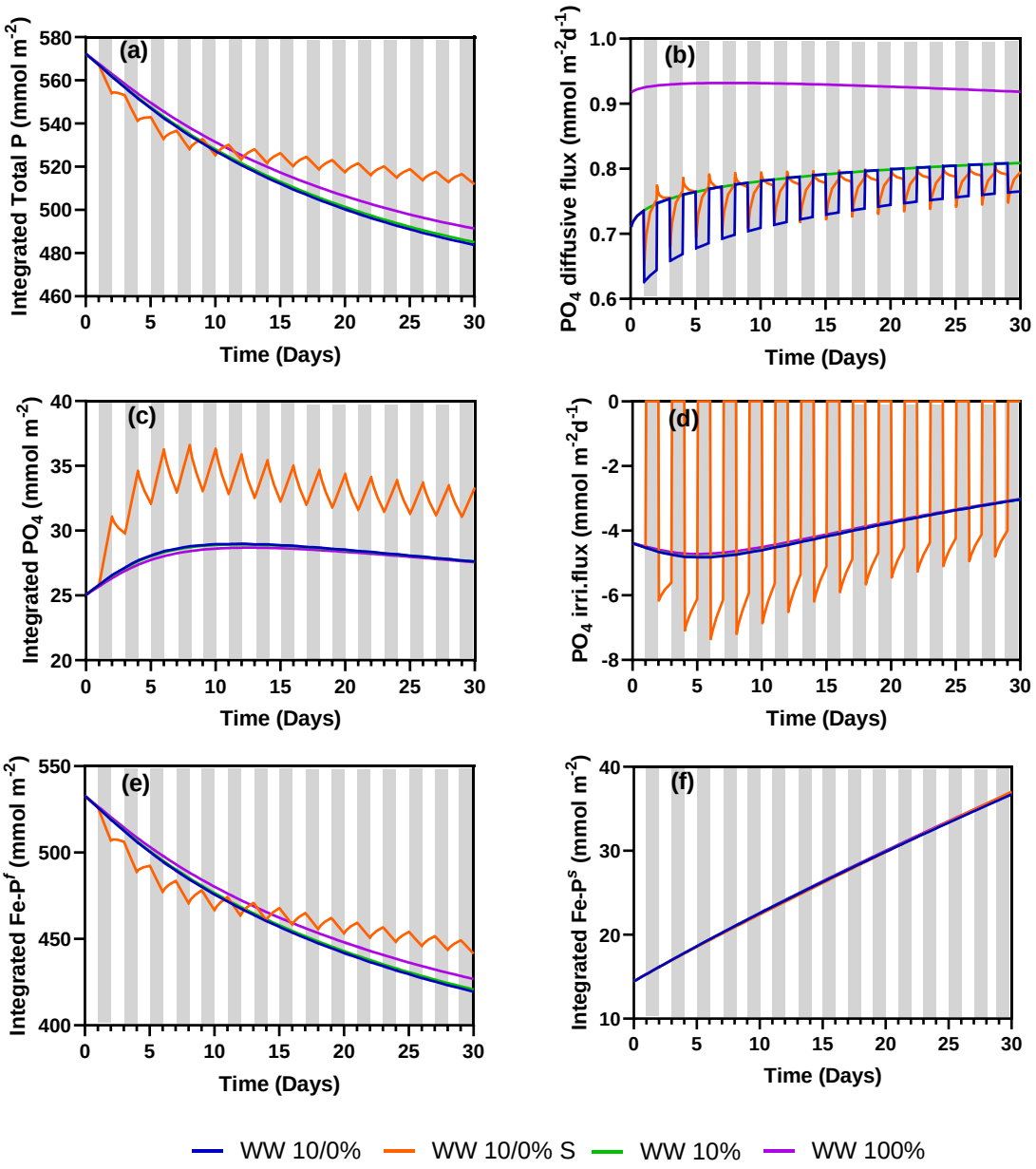

Figure 4.3. Comparison of P uptake/release during the 30 day incubation of cores in presence of worms subjected to constant and recurrent oxygen conditions. Bioirrigation coefficient α equals 46.5, carbon loading 1% and $FeOOH^f$ 1%. White bars denote oxic conditions and dark bars denote anoxic conditions (where applicable). WW 10-0 represent worm treatment with altering 10%oxic/anoxic days. WW 10-0 S has irrigation turned off on anoxic days. WW 10 is worm treatment at constant 10% oxic condition and WW 100 at constant 100% oxic condition. Negative value means out of the sediment.

Surprisingly, the PO_4^{3-} fluxes and FeP^f pool patterns varied among all –worm treatments as opposed to treatments with worms. The Fe bound P pool (FeP^f) dominated the total sediment pool with concentrations ranging between 380-460 mmol m^{-2} (Fig. 4.4a, 4.4e). The N100% treatment led to a build-up of the iron oxyhydroxide bound P pool as expected and no phosphorus was found in the

water column. The N100/0% treatment showed a slight increase in the overall FeP^f pool and the PO_4^{3-} flux altered during the oxic anoxic transition. The N10/0% treatment led to a decrease in the FeP^f pool suggesting anoxia leading to iron reduction and release of bound P. There was a sharp release of phosphorus after seven days of incubation in the N10/0% and N10% treatments indicating a collapse of iron oxyhydroxide cap that was acting as a buffer (Fig. 4.4b). The enhanced PO_4^{3-} flux also led to an immediate fall in total iron oxyhydroxide bound P pool indicating that the iron oxyhydroxide inventory acts as a control on the feedback mechanism.

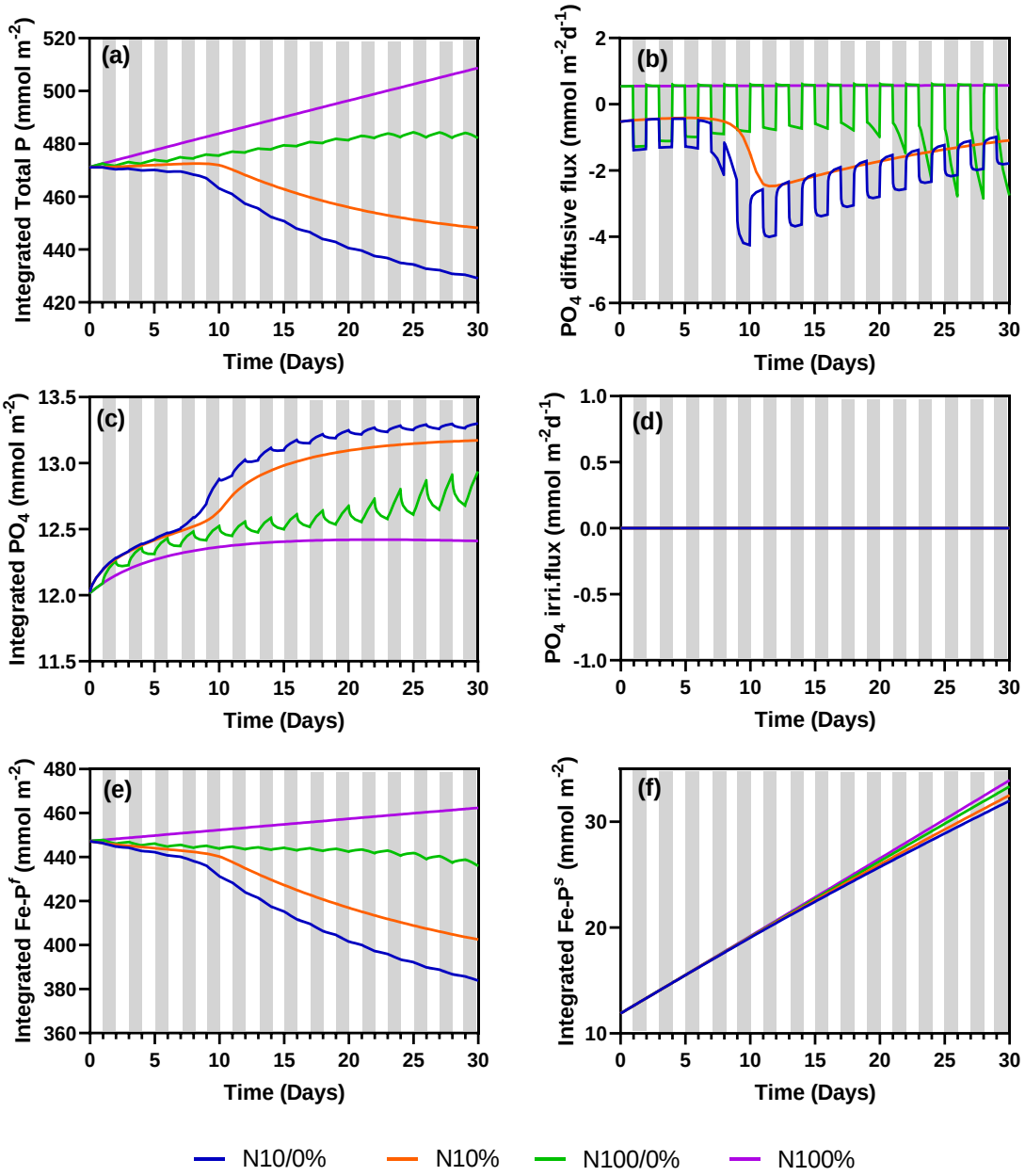

Figure 4.4. Comparison of P uptake/release during the 30 days incubation of cores without addition of worms subjected to constant and recurrent oxygen conditions. No bioirrigation, carbon loading 1% and $FeOOH^f$ 1%. White bars denote oxic conditions and dark bars denote anoxic conditions (where applicable). N10/0% represent treatment with altering 10%/anoxic days. N10% is treatment at constant 10% oxic condition and N100/0% with altering 100%oxic/anoxic days. N100% at constant 100% oxic codition. Negative value means out of the sediment.

4.4.5. *Sensitivity to carbon loading*

The sensitivity of phosphorus fluxes to change in organic matter loading was simulated by varying carbon from 1% to 5% for all treatments following the initial baseline scenarios (Fig. 4.5). After 5% organic matter addition in worm treatment, the PO_4^{3-} irrigation fluxes substantially increased corresponding to a mean concentration of 13 mmol m^{-2} d^{-1} as compared to 5.3 mmol m^{-2} d^{-1} observed during the simulations at 1% carbon loading (Fig. 4.3d, 4.5d). The presence of much larger irrigation fluxes and higher iron reduction rates in response to organic matter mineralisation implied more PO_4^{3-} leaves the system as indicated by a much smaller FeP^f pool and a much larger integrated PO_4^{3-} pool (Fig. 4.5c, 4.5d, 4.5e). The overall behaviour for the fluxes and sedimentary pools was largely the same for all treatments.

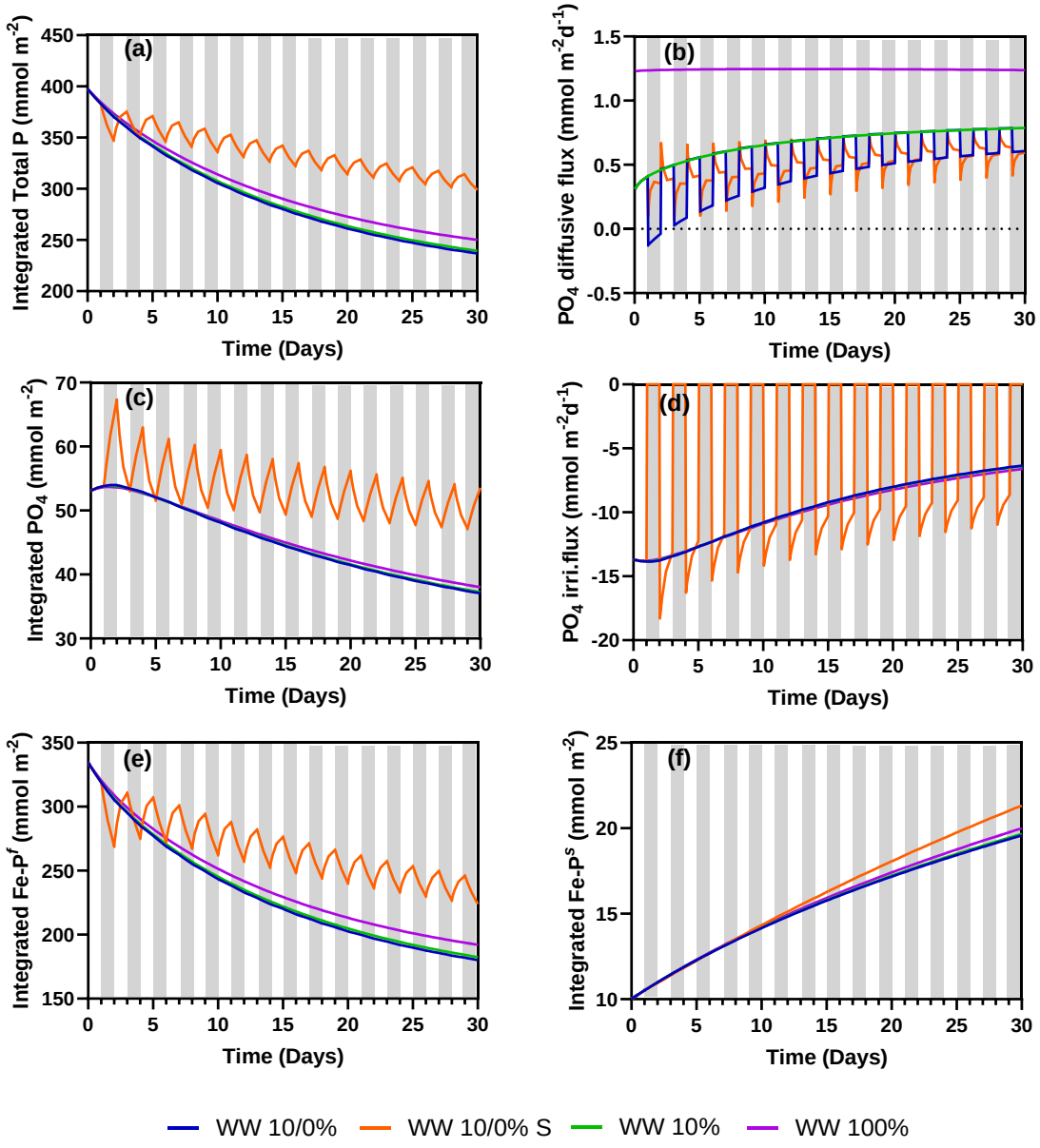

Figure 4.5. Comparison of P uptake/release during the 30 day incubation of cores in presence of worms subjected to high carbon loading (5%) conditions. Bioirrigation coefficient α equals 46.5 and $FeOOH^f$ 1%. White bars denote oxic conditions and dark bars denote anoxic conditions (where applicable). WW 10-0 represent worm treatment with altering 10%oxic/anoxic days. WW 10-0 S has irrigation turned off on anoxic days. WW 10 is worm treatment at constant 10% oxic condition and WW 100 at constant 100% oxic codition. Negative value means out of the sediment.

A much clearer trend was followed by all simulations run on the baseline scenario without worms at 5% carbon loading. The N100% oxic treatment resulted in a larger FeP^f pool at the end of 30 days (Fig. 4.6e). A much larger P flux for treatments with anoxic cycles as compared to simulations run under stable oxic conditions suggests more iron oxyhydroxide reduction during anoxia. There was little variation in the total sedimentary P pools over the entire course of the experiment with a mean concentration of 375 mmol m^{-2} over the 30 days (Fig. 4.6a). After the addition of organic matter, the PO_4^{3-} fluxes increased to a maximum of 5.8 mmol m^{-2} d^{-1} before rapidly decreasing and stabilizing in the range of 1.6 mmol m^{-2} d^{-1}. The most likely explanation for this observation is that there was a build-up of large pool of FeP^f during the initial pre-treatment which was subsequently reduced upon the onset of anoxia as part of dissimilatory iron reduction (Fig. 4.6b). A 5% carbon loading also meant absence of iron bound P pools into the sediment (Supplementary material, Fig. S1).

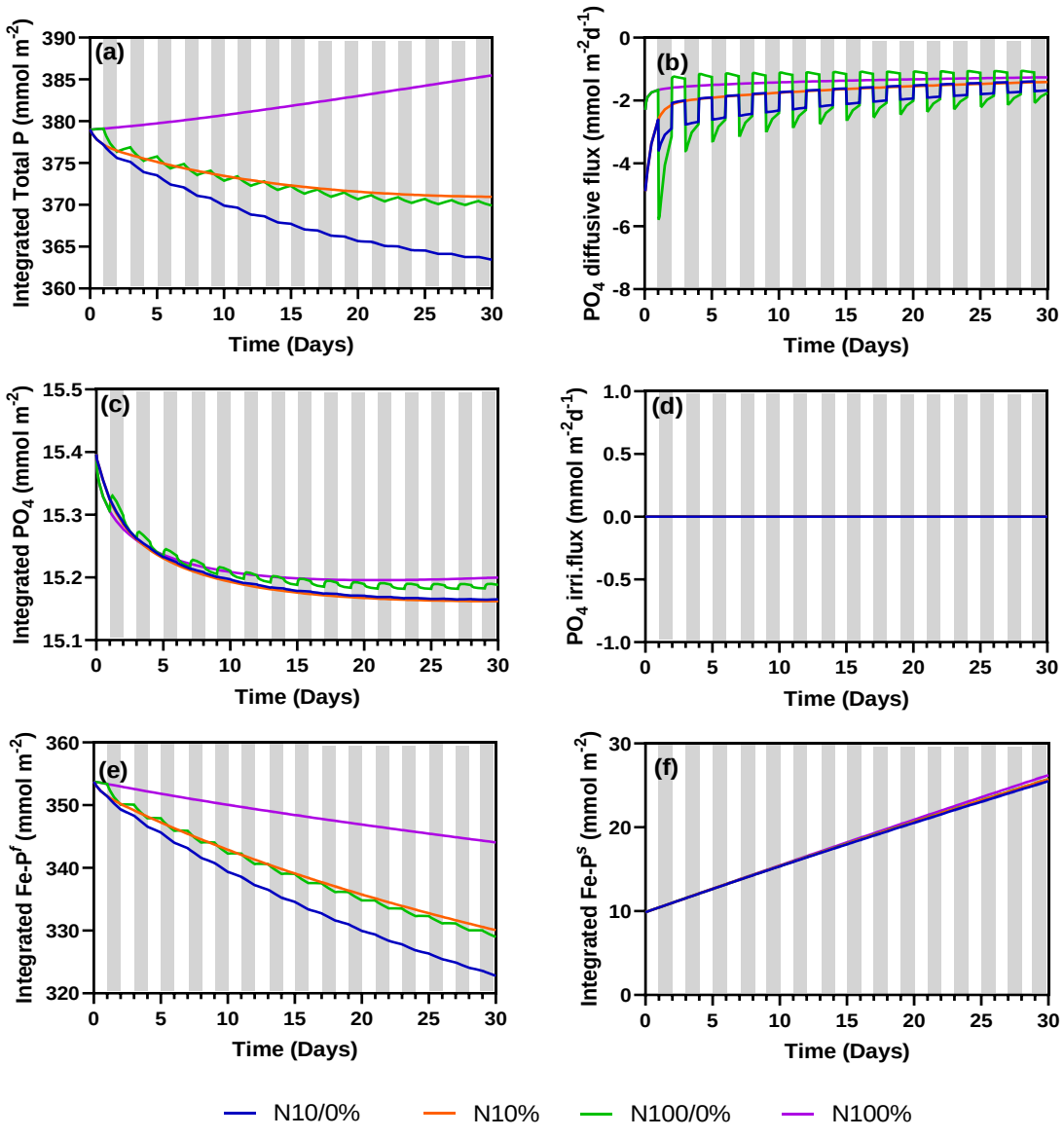

Figure 4.6. Comparison of P uptake/release during the 30 days incubation of cores in presence of worms subjected to high carbon loading (5%) conditions. No bioirrigation and $FeOOH^f$ 1%. White bars denote oxic conditions and dark bars denote anoxic conditions (where applicable). N10/0% represent treatment with altering 10%/anoxic days. N10% is treatment at constant 10% oxic condition and N100/0% with altering 100%oxic/anoxic days. N100% at constant 100% oxic codition. Negative value means out of the sediment.

4.4.5. Fe sensitivity

It was observed that the availability of iron oxides in the sediment controls the flux of phosphorus across the sediment water interface (Fig. 4.7b, 4.7d). The fluxes of phosphorus were sensitive to the initial concentration of Fe present in the sediment. The higher Fe concentrations resulted in larger iron oxyhydroxide bound P pools at the end of 30 days incubation (Fig. 4.7e). There was a variation in trend for the phosphorus fluxes resulting from the three Fe addition simulations. The addition of 41 μmol Fe g^{-1} dry sediment (0.22%) resulted in much higher fluxes for the entire course of experiment as compared to the treatment with 94.9 μmol Fe g^{-1} dry sediment (0.53%). A possible explanation for this unexpected behaviour is the presence of a much smaller surface sediment Fe cap in the 0.22% treatment, which acts as a buffer in model simulations. A small Fe inventory cap and high initial reduction rate meant there was a sharp release of phosphorus from the sediment before re-equilibration. The more crystalline Fe bound P pool (FeP^s) increased from 11 to 26 mmol m^{-2} for the altering 10/0 treatment having 94.9 μmol Fe g^{-1} dry sediment while it remained relatively stable in the range of 6.5 mmol m^{-2} for the altering 10/0 treatment having 41μmol Fe g^{-1} dry sediment (Fig. 4.7f). This was expected, as the larger PO_4^{3-} and irrigation fluxes in the 0.22% Fe treatment consumed the large FeP^f pools present in the sediment preventing conversion into more crystalline FeP^s pools.

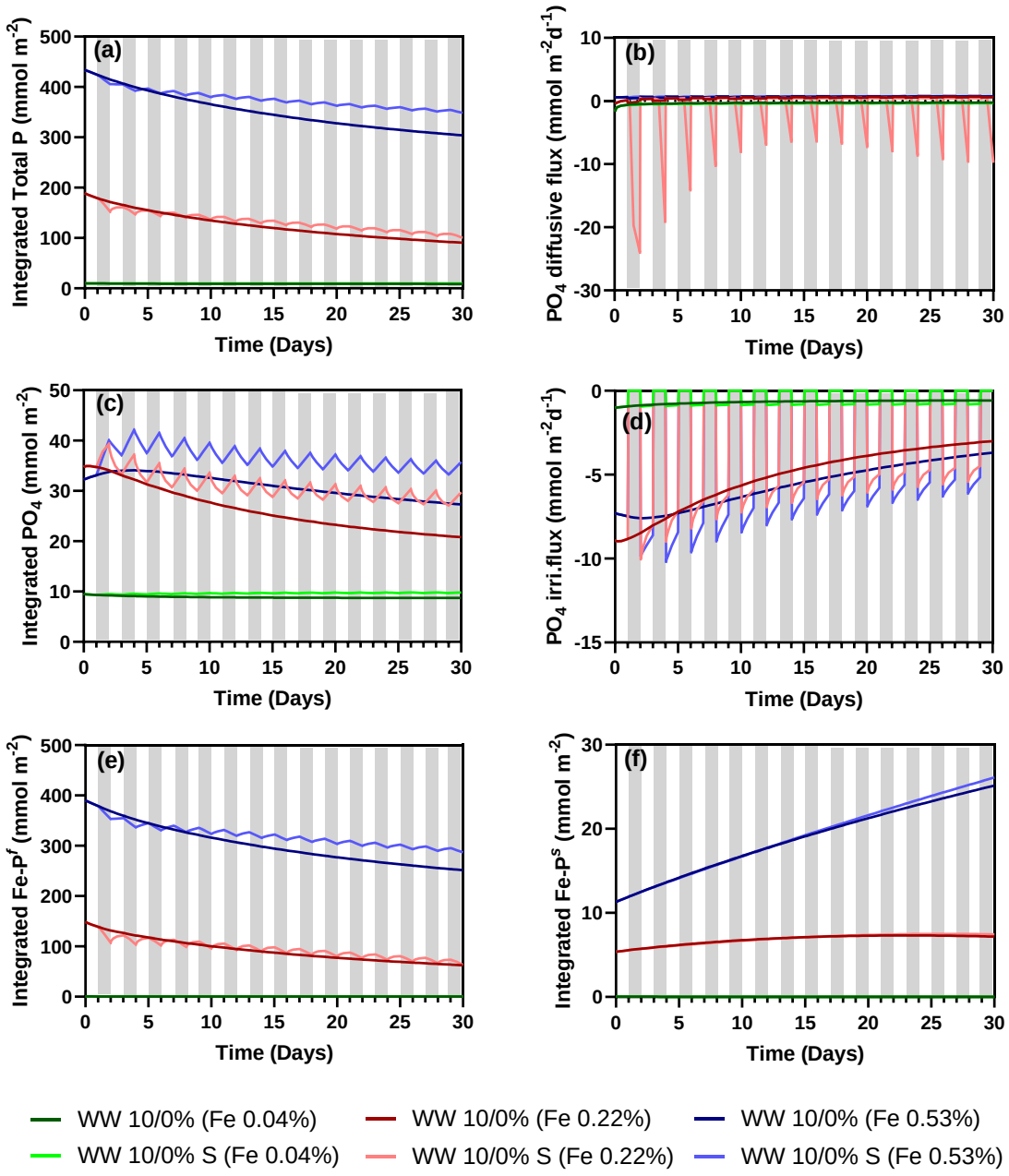

Figure 4.7. Fe bound P pool and flux of P for a simulation of 30 day period with an imposed Fe conc. of 7.6, 40 and 179 µmol g−1 sediment in bioturbed and non-bioturbed sediments. Bioirrigation coefficient α equals 46.5 and carbon loading 1%. White bars denote oxic conditions and dark bars denote anoxic conditions (where applicable). WW 10/0% (Fe 0.04%) represent worm treatment with altering 10%oxic/anoxic days applied $FeOOH^f$ conc. 0.04 and WW 10/0% S (Fe 0.04%) has irrigation turned off on anoxic days with $FeOOH^f$ conc. 0.04%. Similarly, WW 10/0% (Fe 0.22%) and WW 10/0% S (Fe 0.22%) indicate $FeOOH^f$ conc. 0.22% and WW 10/0% (Fe 0.53%) and WW 10/0% S (Fe 0.53%) indicate $FeOOH^f$ conc. 0.53%. Negative value means out of the sediment.

4.4.5. Sensitivity to rate of bioirrigation

Varied bioirrigation simulations reveal that the enhanced worm activity increases the phosphorus fluxes in the water column above the sediment and the fluxes were highly variable (Fig. 4.8d). The higher bioirrigation rates (465 yr^{-1}) led to increased phosphorus flux from the sediments as compared to PO_4^{3-} fluxes resulting from treatments with lower irrigation rates. The cyclic treatments also tend to show higher irrigation fluxes compared to treatments under stable oxygen conditions. At the end

of the 30 day simulation run, lower bioirrigation values tend to produce much smaller fluxes with the anoxic cycle leading to a positive feedback. The initially high phosphorus fluxes resulting from irrigation rates of 465 yr^{-1}, also reduced in size at the end of the 30 day run and produced fluxes similar in size to treatments with 46.5 yr^{-1} irrigation rates. A possible explanation for this behaviour was the reduced reduction rate towards the end of the experiment resulting in much smaller phosphorus fluxes. The FeP^f pool was initially high in all treatments at the start of the experiment, steadily decreasing to a mean concentration of 420 mmol m^{-2} after 30 days (Fig. 4.8e). The initial incubation led to the formation of a much higher iron oxyhydroxide pool, which was subsequently reduced during anoxic cycles and the Fe cap with P being replaced with Fe cap without P.

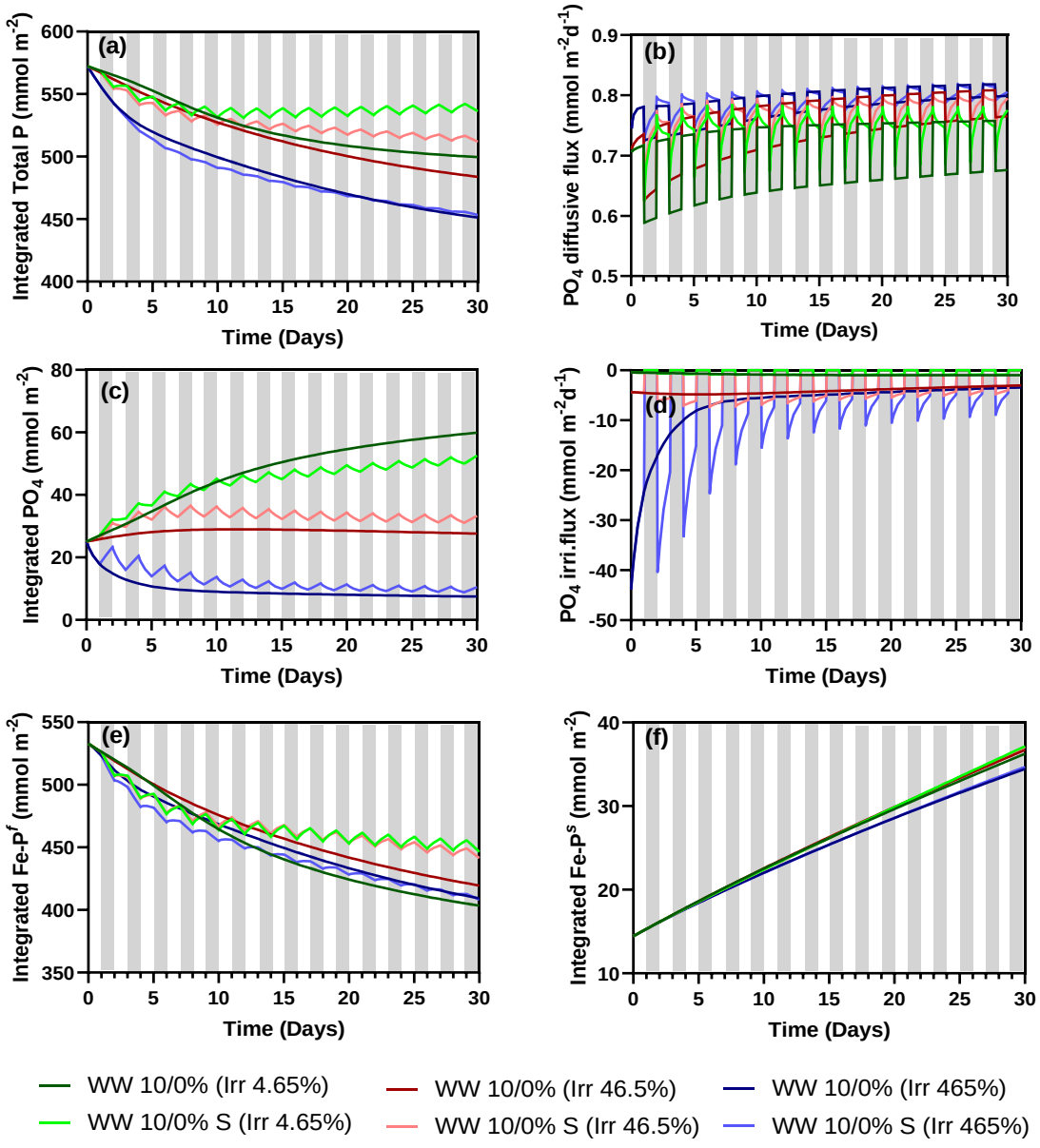

Figure 4.8. Effluxes of P for a simulation of 30 day period with an imposed α value of 4.65, 46.5 and 465 in bioturbed and non-bioturbed sediments keeping $FeOOH^f$ 1% and carbon loading 1%. White bars denote oxic conditions and dark bars denote anoxic conditions (where applicable). WW 10/0% (Irr 4.65%) represent worm treatment with altering 10%oxic/anoxic days applied α value of 4.65 and WW 10/0% S (Irr 4.65%) has irrigation turned off on anoxic days with α value of 4.65. Similarly, WW 10/0% (Irr 46.5%) and WW 10/0% S (Irr 46.5%) indicate α value of 46.5 and WW 10/0% (Irr 465%) and WW 10/0% S (Irr 465%) indicate α value of 465. Negative value means out of the sediment.

4.5. Discussion

4.5.1. Effect of worms on sediment P accumulation

It is well known that benthic fauna can oxygenate the sediment through burrow formation leading to an increase in iron oxides and sediment bound P (Dale et al., 2016; Hupfer et al., 2019). Consistent with this, simulations with worms addition showed a larger accumulation of FeP^f (19 %) in the sediment compared to simulations with no worms in the oxic pre-incubation period (Fig. 4.2e). This also agreed with the experimental work (chapter 3), which showed a greater accumulation of FeP in the + worms treatment. The modelled FeP^f pool was, however, much larger than the observed pool (65 %). The presence of enhanced FeOOH bound P pool for model simulations with irrigation suggest ventilation led oxidation of sediment at depth leading to the formation of FeOOH bound P pool deeper into the sediments. The model was therefore broadly able to simulate an increased uptake of FeP^f under oxic conditions. This further proves that in Fe rich sediments where worm activity could increase FeP^f pool, bioirrigation and bio mixing can be termed as major factors that control the concentration of P in the water column.

4.5.2. Interactions between worm irrigation activity and oxygen concentrations in controlling the P fluxes across the sediment water interface

In the literature, faunal activities under anoxic-hypoxic conditions are not well documented and are often linked to low intensity of bioirrigation but it is at least known for a long time (e.g. Herreid, 1980) that invertebrates can show increased activity under hypoxia (Dale et al., 2015; Middelburg & Levin, 2009). There was a general disagreement between the experimental P flux data and the model simulations output. Experimental data shows that benthic fauna strongly influence the sediment nutrient fluxes through increased bioirrigation activities acting as a significant source of P on the onset of anoxia in altering anoxic-hypoxic experiment. In the model simulations, the W10/0% treatment showed no change in PO_4^{3-} irrigation fluxes under altering anoxic-hypoxic conditions. The altering anoxic days had no effect on P release with bioirrigation turned on but with irrigation turned off in the W10/0% S treatment, larger PO_4^{3-} fluxes out of the sediment due to anoxia were observed, resulting in reduced total integrated P pool (Fig. 3d, 3a, S5). In addition, PO_4^{3-} irrigation fluxes followed a decreasing pattern over the 30-day period in simulations with worms (Fig. 4.3d). A possible explanation is that P (128 $mol\ l^{-1}$) added to the overlying water at the start of initial incubation was reduced (5 $mol\ l^{-1}$) at the start of the actual treatment simulation. The PO_4^{3-} irrigation flux decrease is possibly linked with the rapid exchange of P between sediment porewater and overlying water column for equilibrium establishment. This also led to a reduction in the size of large FeP^f pool present at the start of the simulation outputs (Fig. 4.3e).

In the model simulations, the W10/0% S treatment showed a sharp variation in uptake and release of PO_4^{3-} on altering days suggesting an uptake upon 10% oxygenation with bioirrigation and release due to anoxia without bioirrigation. The mean PO_4^{3-} flux (out of the sediment) output concentration of 5.3 mmol m^{-2} d^{-1} over the 30 day period was nearly three times higher than the concentrations observed during the laboratory experimental run for cyclic anoxic-hypoxic treatment (Fig. 4.3d). The much larger P fluxes observed in model simulation could be explained by the fact that the phosphorus bound to Fe in the model simulations is not a permanent sink of phosphorus. This is because the model assumes a well-mixed sediment and is not implemented to crystallize Fe bound P into forms unavailable for dissimilatory iron reduction, and as a consequence anoxia can lead to an intense P

turnover. Neglecting this limitation of the 1D model, the model outputs compare well with the experimental data and the literature. Sustained hypoxia results in loss of sediment P content due to dissolution of P bearing iron oxyhydroxides, resulting in a pulse of PO_4^{3-} to overlying porewater. Dissolution of iron oxyhydroxides following in response to hypoxia could increase Fe^{2+} and PO_4^{3-} concentrations in the reduced sediment (Lewandowski et al., 2007; Meile et al., 2005). Benthic fauna can induce, via bio-irrigation, a substantial transfer of Fe^{2+} and PO_4^{3-} from the sediment to the overlying porewater (van de Velde & Meysman, 2016). Reed et al. (2011) suggested that phosphorus cycling in sediments is dominated by Fe bound P due to rapid dissimilatory iron reduction coupled with iron oxyhydroxide formation. Zhu et al. (2016) simulated that bioirrigation could increase oxic layer depth and enhance P retention under oxic condition. However, upon onset of anoxia, significant P release could occur due to enhanced diffusion.

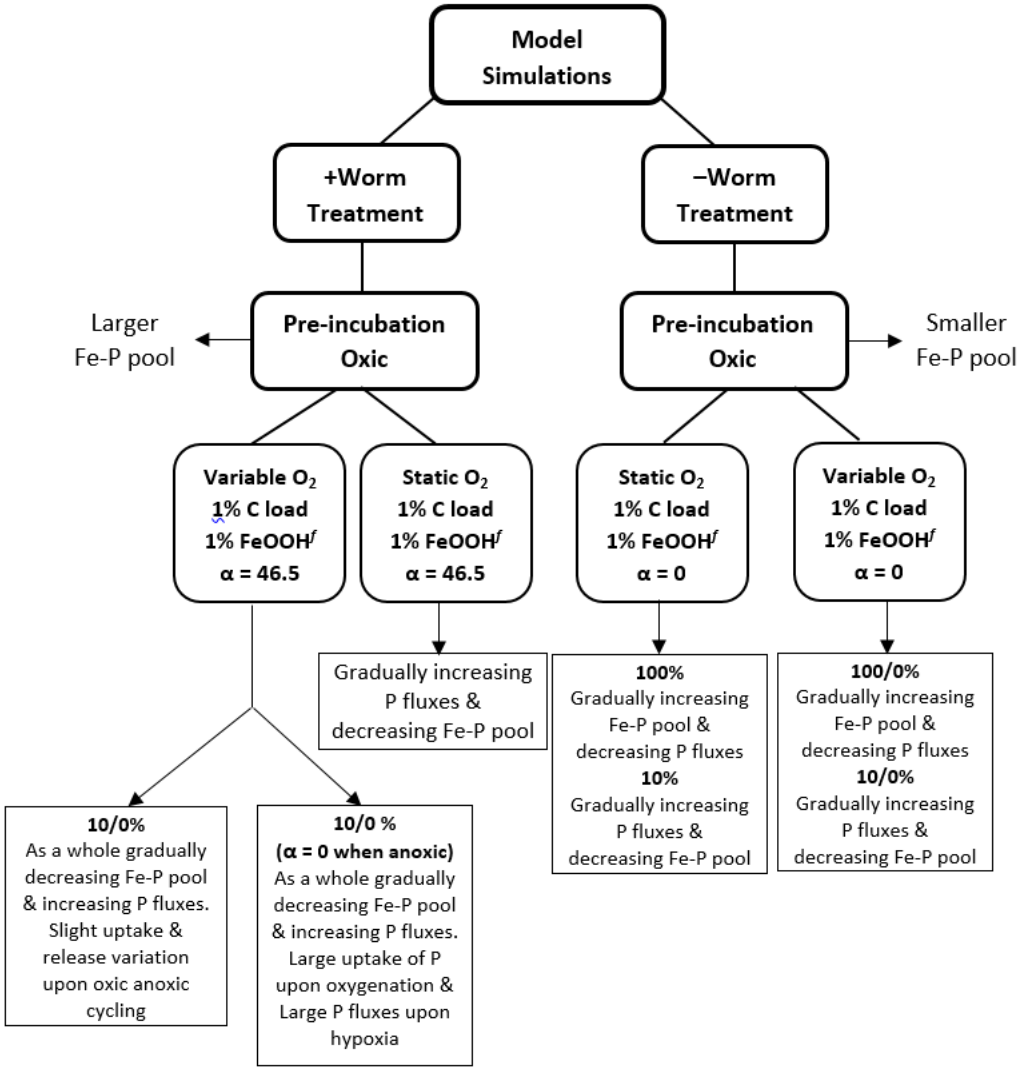

Figure 4.9. *Summary of the model simulation outcomes under different scenarios*

4.5.3. Model sensitivity towards reactive iron content, sediment carbon loading and irrigation rates

The model simulation suggests that the delivery of fresh solid phase iron oxyhydroxide controls how much PO_4^{3-} is released to the surface waters (Fig. 4.7). For simulations with 95 μmol Fe g^{-1} dry sediment, the PO_4^{3-} irrigation fluxes were roughly ten times higher than those observed with 7.1 μmol

Fe g^{-1} dry sediment input. The apparent dependency on Fe inventory meant much larger P effluxes with worms than without worms (Fig. 4.3b, 4.3d, 4.4b, 4.4d). This resulted in a much larger iron bound P pool in the treatment without worms than with worms at the end of the experiment. The model sensitivity to iron supply agrees with the literature, which suggests that iron acts as a limiting species in high carbon systems controlling FeS_2 burial (Faber et al., 2012; Hu & Cai, 2011). In terms of sedimentary Fe bound P depth profiles, the worms treatment with bioirrigation turned off showed a much larger shift in iron bound P pools from deep into the sediment towards the sediment surface for simulations with 95 μmol Fe g^{-1} dry sediment compared to simulations with 41 μmol Fe g^{-1} dry sediment. The sediment profile suggests release of PO_4^{3-} from deeper sediment upon anoxia and its subsequent uptake near the surface as indicated by spikes near the surface for WW10/0% S treatment (Supplementary material, Fig. S3).

The presence of the iron oxyhydroxide bound P pool was restricted to the first one centimetre through elevated organic matter mineralisation rates in simulations with 5% C load. In all other treatments with worms and 1%C load, the iron oxyhydroxide bound P pool was present up to a few centimetres into the sediment. An increase in carbon loading led to remarkably high P fluxes. This can be attributed to the enhanced iron reduction rates (FeOOH consumption) and the S^{2-} fluxes occurring at the sediment water interface during the simulations. The positive flux coming from the organic matter degradation was nearly five times higher than the flux observed in simulations with a 1% C load. Ait Ballagh et al. (2021) showed extremely high mineralization rates and ten times higher Fe bound P fluxes linked to increased organic matter inputs compared to a site with decreased organic matter inputs. The sediment profile of W10/0% S treatment with 1%C load showed Fe bound P pool spike near the sediment surface on alternate days suggesting the capture of released P by the iron oxyhydroxide pool. The profile of the W10/0% S treatment with a 5%C load showed an Fe bound P pool depleted to the sediment surface (~0.2-0.4 cm) with no real spikes suggesting enhanced organic matter mineralization through respiration and exhaustion of P binding sites resulting in the higher loss of P from the system through efflux (Supplementary material, Fig. S1).

The effect of bioirrigation on sediment PO_4^{3-} fluxes and Fe-P pool was evaluated by increasing the bioirrigation coefficient (α value from 4.65 to 465 yr^{1-}). The sediment profile suggest an uptake spike of P near the sediment surface for treatments with irrigation turned off (Fig. S4). In the model simulations, a large α value (465 yr^{1-}) led to higher PO_4^{3-} fluxes and a corresponding lower integrated total P pool as compared to simulations with an α value of 4.6 yr^{-1}. This suggests organic matter mineralisation coupled to dissimilatory iron reduction under hypoxic condition increases with irrigation intensity. Similarly, higher Fe bound P fluxes in Aulne estuary linked to larger irrigation value and depth were observed (Ait Ballagh et al., 2020). Similarly, an increase in bioirrigation from α value 0.1 to 1 d^{1-} produced several fold rise in Fe^{2+} flushing (van de Velde & Meysman, 2016).
The sensitivity analysis to quantify the effects of irrigation rates, Fe content and carbon loading suggests that the model parameters outcome agrees with literature.

4.5.4. Model artefacts and limitations

Of critical importance to this study, the 1D model was unable to simulate deep pools of FeOOH and associated P. Classical 1D model are simple and have reduced computational resource requirements. It was hypothesized that the model would be able to simulate the P dynamics observed during the laboratory experiment. The failure to reproduce observations is because the 1D model assumes a well-

mixed sediment at each depth interval, which means that model simulations cannot have "pockets" of FeOOH at depth surrounded by reduced sediment. In other words, a 1D model is based on a single depth dependent coefficient assuming uniformity along a single grid and lacks horizontal heterogeneity to capture an oxidised burrow surrounded by reduced sediment. In a study on the assessment of model complexities, Meysman concluded that the 1D model fails to capture the essential process that drives bioirrigation (Meysman et al., 2006). The effects of burrow geometry, distribution and flushing cannot be represented by a single depth dependent bioirrigation coefficient function in 1D model (Meile et al., 2005). Dale et al. (2013) suggested the need for addressing the limitation of the 1D model approach to simulate ironoxyhydroxides formation and dissolution on burrow walls. In agreement with these studies, there was a discrepancy between data and model output using the classical 1D modelling method. The experimental outcomes could not be replicated by varying the parameters in 1D model. So, that leaves our experimental hypothesis concerning faunal activity under hypoxic conditions as plausible. The limitations of the 1D model suggest more complex modelling is probably required to simulate localised burrow induced phenomena for Fe and P biogeochemistry. A mechanistic 2D pocket injection model includes lateral heterogeneity to address the bioirrigation associated issue of 1D model. The 2D model with its predictive capacity and model simplicity provides an optimal balance as compared to 1D and 3D models (Meysman et al., 2006).

Another issue observed in the present study with the 1D model is the loss of phosphorus from the system even under oxic conditions as a result of benthic faunal activity (Fig. 4.2e). Since the model is not implemented for a temporal switch of Fe bound P pool to more crystalline forms, the vast decrease in iron bound P pool and the release of associated P appears to be an artefact of model simulation. Also, the 1D model may not be applicable in scenarios involving past and future parameterizations, spatial differences in biomass abundance, specie interactions and their stochastic effects as a lot of the intricacies of what happens in a bioirrigated sediment depend upon the behaviour of the fauna. (Kanzaki et al., 2019; Kristensen et al., 2012; Meysman et al., 2006).

4.6. Conclusions

A reactive 1D transport model was modified with the aim of estimating the sedimentary phosphorus fluxes under oscillating hypoxic anoxic conditions. The sensitivity of the model to Fe supply suggests uptake upon oxygenation and release of P by benthic fauna upon hypoxia in bioturbated and bioirrigated sediments. Although the model formulated for the simulation study comprised both the bioirrigation rate and the attenuation coefficient, it failed to replicate the experimental data outcome highlighting the lateral averaging limitation of one-dimensional model. The model outcomes suggest that the mechanistic sedimentary physics we understand now is not enough to reproduce some real laboratory outcomes. A valuable next step to better (spatially) resolve the predictive capacity of 1D models includes understanding of the complex mechanisms determining the dynamics of coastal lagoon system and accurate spatiotemporal information to enforce accuracy of bioturbation estimates. A possible alternative to overcome spatial heterogeneity would be the use of 2D or 3D models to explicitly represent the burrow networks and associated biogeochemical processes.

4.7. References

Ait Ballagh, F. E., Rabouille, C., Andrieux-Loyer, F., Soetaert, K., Elkalay, K., & Khalil, K. (2020). Spatio-temporal dynamics of sedimentary phosphorus along two temperate eutrophic estuaries: A data-modelling approach. *Continental Shelf Research, 193*, 104037. doi:https://doi.org/10.1016/j.csr.2019.104037

Ait Ballagh, F. E., Rabouille, C., Andrieux-Loyer, F., Soetaert, K., LANSARD, B., Bombled, B., . . . KHALIL, K. (2021). Spatial Variability of Organic Matter and Phosphorus Cycling in Rhône River Prodelta Sediments (NW Mediterranean Sea, France): a Model-Data Approach. *Estuaries and Coasts*. doi:https://doi.org/10.1007/s12237-020-00889-9

Aller, R. C. (1980). Quantifying solute distributions in the bioturbated zone of marine sediments by defining an average microenvironment. *Geochimica et Cosmochimica Acta, 44*(12), 1955-1965. doi:https://doi.org/10.1016/0016-7037(80)90195-7

Aller, R. C. (1982). The Effects of Macrobenthos on Chemical Properties of Marine Sediment and Overlying Water, *Topics in geobiology*, *100*, 53-102. doi:https://doi.org/10.1007/978-1-4757-1317-6_2

Belley, R., Snelgrove, P. V., Archambault, P., & Juniper, S. K. (2016). Environmental Drivers of Benthic Flux Variation and Ecosystem Functioning in Salish Sea and Northeast Pacific Sediments. *PLOS ONE, 11*(3), e0151110. doi:https://doi.org/10.1371/journal.pone.0151110

Berezina, N., Maximov, A., & Vladimirova, O. (2019). The influence of benthic invertebrates on the phosphorus flux at the sediment-water interface in the easternmost Baltic Sea. *Marine Ecology Progress Series, 608*, 33-43. doi:https://doi.org/10.3354/meps12824

Berg, P. (2003). Dynamic Modeling of Early Diagenesis and Nutrient Cycling. A Case Study in an Artic Marine Sediment. *American Journal of Science - AMER J SCI, 303*, 905-955. doi:https://doi.org/10.2475/ajs.303.10.905

Boudreau, B. P. (1997). Diagenetic models and their implementation, *505*, *Berlin*, Springer.

Boudreau, B. P. (1998). Mean mixed depth of sediments: The wherefore and the why. *Limnology and Oceanography, 43*(3), 524-526. doi:https://doi.org/10.4319/lo.1998.43.3.0524

Brigolin, D., Rabouille, C., Bombled, B., Colla, S., Vizzini, S., Pastres, R., & Pranovi, F. (2017). Modelling biogeochemical processes in sediments from the north western Adriatic Sea: response to enhanced POC fluxes, *Biogeosciences, 15*, 1347-1366. doi:https://doi.org/10.5194/bg-15-1347-2018

Dale, A., Nickelsen, L., Scholz, F., Hensen, C., Oschlies, A., & Wallmann, K. (2015). A revised global estimate of dissolved iron fluxes from marine sediments. *Global Biogeochemical Cycles, 29*,691-707. doi:https://doi.org/10.1002/2014GB005017

Dale, A. W., Bertics, V. J., Treude, T., Sommer, S., & Wallmann, K. (2013). Modeling benthic–pelagic nutrient exchange processes and porewater distributions in a seasonally hypoxic sediment: evidence for massive phosphate release by Beggiatoa? *Biogeosciences, 10*(2), 629-651. doi:https://doi.org/10.5194/bg-10-629-2013

Dale, A. W., Boyle, R. A., Lenton, T. M., Ingall, E. D., & Wallmann, K. (2016). A model for microbial phosphorus cycling in bioturbated marine sediments: Significance for phosphorus burial in the early Paleozoic. *Geochimica et Cosmochimica Acta, 189*, 251-268. doi:https://doi.org/10.1016/j.gca.2016.05.046

Borger, E., Tiano, J., Braeckman, U., Ysebaert, T., & Soetaert, K. (2019). Biological and biogeochemical methods for estimating bio-irrigation: a case study in the Oosterschelde estuary, *Biogeosciences, 17*, 1701-1715. doi:https://doi.org/10.5194/bg-17-1701-2020

Faber, P., Kessler, A., Bull, J., Id, M., Meysman, F., & Cook, P. (2012). The role of alkalinity generation in controlling the fluxes of CO2 during exposure and inundation on tidal flats. *Biogeosciences, 9*, 4087-4097.

doi:https://doi.org/10.5194/bg-9-4087-2012

Herreid, C. F. (1980). Hypoxia in invertebrates. *Comparative Biochemistry and Physiology Part A: Physiology*, *67*(3), 311-320.

doi:https://doi.org/10.1016/S0300-9629(80)80002-8

Hu, X., & Cai, W.-J. (2011). An assessment of ocean margin anaerobic processes on oceanic alkalinity budget. *Global Biogeochemical Cycles, 25*(3), 1-11. doi:https://doi.org/10.1029/2010GB003859

Hupfer, M., Jordan, S., Herzog, C., Ebeling, C., Ladwig, R., Rothe, M., & Lewandowski, J. (2019). Chironomid larvae enhance phosphorus burial in lake sediments: Insights from long and short-term experiments. *Science of The Total Environment*, *663*, 254-264.

doi:https://doi.org/10.1016/j.scitotenv.2019.01.274

Kanzaki, Y., Boudreau, B., Turner, S., & Ridgwell, A. (2019). A lattice-automaton bioturbation simulator for the coupled physics, chemistry, and biology of marine sediments (eLABS v0.1). *Geoscientific Model Development Discussions, 0.1*,1-39. doi:https://doi.org/10.5194/gmd-2019-62

Kristensen, E., Penha-Lopes, G., Delefosse, M., Valdemarsen, T., Organo Quintana, C., & Banta, G. (2012). What is bioturbation? Need for a precise definition for fauna in aquatic science, *Marine Ecology Progress Series, 446*, 285-302. doi:https://doi.org/10.3354/meps09506

Kristensen, E., Røy, H., Debrabant, K., & Valdemarsen, T. (2018). Carbon oxidation and bioirrigation in sediments along a Skagerrak-Kattegat-Belt Sea depth transect. *Marine Ecology Progress Series,604*, 33-50. doi:https://doi.org/10.3354/meps12734

Lewandowski, J., Laskov, C., & Hupfer, M. (2007). The relationship between Chironomus plumosus burrows and the spatial distribution of pore-water phosphate, iron and ammonium in lake sediments. *Freshwater Biology, 52*(2), 331-343. doi:https://doi.org/10.1111/j.1365-2427.2006.01702.x

Liu, Y., Reible, D., Hussain, F., & Fang, H. (2019). Role of Bioroughness, Bioirrigation, and Turbulence on Oxygen Dynamics at the Sediment-Water Interface. *Water Resources Research, 55*(10), 8061-8075. doi:https://doi.org/10.1029/2019WR025098

Meile, C. D., Berg, P., Van Cappellen, P., & Tuncay, K. (2005). Solute-specific pore water irrigation: Implications for chemical cycling in early diagenesis. *Journal of Marine Research, 63*, 601-621. doi:https://doi.org/10.1357/0022240054307885

Meysman, F., Boudreau, B., & Middelburg, J. (2005). Modeling reactive transport in sediments subject to bioturbation and compaction. *Geochimica et Cosmochimica Acta, 69*, 3601-3617. doi:https://doi.org/10.1016/j.gca.2005.01.004

Meysman, F., Galaktionov, O., Gribsholt, B., & Middelburg, J. (2006). Bio-irrigation in permeable sediments: An assessment of model complexity. *Journal of Marine Research - J MAR RES, 64*, 589-627. doi:https://doi.org/10.1357/002224006778715757

Miatta, M., & Snelgrove, P. V. R. (2021). Benthic nutrient fluxes in deep-sea sediments within the Laurentian Channel MPA (eastern Canada): The relative roles of macrofauna, environment, and sea pen octocorals. *Deep Sea Research Part I: Oceanographic Research Papers*, *178*, 103655. doi:https://doi.org/10.1016/j.dsr.2021.103655

Middelburg, J. J., & Levin, L. A. (2009). Coastal hypoxia and sediment biogeochemistry. *Biogeosciences*, *6*(7), 1273-1293. doi:https://doi.org/10.5194/bg-6-1273-2009

Norkko, J., Reed, D. C., Timmermann, K., Norkko, A., Gustafsson, B. G., Bonsdorff, E., . . . Conley, D. J. (2012). A welcome can of worms? Hypoxia mitigation by an invasive species. *Global Change Biology*, *18*(2), 422-434. doi:https://doi.org/10.1111/j.1365-2486.2011.02513.x

Paraska, D. W., Hipsey, M. R., & Salmon, S. U. (2014). Sediment diagenesis models: Review of approaches, challenges and opportunities. *Environ. Modelling & Software*, 61, 297-325. doi:https://doi.org/doi.org/10.1016/j.envsoft.2014.05.011

Quintana, C. O., Raymond, C., Nascimento, F. J. A., Bonaglia, S., Forster, S., Gunnarsson, J. S., & Kristensen, E. (2018). Functional Performance of Three Invasive Marenzelleria Species Under Contrasting Ecological Conditions Within the Baltic Sea. *Estuaries and Coasts*, *41*(6), 1766-1781. doi:https://doi.org/10.1007/s12237-018-0376-9

Quintana, C. O., Tang, M., & Kristensen, E. (2007). Simultaneous study of particle reworking, irrigation transport and reaction rates in sediment bioturbated by the polychaetes Heteromastus and Marenzelleria. *Journal of Experimental Marine Biology and Ecology*, *352*(2), 392-406. doi:https://doi.org/10.1016/j.jembe.2007.08.015

Rabalais, N. N., Cai, W.-J., Carstensen, J., Conley, D. J., Fry, B., Hu, X., Zhang, J. (2014). Eutrophication-Driven Deoxygenation in the Coastal Ocean. *Oceanography*, *27*(1), 172-183. doi:https://doi.org/10.5670/oceanog.2014.21

Reed, D. C., Slomp, C. P., & Gustafsson, B. G. (2011). Sedimentary phosphorus dynamics and the evolution of bottom-water hypoxia: A coupled benthic–pelagic model of a coastal system. *Limnology and Oceanography*, *56*(3), 1075-1092. doi:https://doi.org/10.4319/lo.2011.56.3.1075

Scicluna, T. R., Woodland, R. J., Zhu, Y., Grace, M. R., & Cook, P. L. M. (2015). Deep dynamic pools of phosphorus in the sediment of a temperate lagoon with recurring blooms of diazotrophic cyanobacteria. *Limnology and Oceanography*, *60*(6), 2185-2196. doi:https://doi.org/10.1002/lno.10162

Soetaert, K., & Meysman, F. (2012). Reactive transport in aquatic ecosystems: Rapid model prototyping in the open source software R. *Environmental Modelling & Software*, *32*, 49-60. doi:https://doi.org/10.1016/j.envsoft.2011.08.011

Soetaert, K., Petzoldt, T., & Setzer, R. W. (2010). Solving Differential Equations in R: Package deSolve. *Journal of Statistical Software*, *33*(9), 1 - 25. doi:https://doi.org/10.18637/jss.v033.i09

Sturdivant, S. K., Díaz, R. J., & Cutter, G. R. (2012). Bioturbation in a Declining Oxygen Environment, in situ Observations from Wormcam. *PLOS ONE*, *7*(4), e34539. doi:https://doi.org/10.1371/journal.pone.0034539

Tarhan, L. G., Zhao, M., & Planavsky, N. J. (2021). Bioturbation feedbacks on the phosphorus cycle. *Earth and Planetary Science Letters*, *566*, 116961. doi:https://doi.org/10.1016/j.epsl.2021.116961

van de Velde, S., & Meysman, F. (2016). The Influence of Bioturbation on Iron and Sulphur Cycling in Marine Sediments: A Model Analysis. *Aquatic Geochemistry*, *22*,469-504. doi:https://doi.org/10.1007/s10498-016-9301-7

Wang H, A. A., Gulliver JS. (2003). Modeling of phosphorus dynamics in aquatic sediments: II--examination of model performance. *Water Research, 37*(16), 3939-3953.

doi:https://doi.org/10.1016/s0043-1354(03)00305-1

Zhang, W., Neumann, A., Daewel, U., Wirtz, K., van Beusekom, J., Eisele, A., Schrum, C. (2021). Quantifying Importance of Macrobenthos for Benthic-Pelagic Coupling in a Temperate Coastal Shelf Sea. *Journal of Geophysical Research: Oceans, 126*, e2020JC016995.
doi:https://doi.org/10.1029/2020JC016995

Zhao, M., Zhang, S., Tarhan, L., Reinhard, C., & Planavsky, N. (2020). The role of calcium in regulating marine phosphorus burial and atmospheric oxygenation. *Nature Communications, 11*, 2232.
doi:https://doi.org/10.1038/s41467-020-15673-3

Zhu, Y., Hipsey, M. R., McCowan, A., Beardall, J., & Cook, P. L. M. (2016). The role of bioirrigation in sediment phosphorus dynamics and blooms of toxic cyanobacteria in a temperate lagoon. *Environmental Modelling & Software, 86*, 277-304.
doi:https://doi.org/10.1016/j.envsoft.2016.09.023

Zhu, Y., McCowan, A., & Cook, P. (2017). Effects of changes in nutrient loading and composition on hypoxia dynamics and internal nutrient cycling of a stratified coastal lagoon. *Biogeosciences, 14*, 4423-4433.

doi:https://doi.org/10.5194/bg-14-4423-2017

4.8. Supplementary material

Table S1. List of constants included in the reactive transport model.

Constant	Name	Value	Unit	Ref.*
K_f	Decay constant of fast-decaying organic matter	10	y-1	a
K_s	Decay constant of slow-decaying organic matter	0.1	y-1	a
K_{O_2}	Monod constant for aerobic respiration	0.02	μmol cm-3	b
K_{FeOOH}	Monod constant for iron reduction	65	μmol cm-3	a
K_{SO_4}	Monod constant for sulphate reduction	1.6	μmol cm-3	a
K_{IO}	Reed constant for iron oxidation	35000	μmol-1 cm3 y-1	a
$K_{Fe.s}$	Kinetic constant for FeOOH crystallization	0.6	μmol-1 cm3 y-1	a
$K_{FeS.ox}$	Kinetic constant for iron sulphide oxidation	300	μmol-1 cm3 y-1	c
$K_{FeS_2.ox}$	Kinetic constant for pyrite oxidation	1/2	μmol-1 cm3 y-1	b
K_{SO}	Kinetic constant for sulphide oxidation	160	μmol-1 cm3 y-1	a
$K_{Fe.HS}$	Kinetic constant for Fe/HS redox reaction	100	μmol-1 cm3 y-1	c
$K_{FeOOH.HS}$	Kinetic constant for FeOOH/HS redox reaction	8/2	μmol-1 cm3 y-1	c
$K_{FeS.SO_4}$	Kinetic constant for $FeS.SO_4$	7	μmol-1 cm3 y-1	c
Ψ	Attenuation factor for SO_4^{2-} reduction	0.075	-	b

† References: a: van de Velde and Meysman (2016); b: Reed et al. (2011); c: Faber et al. (2012)

Table S2. List of species included in the reactive transport model.

Species Name	Notation
Solids	
Organic matter (OM)	$\{(CH_2O)(PO_4^{3-})_{1/106}\}_{f,s}$
Iron oxyhydroxide	FeOOH
Iron sulphide	FeS
Pyrite	FeS2
Crystalline Iron oxyhydroxide	FeOOH.s
PO_4 adsorbed onto Iron oxyhydroxide	$FeOOH.PO_4$
PO_4 adsorbed onto crystalline Iron oxyhydroxide	$FeOOH.PO_4$.s
Solutes	
Oxygen	O_2
Carbon dioxide	CO_2
Water	H_2O
Hydrogen ion	H^+
Phosphate	PO_4^{-2}
Sulphate	SO_4^{2-}
Sulphide	HS^-
Iron	Fe^{2+}

Table S3. List of environmental and transport parameters.

Parameter	Name	Value	Unit
L	Depth of sediment domain	10	cm
N	Number of grid layers	100	-
S	Salinity	35	ppt
P	Pressure	1.013	bar
T_c	Temperature	10	^{o}C
φ	Porosity	0.8	-
ρ	Density of sediment	2.6	g cm^{-3}
u	Sedimentation velocity in porewater	0	cm yr^{-1}
v	Sedimentation velocity in solid phase	0	cm yr^{-1}
$D_b{}^0$	Bio mixing	28	Cm^2 yr^{-1}
α^o	Bio irrigation	46.5‡	yr^{-1}
DBL	Thickness of diffusive boundary layer	0	cm

‡ Bio irrigation 46.5 yr^{-1} if not specified

Table S4. Iron reduction rates in simulation with worms (C loading 1%, FeOOH^f 1% and α equals 46.5).

Time in days	WW 10/0% S	WW 10/0%	WW 10%	WW 100%
0.00	3728.95	3728.95	3728.95	3728.95
1.00	3950.70	3950.70	3950.70	3713.07
2.00	3614.81	4061.62	3925.71	3696.59
3.00	3569.95	3898.41	3902.02	3679.55
4.00	3290.90	4009.23	3878.76	3662.02
5.00	3317.87	3849.83	3855.74	3644.04
6.00	3075.51	3959.16	3832.97	3625.65
7.00	3151.58	3803.06	3810.42	3606.91
8.00	2935.13	3910.79	3788.05	3587.83
9.00	3041.17	3757.59	3765.81	3568.46
10.00	2842.27	3863.42	3743.63	3548.83
11.00	2962.75	3712.74	3721.46	3528.96
12.00	2775.70	3816.44	3699.28	3508.87
13.00	2900.92	3668.00	3677.04	3488.60
14.00	2722.43	3769.45	3654.74	3468.15
15.00	2847.23	3623.12	3632.37	3447.55
16.00	2675.57	3722.29	3609.92	3426.82
17.00	2797.50	3577.99	3587.41	3405.98
18.00	2631.79	3674.92	3564.82	3385.03
19.00	2749.80	3532.62	3542.18	3363.99
20.00	2589.56	3627.36	3519.48	3342.87
21.00	2703.30	3487.06	3496.74	3321.70
22.00	2548.26	3579.68	3473.97	3300.46
23.00	2657.69	3441.38	3451.17	3279.19
24.00	2507.65	3531.94	3428.35	3257.88
25.00	2612.88	3395.63	3405.52	3236.54
26.00	2467.69	3484.21	3382.69	3215.18
27.00	2568.88	3349.88	3359.86	3193.82
28.00	2428.38	3436.53	3337.04	3172.45
29.00	2525.70	3304.18	3314.24	3151.08
30.00	2389.75	3388.96	3291.47	3129.72

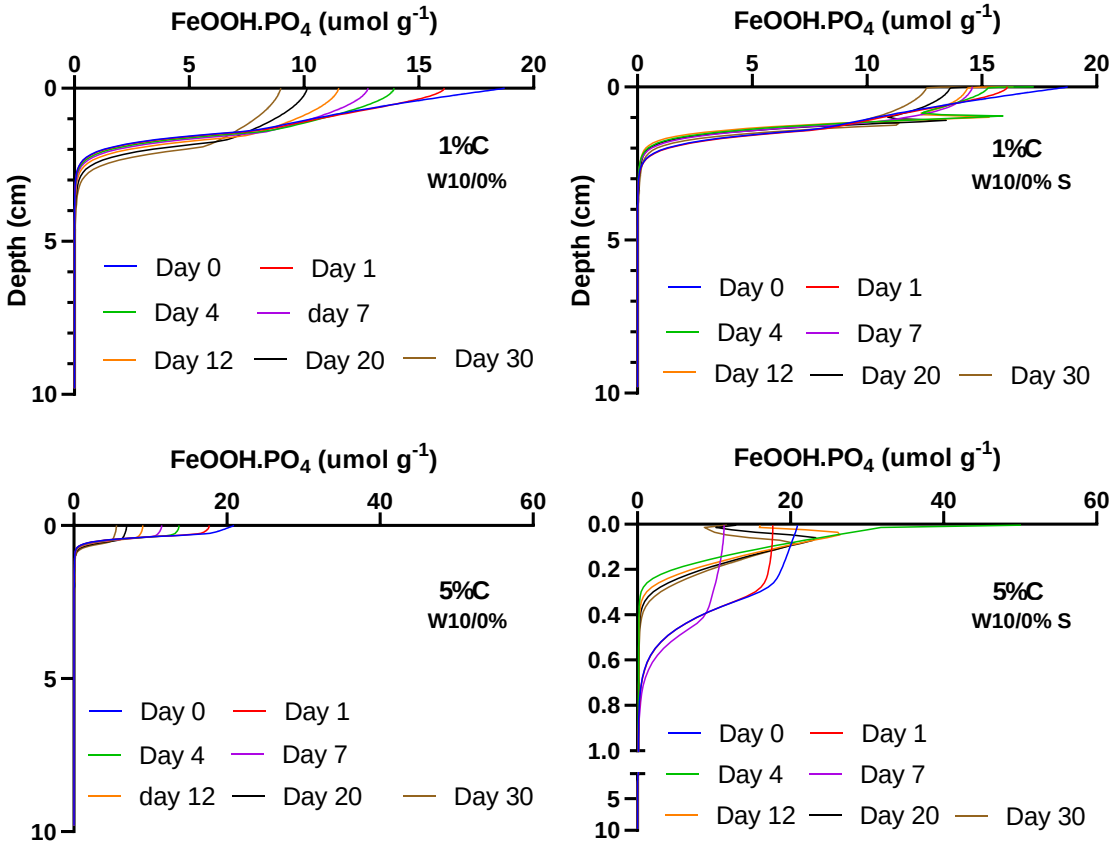

Figure S1. Sediment depth profile of Fe bound P in simulation with worms for 1% and 5% carbon loading. 1%C W10/0% represent worm treatment with altering 10%oxic/anoxic days at 1% carbon loading and 1%C W10/0% S has irrigation turned off on anoxic days. Similarly. %%C W10/0% represent worm treatment with altering 10%oxic/anoxic days at 5% carbon loading and 5%C W10/0% S has irrigation turned off on anoxic days.

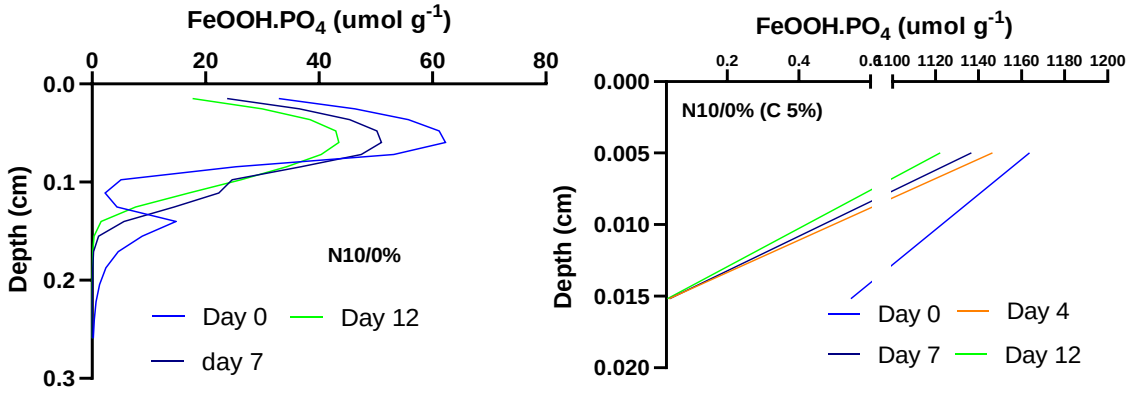

Figure S2. Sediment depth profile of Fe bound P in simulation with 1% and 5% carbon loading without worms. N10/0% represent treatment with altering 10%oxic/anoxic days at 1% carbon loading and N10/0% (C 5%) represent treatment with altering 10%oxic/anoxic days at 5% carbon loading.

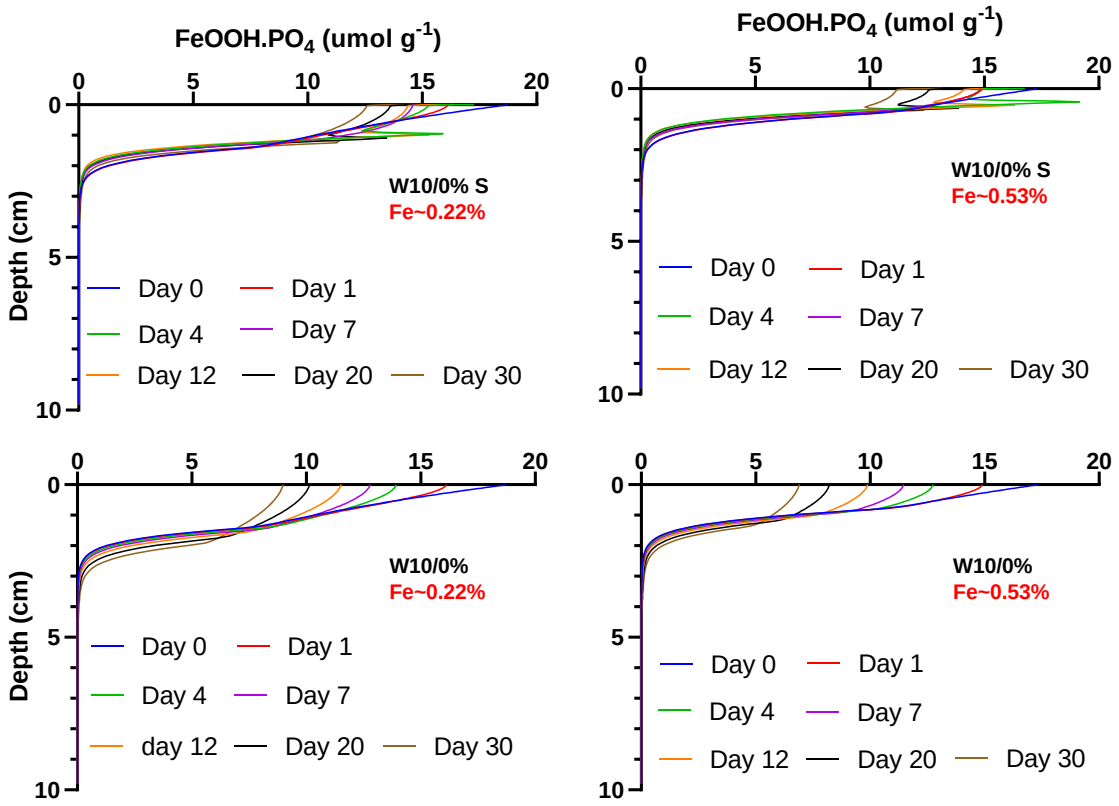

Figure S3. Sediment depth profile of Fe bound P in simulation with worms for 0.22% and 0.53% Fe.). W10/0% (Fe 0.22%) represent worm treatment with altering 10%oxic/anoxic days applied $FeOOH^f$ conc. 0.22% and WW 10/0% S (Fe 0.22%) has irrigation turned off on anoxic days with $FeOOH^f$ conc. 0.22%. Similarly, W10/0% (Fe 0.53%) and WW 10/0% S (Fe 0.53%) indicate $FeOOH^f$ conc. 0.53%.

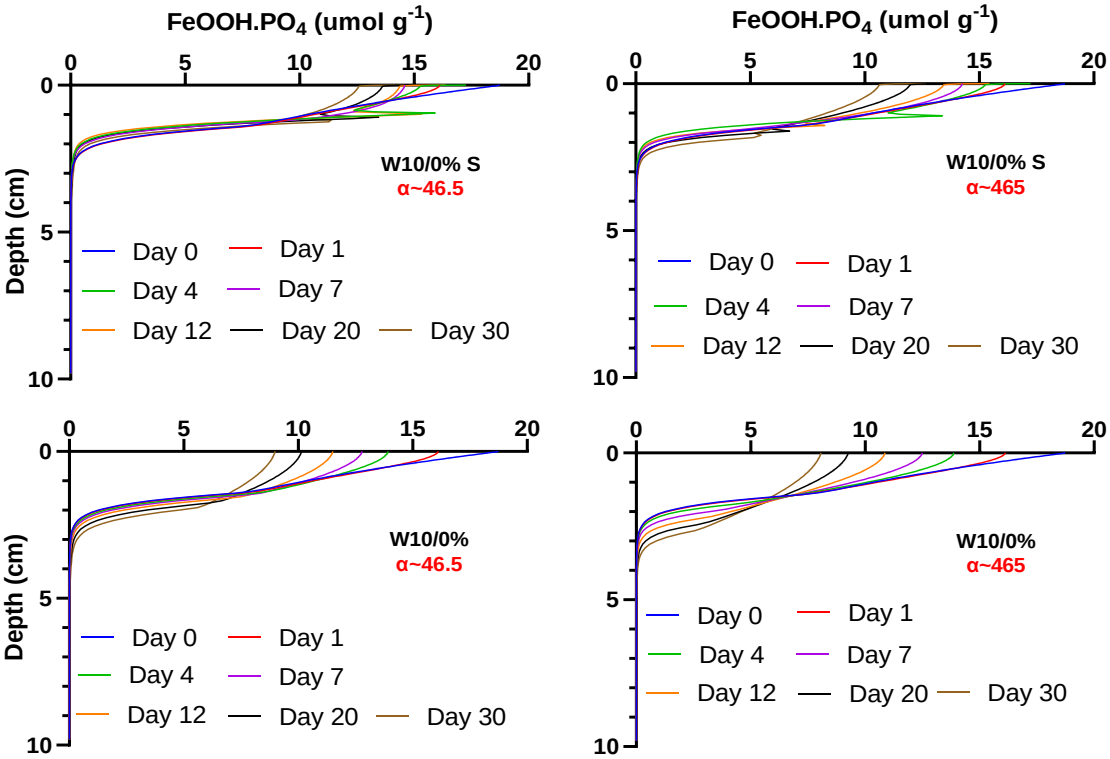

Figure S4. Sediment depth profile of Fe bound P in simulations with worms for bioirrigation value 46.5 & 465. W10/0% (α 46.5) represent worm treatment with altering 10%oxic/anoxic days applied α value of 46.5 and WW 10/0% S (α 46.5) has irrigation turned off on anoxic days with α value of 46.5. Similarly, W10/0% (α 465) and W10/0% S (α 46.5) indicate α value of 465.

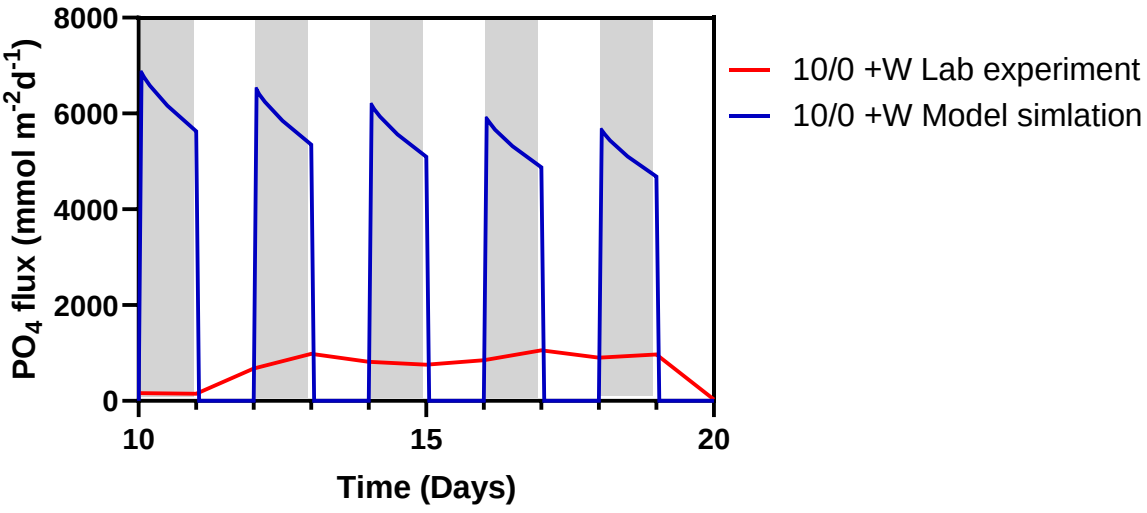

Figure S5. Comparison of effluxes of P for a lab based experiment on cores with worms under cyclic oxygen condition (cyclic 10% oxic period and anoxia every 24 hours) and simulation of 1D model with worms under cyclic oxygen condition (cyclic 10% oxic period and anoxia every 24 hours) with an imposed α value of 465 in bioturbed sediments keeping FeOOHf 1% and carbon loading 1% during 20-30 day timeframe

5. *Synthesis and conclusions*

In this synthesis and conclusions chapter, the overall research findings are summarised and the ecological implications of the research outcomes are highlighted. Finally, I have pointed towards some promising future research directions that would deliver information to uncover some of the complexities of sedimentary P biogeochemical processes.

5.1. Summary of research findings

At the start of research work, some research objectives were defined based on the interesting research findings and recommendations of Todd R Scicluna. His research work highlighted the mechanism behind P release from sediments and potential role of *C. capitata* in uptake and release of phosphorus. This led to outlining the following three main research objectives:

(1) Study of the iron phosphorus dynamics within the Gippsland lakes to investigate the sediment P recharge mechanism

(2) investigate the role of *C. capitata* activity on sediment P biogeochemistry under variable oxygen regime

(3) explore the potential of a one-dimensional model to capture interaction between bioirrigation and phosphorus release and storage within the sediment

This thesis reveals new insights into the significance of variable oxygen conditions as a mean to control sediment P release, quantitative understanding of benthic fauna activity and impacts on sediment biogeochemistry and the need of advancing in existing mechanistic models to elucidate the effects of environmental change on sediment P biogeochemistry.

5.1.1. Controls on P release in sediments

The Gippsland Lakes monitoring study aimed at identifying the key variables causing changes in sedimentary P pools over short and long term. The research outcomes presented provided an insight into the sediment amorphous iron bound P dynamics and its controls. The site experienced periods of oxygenation lasting more than two years on two occasions. On both occasions, the net change in sedimentary P pools was negligible suggesting that the gradual accumulation of P in to sediments is not applicable to the lake under study. Statistical analysis performed on the decade long monitoring data suggested a very strong association of bottom water TP with Chl-*a* and Asc-P indicating that inflow events are more important in controlling iron oxyhydroxide bound P pool than longer term oxidised conditions. Interestingly, Asc-P showed no clear response to inflows suggesting that not all inflow events result in an increase of Asc-Fe and Asc-P pool. An important aspect associated with the inflow events is the delivery of fresh Fe and P to the system that supports Asc-P enrichment in sediments. The surface sediment FRP was also able to demonstrate the sediment P behaviour in response to inflow events. The year 2018 marks a period when relatively small inflow event (~2400 ML d^{-1}) led to delivery of fresh P resulting in a 25% rise in Asc-P and ten times in FRP concentrations. The relatively small Asc-P enrichment of 25% can be explained by the presence of relatively small Asc-Fe pool recorded for the monitoring period. This highlight the significance of iron oxyhydroxide pool as another factor that controls Asc-P in sediments. Further monitoring could provide critical information for predicting the long-term behaviour of the lakes.

In this thesis, the association of river inflow events and environmental variables (temperature, salinity, DO, turbidity, pH, Chlorophyll, NH_4^+, FRP, NO_X, TP and TN) with the changes in reactive Fe bound P pool of the sediments was monitored. The promising avenues for further research are mainly derived from a continuation of the present study while taking into account some of the limitations encountered in this study. In-situ water quality investigations similar to those of this research but on a spatial scale incorporating different areas of the Gippsland Lakes needs to be executed. The sedimentary P pools also need to be studied across the Gippsland Lakes. The purpose of the study would be to identify the spatiotemporal heterogeneity of the sedimentary P pools. Secondly, tracking the delivery of Fe and P input through inflow events will help demonstrate the spatial variation of Fe and P uptake from the point of entrance where the inflow enters the Lake to further downward stream areas where P remains available to the sediment. It is expected that variability in factors across the lake will favour spatially altering biogeochemistry. A study on spatial scale was conducted in Lake Wairewa to investigate the poorly understood mechanisms controlling P dynamics. The results indicated the presence of legacy P deposited reactive P pool as a ready source for internal P. However, the low oxygen conditions were not spatially extensive in the Lake suggesting that the hypoxic events could drive asymmetrical P release (Waters et al., 2021). In a study to understand the P dynamics in Lake Chaohu, short term and long term (years to decades) outcomes were combined to quantify the P release potential. The rates of P release were much larger at sites near the riverine inputs and the trends were opposite at sites away from inputs. Legacy P accounted for 81% of the P fluxes observed in form of Fe bound P. The study highlighted the potential role of internal and external P in sediment P dynamics (Yang et al., 2022). Another point to ponder in the proposed study would be the impact of timescale variation in inflow events that is the influence of longer lasting inflows on the Lakes P dynamics as compared to short-term inflows. PCA analysis can be combined with spatial data as useful tool for investigation. In literature as well, a combination of spatial analysis and PCA has been suggested as a useful tool for investigation (Deng, 2021; Li et al., 2017). The data analysis can then help answer the questions related to the variation in major influencing factors of water quality across the different areas and seasons. Does legacy P have a significant effect on Lakes? The potential role of inflow events and oxygen regime in relation to sedimentary P dynamics? The results can then be transformed into a predictive framework allowing to speculate the possible impacts of an inflow event in different environment.

5.1.2. Significance of benthic fauna and variable oxygen condition in mediating P removal

This study underscores the importance of benthic fauna irrigation activity in relation to the sediment P cycling. Most studies emphasizing the role of benthic fauna and oxygen conditions as control of P release from sediments involve monitored field observations. Laboratory experiments provide an alternative way of studying the biogeochemical processes under controlled conditions. In the present study, potential impact of benthic fauna under varying oxygen conditions on cycling of P within the sediments was observed. An oxic pre-incubation resulted in an enhanced enrichment of iron oxyhydroxides bound P in cores with worms showing the strong influence of burrowing activity indicated by yellowish brown color deeper in to the sediments. This behaviour can be explained by the combined effect of oxic conditions and worm irrigation activity transporting oxygen into the area surrounding the burrows generating oxidized compounds (iron oxyhydroxides) leading to the co-precipitation of P with freshly precipitated iron oxyhydroxides (Beam et al., 2020). An important

aspect of my result was the change in iron bound P pool to a more crystalline phase in worms treatment that was kept oxygenated post incubation.

According to the findings of this study, oscillating hypoxic-anoxic conditions led to an enhanced P-flux from the sediment in treatment with worms under cyclic 10% oxic and anoxic conditions compared to completely anoxic treatment. This suggest oxygen deficiency in the bottom water resulting in stress prompted sustained and enhanced reductive dissolution of Fe oxides and P release while completely anoxic conditions led to enhanced rapid P release from sediments, however, the treatment resulted in *C. capitata* mortality within a few days. *C. capitata* is known for its resilience to hypoxic conditions and it is most likely that stress induced conditions might have led to an enhanced irrigation activity for transporting oxygen into the sediment and consequently pumping out P into the overlying water (Gamenick et al., 1998; Rosenberg et al., 2001). The hypothesis is further supported by the change in sediment color from brown to black. In coastal lagoons, wind forcing and tidal effects can cause variability in oxygen conditions at the sediment water interface leading to complex P dynamics (Verschelling et al., 2017). The study outcomes also highlight the importance of the modified sequential extraction schemes used in the study for Fe and P fractions that allowed distinguishing reactive Fe and P in the sediment.

The range of P flux in cores with and without worms highlight the significance of oxygen conditions and fauna presence for sedimentary P cycling. All experiments involving *C. capitata* were performed on well-mixed sediments packed into core liners after homogenising. In the literature, studies related to the influence of benthic fauna on ecosystem functioning suggest that the effect of benthic fauna depend on both the physiochemical property and the traits of the fauna. For example, the presence of iron or sulphur, temperature, oxygen condition or the carbonate nature of the sediments can alter influence of benthic fauna (Bernard et al., 2020). To further investigate the role of benthic fauna and to address sediment heterogeneity, the *C. capitata* experiments could be executed using intact Gippsland Lakes sediments. The P fluxes measurement of the experiments will result in a more accurate and real representation of the *C. capitata* potential for P fluxes than those measured in the chapter 3, and provide a more detailed information on the potential of *C. capitata* to influence sediment Fe bound P pools under varying oxygen conditions. Similar to the present study, Kendzierska et al. (2020) investigated the size and direction of benthic P fluxes from sediments under variable oxygen conditions to assess the impact of fauna. The highest P-effluxes were observed in sediments exposed to occasional hypoxic or anoxic conditions. Furthermore, based on the success of the modified extraction scheme particularly ascorbate and dithionite extractions to display amorphous and crystalline iron oxides and associated P phases, further experiments could be performed to investigate the conversion of amorphous iron oxyhydroxide bound P pools to more crystalline Fe-P pools over longer periods. The study would help understand the dynamics of Fe and P pools in sediments and the role of benthic fauna in P storage over longer timescales. It is suggested that the presence of benthic fauna can enhance P retention within the sediments and conversion into stable forms unavailable for easy dissolution (Hupfer et al., 2019). Formation of more crystalline phase iron oxyhydroxide from amorphous can occur in as little as 100 days (Schwertmann & Murad, 1983). The aim of study should be to determine the importance of benthic fauna in relation to rate of conversion of reactive Fe-P into more stable Fe-P and the link between the biogeochemical P cycles and life cycle of these fauna.

5.1.3. Advancing models for sediment P cycling

Models provide an alternate way of studying the sedimentary biogeochemical processes and their interactions. In the present study, a 1D model was used to investigate the potential of the model to simulate the interaction between oxygen regime and faunal activity, and resulting P fluxes. Consistent with experimental outcome, the baseline simulations in oxic pre-incubation led to an enrichment of amorphous Fe bound P pool indicating that bioirrigation in model acts as a major sink of P. The Fe-P pool was much larger in size compared to simulations without worms suggesting pumping action of the host organisms ventilate burrows, leading to a formation of iron oxyhydroxides on the exposed burrow walls. Based on the mechanistic understanding from the 1D model, it was hypothesized that the model simulations will also be able to address the bioirrigation P release effect. Unlike the experimental outcome, the cyclic hypoxic-anoxic conditions had no enhanced irrigation effect on P fluxes in simulations with worms. The results suggest that the oxygen condition has a more pronounced effect on sedimentary P cycling in the 1D model. A possible explanation for this behaviour is the lack of lateral heterogeneity in the model as it relies on a single depth dependent coefficient function. A 1D model assumes a well mixed sediment at depth intervals which can't have deep pockets of iron oxyhydroxides surrounded by anoxic sediment. Secondly, reactive-transport models simulate benthic fauna effects implicitly, e.g., considering bioturbation and/or bioirrigation coefficient only. The approach may not be successful in coastal systems that experience greater variability suggesting a strong need to couple detailed sediment processes with faunal activity (Ehrnsten et al., 2020).

A mechanistic 2D model includes lateral heterogeneity to possibly address the bioirrigation associated issues faced in simulations performed on the 1D model. Compared to 3D model which are complex, the 2D model with its predictive capacity and simplicity provides an optimal balance. The choice of the model depend up on the scale of the domain and 2D models offers a good compromise with economic and simplicity gains and simulation outcomes tend to be closer to the 3D models (Gharbi et al., 2016). It is therefore recommended that the experiments be done using a more mechanistic 2D model. It is hypothesized that a 2D model with lateral heterogeneity will be able to produce the bioirrigation effects observed in the laboratory experiments. In 1D models, sediment concentrations are only depth averaged whereas a 2D model can be classified as depth integrated as well as laterally integrated (Lai, 2020). A 2D model was applied to simulate the spatial distribution of phosphate for Baiyangdian Lake. A depth dependent advection diffusion equation allowed for the direction of the depth averaged pollutant concentration. The established 2D model simulated with a maximum relative error less than 4% (Tang et al, 2018). Compared to 3D models that are complex and resource consuming in their implementation, the 2D models are more informative than 1D models and less complex and cost effective than 3D models (Guan et al, 2018). Bioirrigation zones are complex 3D environments and a 2D pocket injection model can simplify the 3D micro-environments into 2D formulations to describe the radial solute movements caused by bioirrigation (Meysman et al., 2006). Further, a more mechanistic 2D model could be implemented for Fe-P crystallization into stable Fe oxides to incorporate long-term influence of bioirrigation activity by benthic fauna into modelling work to observe longer timescale variation in sediment Fe and P dynamics.

5.2. Implications of research findings

From a management perspective, the results from the present Gippsland Lakes monitoring study

suggest that the fate of iron oxide bound phosphorus in sediments is strongly affected by the delivery of fresh Fe and P through inflows. This mechanism of P accumulation support the notion that reducing the input of nutrient from the upper catchment via inflows into the Gippsland Lakes is critical in reducing the occurrence and timescale of algal blooms in the system. This study has some major implications for Lakes health management because it suggests that even artificially oxygenating the Gippsland Lakes to alleviate stratified conditions and enhance P uptake by iron oxides may not always work since the system might be experiencing low Fe:P ratios or continued inflows over longer periods of time. Also, it normally takes several years for strategies focussed on reduced external P loads to reap full benefits (Giudice et al., 2018). Based on the outcomes of chapter 3, the presence of *C. capitata* in the Gippsland Lakes may significantly help to enhance the sink of P into the sediments from the water column. However, phosphorus enriched sediments will act as additional P source over shorter periods and may worsen the situation through P release upon anoxia. Therefore, management strategies targeting reduce P delivery into the system will be as important as those that enhance the accumulation of P within the sediment. The EPA and DELWP should incorporate strategies to reduce impacts of inflow events in their established operational guidelines for sediment management apart from investigating the impacts of high nutrient loads.

From a global perspective, the findings of the present study demonstrate the importance of internal P and external P loads as two relatively distinct and influential mechanisms of deteriorating water quality. The monitoring part of present study suggest how the inflow events through delivery of P control lake water quality and how sediment P dynamics are influenced by a large variety of factors. While the experimental study, emphasize the potential of benthic fauna and the dependence on oxygen condition as mechanism for possible sedimentary P recharge and release. This meant that the fauna assisted enhanced P uptake by sediments under oxic conditions, switches to potential P source under short-term anoxic pulses. The study also suggest that the basic paradigm regarding internal and external P load in estuaries which controls accumulation and release of P from sediments is rather much more complex. The estuarine responses to nutrient loading varies according to the biogeochemical and physical dynamics of the system. For example, delivery of P through continued high inflow event led to an algal bloom in the present study, however, the presence of *C. capitata* would have led to an accumulation of P in the sediments. Similarly, stratification in shallower lakes is greatly influenced by strong winds as compared to deep lakes. A decade long study on the Neuse estuary suggested that the increase in benthic fauna concentration was not correlated with the changes in salinity, temperature or dissolved oxygen (factors commonly associated with benthic fauna) (Froelich et al., 2019). The impact of nutrient loads on lake water quality are associated with the dynamics of large variety of factors including but not limited to oxygen condition, temperature, benthic community, pH, hydrodynamic conditions and salinity (Giudice et al., 2018; Papatheodorou et al., 2006; Yang et al., 2022).

5.4. Conclusions

Undoubtedly, the uptake and release of phosphorus by sediments represents an important component of phosphorus cycling in estuaries. Hypoxia or anoxia are known to drastically change ecosystem functioning through enhanced benthic P fluxes from the sediments. However, the timescale and the sources of P that drive sediment phosphorus recharge are not always completely understood. In this research on the Gippsland Lakes (chapter II), sedimentary reactive Fe and P pools coincided with the

river inflows and bottom water TP levels. No clear trends for the build-up of legacy P in the system were observed. Just as important in sediment P recharge mechanism is the delivery of fresh Fe and P into the system, for high inflow events to have a significant impact on LKN water quality. In the laboratory experiments (chapter III), we explored benthic worms as significant sink of P up on oxygenation and a source of P up on hypoxia. The presence of iron in the sediments appeared to be an important factor as it controls P uptake and release through iron oxyhydroxide formation and dissolution. Oxic conditions in the water column allow uptake of P by iron oxyhydroxide as part of burrowing activity by benthic fauna. The survivability of benthic fauna under hypoxic-anoxic conditions control the extent of P release from the sediment. Lastly (chapter IV), modelling was explored as an alternative way of understanding sedimentary P dynamics in the Gippsland Lakes by applying different Fe, P, irrigation and oxygen perspectives. The model failed to capture the real description of scenarios involving bioirrigation. This suggests that bioirrigation activities by benthic fauna are complex phenomena that demand lateral heterogeneity apart from the traditional depth dependent coefficient function. A 2D model with its lateral heterogeneity and predictive capacity may be able to capture scenarios involving bioirrigation associated complexities. The understanding of the environmental variables and their interactions and knowledge of the sediment P contents are needed to obtain a more complete understanding of the complex local P cycling within the sediments of estuaries and coastal marine sediments.

5.5. References

Beam, J. P., George, S., Record, N. R., Countway, P. D., Johnston, D. T., Girguis, P. R., & Emerson, D. (2020). Mud, Microbes, and Macrofauna: Seasonal Dynamics of the Iron Biogeochemical Cycle in an Intertidal Mudflat. *Frontiers in Marine Science, 7*. doi:https://doi.org/10.3389/fmars.2020.562617

Bernard, G., Kauppi, L., Lavesque, N., Ciutat, A., Grémare, A., Massé, C., & Maire, O. (2020). An Invasive Mussel (Arcuatula senhousia, Benson 1842) Interacts with Resident Biota in Controlling Benthic Ecosystem Functioning. *Journal of Marine Science and Engineering, 8*(12), 963.

Retrieved from https://www.mdpi.com/2077-1312/8/12/963

Cook, P. L. M., Holland, D. P., & Longmore, A. R. (2010). Effect of a flood event on the dynamics of phytoplankton and biogeochemistry in a large temperate Australian lagoon. *Limnology and Oceanography, 55*(3), 1123-1133. doi:https://doi.org/10.4319/lo.2010.55.3.1123

Deng, C. L., Lusan & Peng, Dingzhi & Li, Haisheng & Zhao, Ziyang & Chunjian, Lyu & Zhang, Zeqian. (2021). Net anthropogenic nitrogen and phosphorus inputs in the Yangtze River economic belt: spatiotemporal dynamics, attribution analysis, and diversity management *Journal of Hydrology, 597*(9), 126221.

doi:https://doi.org/10.1016/j.jhydrol.2021.126221

Ehrnsten, E., Sun, X., Humborg, C., Norkko, A., Savchuk, O. P., Slomp, C. P., . . . Gustafsson, B. G. (2020). Understanding Environmental Changes in Temperate Coastal Seas: Linking Models of Benthic Fauna to Carbon and Nutrient Fluxes. *Frontiers in Marine Science, 7*. doi:10.3389/fmars.2020.00450

Froelich B, G. R., Blackwood D, Lauer K, Noble R. (2019). Decadal monitoring reveals an increase in Vibrio spp. concentrations in the Neuse River Estuary, North Carolina, USA. *PLOS ONE, 14*(4), e0215254.

doi:https://doi.org/10.1371/journal.pone.0215254

Gamenick, I., Vismann, B., Grieshaber, M., & Giere, O. (1998). Ecophysiological differentiation of *Capitella capitata* (Polychaeta). Sibling species from different sulfidic habitats. *Marine Ecology Progress Series, 175*, 155-166.

doi:https://doi.org/10.3354/meps175155

Gharbi, M., Soualmia, A., Dartus, D., & Masbernat, L. (2016). Floods effects on rivers morphological changes application to the Medjerda River in Tunisia. *Journal of Hydrology and Hydromechanics, 64*(1), 56-66. doi:https://doi.org/10.1515/johh-2016-0004

Giudice, D., Zhou, Y., Sinha, E., & Michalak, A. M. (2018). Long-Term Phosphorus Loading and Springtime Temperatures Explain Interannual Variability of Hypoxia in a Large Temperate Lake. *Environmental Science & Technology, 52*(4), 2046-2054.

doi:https://doi.org/10.1021/acs.est.7b04730

Guan, M., Ahilan, S., Yu, D., Peng, Y., & Wright, N. (2018). Numerical modelling of hydro-morphological processes dominated by fine suspended sediment in a stormwater pond. *Journal of Hydrology, 556*, 87-99. doi:https://doi.org/10.1016/j.jhydrol.2017.11.006

Hupfer, M., Jordan, S., Herzog, C., Ebeling, C., Ladwig, R., Rothe, M., & Lewandowski, J. (2019). Chironomid larvae enhance phosphorus burial in lake sediments: Insights from long and short-term experiments. *Science of The Total Environment, 663*, 254-264.

doi:https://doi.org/10.1016/j.scitotenv.2019.01.274

Kendzierska. H, K. Ł.-M., Dorota Burska, Urszula Janas,. (2020). Benthic fluxes of oxygen and nutrients under the influence of macrobenthic fauna on the periphery of the intermittently hypoxic zone in the Baltic Sea. *Journal of Experimental Marine Biology and Ecology, 530*, 151439.

doi:https://doi.org/10.1016/j.jembe.2020.151439

Lai, Y. G. (2020). A Two-Dimensional Depth-Averaged Sediment Transport Mobile-Bed Model with Polygonal Meshes. *Water, 12*(4), 1032.
doi:https://www.mdpi.com/2073-4441/12/4/1032

Li, K., Wang, L., Li, Z., Xie, Y., Wang, X., & Fang, Q. (2017). Exploring the Spatial-Seasonal Dynamics of Water Quality, Submerged Aquatic Plants and Their Influencing Factors in Different Areas of a Lake. *Water, 9*(9), 707.
Retrieved from https://www.mdpi.com/2073-4441/9/9/707

Meysman, F., Galaktionov, O., Gribsholt, B., & Middelburg, J. (2006). Bio-irrigation in permeable sediments: An assessment of model complexity. *Journal of Marine Research - J MAR RES, 64*, 589-627.

doi:https://doi.org/10.1357/002224006778715757

Papatheodorou. G, G. D., Nicolaos Lambrakis. (2006). A long-term study of temporal hydrochemical data in a shallow lake using multivariate statistical techniques. *Ecological Modelling, 193*(3-4), 759-776.

doi:https://doi.org/10.1016/j.ecolmodel.2005.09.004

Rosenberg, R., Nilsson, H. C., & Diaz, R. J. (2001). Response of Benthic Fauna and Changing Sediment Redox Profiles over a Hypoxic Gradient. *Estuarine Coastal and Shelf Science, 53*, 343-350.
doi:https://doi.org/10.1006/ecss.2001.0810

Schwertmann, U., & Murad, E. (1983). Effect of pH on the Formation of Goethite and Hematite from Ferrihydrite. *Clays and Clay Minerals, 31*, 277-284.
doi:https://doi.org/10.1346/CCMN.1983.0310405

Tang. C, Y. Y., Zhifeng Yang, Shanghong Zhang, Haifei Liu. (2018). Effects of ecological flow release patterns on water quality and ecological restoration of a large shallow lake. *Journal of Cleaner Production, 174*, 577-590.

doi:https://doi.org/10.1016/j.jclepro.2017.10.338

Verschelling, E., van der Deijl, E., van der Perk, M., Sloff, K., & Middelkoop, H. (2017). Effects of discharge, wind, and tide on sedimentation in a recently restored tidal freshwater wetland. *Hydrological Processes, 31*(16), 2827-2841.

doi:https://doi.org/10.1002/hyp.11217

Waters, S., Webster-Brown, J. G., & Hawes, I. (2021). The release of legacy phosphorus from deforestation-derived sediments in shallow, coastal lake Forsyth/Te Roto o Wairewa. *New Zealand Journal of Marine and Freshwater Research, 55*(3), 446-465.
doi:https://doi.org/10.1080/00288330.2020.1804408

Yang. C, J. L., Hongbin Yin. (2022). Phosphorus internal loading and sediment diagenesis in a large eutrophic lake (Lake Chaohu, China). *Environmental Pollution, 292*, 118471. doi:https://doi.org/10.1016/j.envpol.2021.118471